INFORMATION TO USERS

This manuscript has been reproduced from the microfilm master. UMI films the text directly from the original or copy submitted. Thus, some thesis and dissertation copies are in typewriter face, while others may be from any type of computer printer.

The quality of this reproduction is dependent upon the quality of the copy submitted. Broken or indistinct print, colored or poor quality illustrations and photographs, print bleedthrough, substandard margins, and improper alignment can adversely affect reproduction.

In the unlikely event that the author did not send UMI a complete manuscript and there are missing pages, these will be noted. Also, if unauthorized copyright material had to be removed, a note will indicate the deletion.

Oversize materials (e.g., maps, drawings, charts) are reproduced by sectioning the original, beginning at the upper left-hand corner and continuing from left to right in equal sections with small overlaps. Each original is also photographed in one exposure and is included in reduced form at the back of the book.

Photographs included in the original manuscript have been reproduced xerographically in this copy. Higher quality 6" x 9" black and white photographic prints are available for any photographs or illustrations appearing in this copy for an additional charge. Contact UMI directly to order.

UMI

A Bell & Howell Information Company
300 North Zeeb Road, Ann Arbor MI 48106-1346 USA
313/761-4700 800/521-0600

Model Fidelity Considerations in the Dynamic Simulation of Equilibrium Staged Separation Operations

by

Shaoqun Huang

A dissertation submitted to the Graduate Faculty in Engineering
in partial fulfillment of the requirements for the degree of Doctor of Philosophy,
The City University of New York

1996

This manuscript has been read and accepted for the Graduate Faculty in Engineering in satisfaction of the dissertation requirement for the degree of Doctor of Philosophy.

20 MAR 96
Date

Prof. Irven H. Rinard
Chair of Examining Committee

3/20/96
Date

Prof. Gerard G. Lowen
Executive Officer

Prof. Reuel Shinnar
Prof. Roberto Mauri
Prof. Alexander Couzis
Dr. Bruce Benjamin

Supervisory Committee

The City University of New York

ABSTRACT

Model Fidelity Considerations

in the Dynamic Simulation of Equilibrium Staged Separation Operations

by

Shaoqun Huang

Advisor: Professor Irven H. Rinard

Model fidelity, namely, how well a particular model represents the behavior of an actual system, is an important consideration in dynamic process simulation. As even more sophisticated models are used in order to obtain a better understanding of both the physical phenomena and expected performance of processes, the trade-offs between model complexity and model fidelity must be considered. There is a need for guidelines or criteria to assist systems engineers and dynamic models in the appropriate choice of model as a function of fidelity and complexity.

In this thesis, model fidelity is studied by using a reference model. These other models may be either simpler or more detailed than the reference model. The object is to develop methodology for making informed choices as to which model to use in a given application. Our approach has been to develop model fidelity indices of various types against which model fidelity errors can be correlated. These should be simple to evaluate *a priori* so that the user can decide which model to use without expending a lot of effort.

Three equilibrium staged separation operations were studied: (1) a single-stage flash drum, (2) an isothermal gas absorber, and (3) a simple multicomponent distillation column. The first two, being relatively simple, were used to develop indices and model fidelity error correlations and guidelines. These were then tested on the more complex distillation column model.

Two aspects of modeling were included in this study. One is the choice of vapor-liquid equilibrium (VLE) model. The other is the choice of what structural details should be included in the model. Two VLE models were compared, namely, ideal and that based on the Wilson activity coefficient model. A number of structural details associated with multi-staged separations were studied.

The results validate the approach, namely, that model fidelity indices can be used to correlate model fidelity errors. Several were developed, the most useful being Index A which allows one to decide what VLE model to use. The results also show that under most circumstances, the vapor holdup can be neglected compared to the liquid holdup. Downcomer dynamics can generally be neglected over the frequency bandwidth of usual engineering interest but flow-over-the-weir dynamics cannot. Most of these models are very stiff and the choice of the appropriate integration method is not always straightforward.

To my grandmother and parents, whose fostering brought about my continuous efforts in life. To my wife Yuzhen and my daughter Min, whose love, patience and encouragement have contributed more than anything else to the completion of this work.

ACKNOWLEDGEMENTS

The author wishes to express his profound appreciation and gratitude to Professor Irven H. Rinard for his continuous guidance, inspiration and contribution at all times during the course of this work. He also wishes to thank all members of the Supervisory Committee for their help and encouragement.

Financial assistance was made available by Robust Systems Technology, Inc., Simulation Sciences, Inc., and a Graduate Fellowship B provided by City College. This aid is gratefully acknowledged.

CONTENTS

LIST OF TABLES

LIST OF FIGURES

CHAPTER ONE. MODEL FIDELITY CONCEPTS

1.1 Introduction

The concern herein is with the modeling aspects of dynamic simulation. On the one hand, a simulation is only as good as the models on which it is based. On the other, if the models are overly complex and detailed, difficulties may arise in the course of the simulation. Thus a tradeoff is required between the fidelity of model and its complexity, the extent of this tradeoff being determined by the purpose of the simulation. It is the nature of this tradeoff which is explored in this work, specifically in regard to equilibrium-stage separation operations.

Great progress has been made during the last decade in the dynamic simulation of chemical processes. It has been driven by the demands for improved process control, process safety evaluation, and the training of operating personnel. And it has been made possible by the rapidly increasing cost effectiveness of high-capability computers. An indicator of this progress is that dynamic simulators are being more widely used by industry. There are now several commercially available dynamic simulators of which one of the better known is SPEEDUP (Pantelides 1988). Marquardt (1991) listed more than twenty dynamic process simulation packages in his summary of dynamic process simulation. *Hydrocarbon Processing* (Sept. 1995) provides information about commercially available chemical and petrochemical dynamic process simulation systems. Benson (1989) provides an overview of what will required of the next generation of simulators, namely, that these be multipurpose

in nature capable of steady-state, dynamic systems engineering, real-time training, and on-line control all using the same basic set of equipment and physical properties models.

Throughout most of its history, dynamic simulation has been limited to the simplest possible models. This limitation was imposed by the finite hardware capabilities of the analog computers used in the 1950's and 60's and by the lack of memory and speed of the digital computers of the 1970's and 1980's. One has only to examine DYFLO, the pioneering digital simulator developed by Roger Franks at DuPont (Franks 1972), to realize just how limited these models are. The only model fidelity question that arose was just how simple could the model be and still provide any useful results at all.

The situation is changing rapidly. The need for tighter and more sophisticated process control and the growing dependence upon simulation for safety system validation and operator training and certification has led to demands for high fidelity models and replica simulators. There should be no discernible differences between the behavior predicted by the simulator and that of the actual system. Further, the use of approximate models is not acceptable for pre-startup simulation of first-of-a-kind facilities since these cannot be validated against plant test data. Even for established facilities, acquisition of high-quality dynamic test ranks somewhere between difficult and impossible. Thus, while far from perfect, the high fidelity model is the only acceptable alternative.

Thus we are now being faced with the situation in dynamic simulation that has long existed in steady-state simulation, namely, the use of complex models with little or no

guidance for the user in how well these models perform. It has been shown for steady-state simulation (Rinard 1987) that as systems become more tightly recycled, their sensitivity to modeling errors increases. This is true not only of entire processes but also of those types of equipment which employ internal recycles, e.g., staged separation operations such as distillation. It is the goal of the present work to explore this problem with respect to the dynamic modeling of equilibrium staged systems.

1.2 Measures of Model Fidelity

Model fidelity is defined as how well a particular model represents the behavior of an actual system. For the reasons mentioned in the previous section, the actual system is seldom available to provide data for comparison. As a surrogate, a reference model is used. The choice of reference model depends upon the specific circumstances. If a validated model containing a full range of detail is available, then this can be used to evaluate the relative fidelity of simpler models. On the other hand, one may choose as a reference model one which has been widely published and studied even though it is known to be based on one or more simplifying assumptions. This choice can be used to evaluate the effects of relaxing one or more of these simplifying assumptions. In this work, both approaches will be used where appropriate.

There are a number of measures that can be used to assess various aspects of model fidelity with respect to a reference model (Rinard 1990):

1) Steady-state accuracy

Steady-state accuracy is a measure of how well the model predicts the behavior of the system operating at steady state. For the obvious reason, it is useful only when dealing with a continuous process. Quantitatively, steady-state accuracy, SSA, is defined as either the absolute value of the difference between the steady-state value from the reference model and the model being evaluated (SSAA) or the relative error (SSAR). For the ith process variable y_i this can be stated as:

$$(1.2\text{-}1) \qquad SSAA_i = |y_i^{rm} - y_i^{m}| \quad or$$

$$SSAR_i = \frac{|y_i^{rm} - y_i^{m}|}{y_i^{rm}}$$

where the superscript rm refers to the reference model and superscript m to the model under evaluation. The SSA must be evaluated for each and every process variable of importance. While a vector norm would simplify the analysis in some ways, it would tend to obscure the tradeoffs between different types, say temperature and composition, which may differ from one situation to another. In this work the process variables will be considered separately. Also, whether to use SSAA or SSAR is a question of context. For instance, an operator or control engineer may be interested in relative errors in flow rates, say, but absolute errors in product composition.

Strange as it may seem, this is probably the most important measure of dynamic model fidelity for the simple reason that the steady-state performance is generally much better known than the dynamic performance, particularly to the operating personnel. If the dynamic model is to have any credibility with them, it must reproduce the steady-state behavior within some acceptable degree of accuracy.

2) Static Accuracy

Static accuracy SA refers to accuracy with which the dynamic model predicts the open-loop process gain matrix $K_p = [k_{pij}]$. It is best defined in terms of a relative error as follows:

$$(1.2\text{-}2) \qquad SA_{ij} = \frac{|k_{pij}^{rm} - k_{pij}^{m}|}{|k_{pij}^{rm}|}$$

This measure is important in judging whether or not a given model is sufficiently accurate to provide proper guidance in the structuring of multivariable control systems.

3) Dynamic accuracy

Dynamic accuracy can be characterized in two ways. One uses the linearized model to explore model structure in any of the transform, frequency, or time domains; the other the unlinearized model in the time domain. When using the linearized model in the frequency domain, the measures of interest are the frequency response gain and phase angle as functions of frequency. In the time domain, these are the eigenvalue spectrum and the condition number. In the time domain there are several characteristics of interest. In some situations the maximum error between the model and its reference model may be of critical importance. In others, an integral error such as the integral squared error (ISE) or the integral of the absolute value of the error (IAE) evaluated over some time interval may be more significant.

The eigenvalue spectrum reveals to what extent the model being evaluated matches the reference model with respect to time response modes. Also, the ratio of the real parts of the largest and smallest eigenvalues of a given model is an indication of its stiffness, a measure of model complexity that is discussed in the next section. The condition number of a model compared to that of the reference model is a measure of their relative sensitivities to modeling error, again a measure of model complexity. Comparison of the transfer functions of the model and its reference model indicates to what extent the order of the system is being modeled. The transfer function also reveals the presence (or absence) of right half plane (RHP) zeroes, important because of their role in inverse response.

The linearized measure that is used most widely in this work is the frequency response. It also reveals the order of the system. Comparison with a reference model at the critical point indicates to what extent the model is suitable for control system design, large errors in either gain or phase angle suggesting a substantial degree of model uncertainty.

In the frequency domain the gain accuracy $GA_{ij}(\omega)$ of the ith output with respect to the jth input is best defined on an absolute basis when the gain is expressed on a logarithmic basis (in, say, decilogs) as follows:

$$(1.2\text{-}3a) \qquad GA_{ij}(\omega) = 10\log_{10}|G_{pij}^{rm}(\omega)| - 10\log_{10}|G_{pij}^{m}(\omega)|$$

This suitable unless one of the two gains is identically zero, in which case the comparison should be made using the arithmetic gain.

The phase accuracy is defined similarly (in either degrees or radian)

$$(1.2\text{-}3b) \qquad PA_{ij}(\omega) = \angle G_{pij}^{rm}(\omega) - \angle G_{pij}^{m}(\omega)$$

Both the gain and phase accuracy measures are functions of frequency. Generally one will want to evaluate them at some reference frequency such as the critical frequency. Otherwise the comparison may be meaningless if comparing two models, one of which is unbounded in either phase or gain while the other is not.

Keep in mind that these measures of model fidelity are based on a linearized model. They are very useful but do require linearization of the model equations which, for a complex model, can be a laborious and exacting task. Therefore it is quite often more convenient, although less revealing, to compare simulated responses in the time domain. As discussed previously, there are two measures of time-domain model fidelity that have their uses. One measure of time-domain accuracy is the maximum difference between the model and its reference model ($TDAM_i$) over a time interval (0,T). It is defined as

$$(1.2\text{-}4) \qquad TDAM_i = \max_t |y_i^{rm}(t) - y_i^{m}(t)|, \quad 0 \le t \le T$$

Similarly, an integral-squared-error measure ($TDAI_i$) is defined as

$$(1.2\text{-}5) \qquad TDAI_i = \int_0^T [y_i^{rm}(t) - y_i^{m}(t)]^2 dt$$

4) Operational accuracy

Operational accuracy concerns the ability of a model to represent the behavior of the system over the entire range of potential operating conditions. A great majority of the dynamic models described in the literature only apply over that narrow range of conditions associated with normal operations. While this is acceptable for some activities such as control system design, it is not for others such as safety system validation and start up and shut down studies. Consider, for example, the operation of a boiler. For normal operations, a change in heat input translates directly into an increase in steam production. However, during start up there is no steam production until the inventory of water in the boiler tubes and steam drum reaches the boiling point. Two different models are required to span this range of operating conditions if start up is an important aspect of the simulation.

1.3 Measures of Model Complexity

There are several measures that can be used to characterize model complexity. These along with the measures of model fidelity can be used to make a choice of the appropriate model to use in a given situation.

1) Number of equations

The simplest and most straightforward measure of model complexity is merely the number of equations required to describe the model. In general these will be both a combination of ordinary differential equations (ODE's) and algebraic equations (AE's), the combined set being described as differential and algebraic equations (DAE's). The basic

equations for some models, though not those in this work, are partial differential equations (PDE's). However, in almost all simulators these are approximated as sets of ODE's either through orthogonal collocation (Michelson 1973) or finite difference approximations by the so-called method-of-lines (Schiesser 1991, Silebi 1992).

2) DAE index

The numerical solution of DAE's for the purposes of simulation is much more difficult than that for ODE's (Brenan 1989). There are few solvers available for DAE's, DASSL being one of the few. What is usually done is to convert the DAE's to ODE's by differentiating the AE's with respect to time to convert them to ODE's. The number of times this differentiating must be performed to completely reduce the AE's to ODE's is referred to as the DAE index. Systems whose index is one can be reliably integrated using ODE solvers, although care must be taken in specifying a consistent set of initial conditions that satisfy the original AE's. Systems with an index higher than one cannot be reliably integrated and so are to be avoided. As will be seen, the models developed in this work are only of index one.

3) Stiffness ratio

Stiffness is a major problem in dynamic simulation, particularly when gas phase flow rate transients must be included in the model. Stiffness is defined as the ratio of the absolute value of the real part of the largest eigenvalue of the model to the absolute value of the real

part of the smallest. The larger this ratio is, the stiffer the system. The reciprocal of the largest eigenvalue determines the maximum step size that can be employed by an explicit ODE solver while the smallest eigenvalue governs how long a perturbed system will take to come to a new steady-state. Thus, the higher the stiffness ratio, the longer the computer time required to simulate a given amount of process time.

Systems are generally considered stiff when the stiffness ratio is greater than 500. Stiffness ratios exceeding 10^6 are not uncommon in process simulation. When stiff system are encountered, one can no longer use the usual explicit ODE solvers such as Euler or Runge-Kutta. Instead an implicit solver must be used (Silebi 1992). To be efficient, implicit solvers require an analytical representation of the Jacobian of the system of model equations. This is identical to the task of linearization discussed previously, namely, time-consuming and exacting. (It should be noted that some relief to the linearization problem is available through the use of symbolic algebra packages such as Maple and Mathematica. However, these were not available to the author at the outset of the present work.)

4) Real Time Factor

A measure of model complexity which is related to stiffness is the real time factor (RTF). This is defined as the ratio of process time interval being simulated to the amount of computer time required to carry out the simulation. For instance, if process transient that will take fifteen minutes in the plant is simulated in nine seconds on a particular computer the RTF = (15)(60)/(9) = 100. Obviously the RTF will depend upon the computing speed

of the computer being used. The faster the computer, the higher the RTF.

RTF is an important measure for both engineering simulators and training simulators. For the former, a high RTF is required so that the engineer can evaluate a reasonable number of case studies within a reasonable period of time. This is particularly true if the dominant time constant for the process is on the order of hours, not unusual in highly recycled system (Rinard 1982, Denn 1982) or high purity distillation (Fuentes & Luyben 1980). For training simulators the RTF does not have to be as large but still must be greater than 1.0 if the simulator is to meet the requirement of responding in real time. How much greater than 1.0 depends, of course, upon the system overhead of the particular computer being used.

One might think that meeting the RTF requirement for engineering simulation would be sufficient. However, this is not generally the case. For a number of reasons engineering simulations are subject to far fewer time discontinuities than are training simulations. This means that they can efficiently employ implicit ODE solvers which permit much larger integration time steps than do explicit ODE solvers. Training simulators on the other hand experience continual discontinuities. Some are deliberately introduced in training exercises such a pump failures and the like. Others result from the interaction between the simulation and the distributed control system (DCS) to which it is interfaced. When the discontinuities occur often enough, the implicit ODE solver loses its efficiency since it must be reinitialized after each discontinuity using an explicit ODE solver.

5) Condition number

The condition number of the state-space matrix derived from the linearization of a model is a measure of its sensitivity to modeling errors. The higher the condition number, the more sensitive the model. Unlike the eigenvalues, the condition number is scaling dependent. Thus, its interpretation on an absolute basis can be problematical. But it still a useful tool in comparing alternative models. Also, as will be seen, the condition number and the stiffness ratio tend to go hand-in-hand.

6) Nonlinearity

All but the simplest process models are nonlinear. This has several ramifications. Nonlinear models can exhibit behavior such as multiple steady-states and bifurcation that linear models cannot (Arbel 1995). Further, all measures of model fidelity and model complexity based on linearization will vary as the steady-state equilibrium point on which the lineariazation is based is varied. The RTF will also vary depending upon how severely the system is perturbed. Unfortunately, there is no simple measure of the degree of nonlinearity of a system.

7) Model branching

Many models, if they are to encompass operational fidelity, have two or more branches. For example, the model for an adiabatic flash will have one branch (liquid phase only) if the flashed feed is below its bubble point, a second branch if in the two-phase region, and a third (vapor phase only) if the flashed feed is above its dew point. Transition from one

branch to another can cause severe difficulties for some ODE solvers. Proper detection and reinitialization is required. Thus, the number of branches required for operational fidelity is another measure of model complexity.

1.4 Source of Model Complexity

There are two basic sources of model complexity. One is model structure; the other physical properties representation.

1) Model structure

Model structure can be made more complex by including more details of the equipment geometry and vessel internals. In the case of a distillation column the simplest model for an equilibrium stage assumes that the liquid on the tray is well mixed and that the liquid and vapor holdups are constant. A more complex model may take into account variable liquid holdup as determined by flow over the tray outlet weir, additional composition dynamics due to downcomer holdup, and pressure dynamics determined by the imbalance between vapor generation and condensation within the column. An even more detailed model will take into account the actual mass transfer rates occurring in the froth zone above the tray (Kooijman and Taylor 1995).

Model complexity can also be increased through the imposition of implicit control of one or more process variables. A flash drum provides a simple example. If one is

interested in the composition dynamics, it can be assumed that the liquid and vapor holdups are constant. This is tantamount to assuming perfect liquid level control and perfect pressure control. The effect on the modeling is to make the vapor and liquid flow rates leaving the drum algebraic variables. The net effect on the model is to make it more heavily a DAE system than it would be otherwise.

2) Physical properties representation

It is well known that the use of realistic physical properties representations such as equations of state, activity coefficient models, and complex mixing rules greatly increase the amount of computer time required to carry out a given simulation. In the early years of dynamic simulation, only the simplest models (ideal gas, Raoult's Law, ideal mixing, etc.) could be used without grossly exceeding the available computing resources. More recently, the widespread availability of sophisticated physical properties systems in steady-state simulators such as ASPEN, have led to similar expectations for dynamic simulators. If for no other reason, steady-state accuracy requires it.

Even with today's greatly improved computing resources, the indiscriminate use of complex physical properties models can result in unacceptably low real time factors. One approach has been to use local thermodynamic models (Barrett 1979, Chimowitz 1983 and 1984, Hillestad 1989, Machietto 1986, Sorlie 1992) but these have disadvantages such as creating discontinuities on updating and requiring frequent updating during severe transients.

1.5 Research Strategy

The goal of this work is to provide the systems engineer with guidelines for choosing the appropriate staged separation model to use in a given situation both with respect to structure and to physical properties representation. Our approach has been to develop a number of indices which can be used to evaluate or estimate the various fidelity and model complexity measures.

1) Model indices

To be useful a model index must be easy to evaluate a priori. It should be based on data which is readily available to the systems engineer. For instance, if we are concerned about the effects of variable liquid density upon the dynamic behavior of mixing tank, the index might be based on the ratio of the liquid molar volumes of the various components. This is illustrated in the last section of this chapter.

2) Study strategy

The following strategy was adopted for this work. First a number of simple situation would be studied with the goal of determining what are suitable indices for physical properties representations and structural complexity. Then these would be applied to more complex situations to see how well they serve as guidelines in these cases. To study the effects of vapor-liquid equilibrium (VLE) models, a simple flash drum was chosen. The

effects of structural details of multi-stage separation systems were evaluated using a simple gas absorber model based on the same assumptions that lead to the Kremser Equation for steady-state design (Kremser 1930, Henley 1981, King 1980). The indices and guidelines extracted from these studies were then evaluated using two distillation column models. The first is based on the assumption of constant molal overflow (CMO). This assumption is relaxed in the second model by including the energy balance in the tray model.

1.6 Basic Model Equations

The following is a development of the dynamic model equations for a well-mixed volume. Based on the conservation of mass for each component in a multicomponent mixture and the conservation of energy, these equations have the general form:

$$\frac{d\Psi}{dt} = F(Y,Z,M) \quad and \tag{1.6-1a}$$

$$G(Y,Z,M) = 0 \tag{1.6-1b}$$

where Ψ is a vector of holdups of conserved quantities, Y is a vector state variables, Z a vector of algebraic variables, and M a vector of input variables. Note that these equations form a set of differential and algebraic equations (DAE's). Specifically Ψ is defined as:

$$\Psi = [\phi\rho x_1, \phi\rho x_2, \ldots, \phi\rho x_{nc}, \phi\rho U]^T \tag{1.6-2}$$

where x_i is the ith component in a mixture of nc components. The right-hand-side of Eqn. 1.6-1a, namely F(Y,Z,M) has the form:

$$(1.6\text{-}3a) \qquad f_i = F_0 x_{0i} - F x_i + \eta_i + \phi\rho \sum_{j=1}^{nr} a_{ij} r_j, \quad i = 1,\ldots,nc \quad and$$

$$(1.6\text{-}3b) \qquad f_{nc+1} = F_0 H_0 - F H + \sum_{i=1}^{nc} \eta_i h_i^* + q_1 + q_2$$

While there may be more, there is at least one algebraic equation in the set G(Y,Z,M) defined in Eqn.1.6-1b, namely,

$$(1.6\text{-}4) \qquad g_1(x_1, x_2, \ldots, x_{nc}) = \sum_{i=1}^{nc} x_i - 1 = 0$$

Eqn. 1.6-4 along with Eqn. 1.6-1a form a set of DAE's of index one. If Eqn. 1.6-4 is differentiated with respect to time, one gets

$$(1.6\text{-}5) \qquad \frac{dg_1}{dt} = \sum_{i=1}^{nc} \frac{dx_i}{dt} = 0.$$

Summing the first nc elements of Eqn. 1.6-1a over i and applying Eqns. 1.6-4 and 1.6-5 gives an overall mass balance of the form

$$(1.6\text{-}6) \qquad \frac{d\phi\rho}{dt} = F_0 - F + \mathrm{N} + \phi\rho \sum_{j=1}^{nr} \sigma_j r_j$$

$$where \ \mathrm{N} = \sum_{i=1}^{nc} \eta_i \quad and \quad \sigma_j = \sum_{i=1}^{nc} a_{ij}$$

Eqn.1.6- 6 can be used to replace g_1 in Eqns. 1.6-1a and 1.6-1b giving an augmented holdup vector of the form

$$(1.6\text{-}7) \qquad \Upsilon = [\phi\rho x_1, \phi\rho x_2, \ldots, \phi\rho x_{nc}, \phi\rho, \phi\rho U]^T$$

and Eqns. 1.6-1a and 1.6-1b become

$$(1.6\text{-}8a) \qquad \frac{d\Upsilon}{dt} = \Gamma(Y,Z,M)$$

$$(1.6\text{-}8b) \quad \textit{and} \qquad \Omega(Y,Z,M) = 0.$$

$$\textit{where } \Gamma = F_0 x_{0i} - F x_i + \eta_i + \phi\rho \sum_{j=1}^{nr} a_{ij} r_j, \quad i = 1,\ldots,nc$$

$$= F_0 - F + N + \phi\rho \sum_{j=1}^{nr} \sigma_j r_j \qquad i = nc+1$$

$$\textit{and} = F_0 H_0 - FH + \sum_{i=1}^{nc} \eta_i h_i^* + q_1 + q_2, \quad i = nc+2$$

Eqn. 1.6-8 can be expanded as follows:

$$(1.6\text{-}9) \qquad J_\Upsilon \frac{dY}{dt} = \Gamma(Y,Z,M)$$

$$\textit{where } J_\Upsilon = \left[\frac{\partial \Psi_i}{\partial y_j}\right]$$

J_Υ will be referred to as the holdup Jacobian. This completes the development of the basic model equations. Their use is illustrated in the next section.

1.7 Illustrative Example - Mixing Tank

A simple example, that of a mixing tank, will serve to illustrate the approach outlined in Section 1.2. The tank is shown schematically in Fig. 1.1. Two cases are considered. In the first, the liquid density is assumed to be constant; in the second, a function of composition according to the ideal solution law. In both cases the tank is assumed to be isothermal.

The model equations for the tank can be extracted from the general model derived in the previous section. Since there is neither mass transfer nor reaction, those terms in Eqn. 1.6-8a are zero. Since the tank isothermal, the energy balance component can be ignored (unless one is interested in the dynamic heat transfer required to maintain isothermality). The model equations are, then,

$$\frac{d[\phi\rho x_i]}{dt} = F_0 x_{0i} - F x_i \tag{1.7-1}$$

$$\frac{d[\phi\rho]}{dt} = F_0 - F \tag{1.7-2}$$

Noting that the volume is variable, i.e., $\phi = Sh$, and reducing to first order form gives:

$$\phi\rho\frac{dx_i}{dt} = F_0(x_{0i} - x_i) \tag{1.7-3}$$

$$S\rho\frac{dh}{dt} = F_0\left[1 - \frac{1}{\rho}\sum_{j=1}^{nc}\frac{\partial\rho}{\partial x_j}(x_{0j} - x_j)\right] - F \tag{1.7-4}$$

Note that at steady state the outlet flow rate and composition must equal the inlet flow rate and composition respectively. This part of the steady state performance is unaffected by the choice of density model. However, the steady-state level will be.

For Case 1 (constant density), we have

$$\rho = constant \quad and \quad \frac{\partial\rho}{\partial x_j} = 0 \tag{1.7-5}$$

while for Case 2 (ideal solution density),

$$(1.7\text{-}6) \qquad \rho = \frac{1}{\sum_{k=1}^{nc} x_k v_k}, \quad and \quad \frac{\partial \rho}{\partial x_j} = -v_j \rho^2$$

where v_j = the molar volume of the jth component. For Case 1 the overall mass balance becomes

$$(1.7\text{-}7) \qquad \frac{dh}{dt} = \frac{1}{S\rho}(F_0 - F) = \frac{1}{S}(Q_0 - Q)$$

where Q = volummetric flow rate. For Case 2, we have

$$(1.7\text{-}8) \qquad \frac{dh}{dt} = \frac{1}{S}\left(\frac{F_0}{\rho_0} - \frac{F}{\rho}\right) = \frac{1}{S}(Q_0 - Q)$$

For Case 1 the only way in which the level can change is if there is an imbalance between molar flow rates in and out of the tank. For Case 2, even if the molar flow rates in and out are equal, the level can change if the composition of the feed to the tank changes. Let us suppose that the tank is running at steady-state conditions (call this State 1) and that the composition of the feed is changed but that the molar flow rate is not. After the composition transient dies out, the tank will come to a new steady state (call this State 2) but its molar hold will not have changed. It is easy to show that the tank level for State 2 will be related to that for State 1 by

$$(1.7\text{-}9) \qquad h_2 = \frac{\rho_1}{\rho_2} h_1$$

and that the steady-state error relative to State 1 is

$$(1.7\text{-}10) \qquad SSAR = \left|\frac{\rho_1}{\rho_2} - 1\right|$$

This suggests that a suitable index for choosing an acceptable liquid density model (call it I_D) is the ratio of maximum density one might expect to the minimum. In the absence of a sharper estimate, one could use the ratio of the largest component molar volume in the mixture to the smallest.

Let us examine how suitable I_D is as an index for the other measures of model fidelity. The linearized model equations for Case 1 are

$$(1.7\text{-}11a) \qquad \frac{d\Delta x_i}{dt} = (\Delta x_{0i} - \Delta x_i)/\tau, \quad i=1,...,nc$$

$$(1.7\text{-}11b) \qquad \frac{d\Delta h}{dt} = \frac{1}{S\rho}(\Delta F_0 - \Delta F)$$

$$where \quad \tau = \frac{Sh\rho}{F}$$

For Case 2 Eqn. 1.7-11a remains the same while Eqn. 1.7-11b becomes

$$(1.7\text{-}12) \qquad \frac{d\Delta h}{dt} = \frac{1}{S\rho}(\Delta F_0 - \Delta F) + \frac{F}{S}\sum_{j=1}^{nc} v_j(\Delta x_{0j} - \Delta x_j)$$

It is simple to show that the state-space matrices for the two cases, while not identical, have the same eigenvalues. If level is to be controlled by manipulating either the inlet or outlet flow rate, then the corresponding steady-state gain is the same for both cases. However, if outlet composition is to be manipulated by adjusting the inlet composition, then the row in the steady-state gain matrix changes, namely, that of the effect of inlet composition on level. All other steady-state gains in the gain matrix remain the same. In evaluating the effect of

inlet composition on level, we must keep in mind that individual components of the inlet composition vector cannot all be changed independently since the sum over all the changes must be zero.

Let us look at the situation for nc = 2. The transfer function relating level to changes in the feed of component for Case 2 is

$$(1.7\text{-}13) \qquad G(s) = \frac{\overline{\Delta h}}{\overline{\Delta x_{01}}} = \frac{h\rho v_2}{\tau s + 1}\left(\frac{v_1}{v_2} - 1\right)$$

where the overline indicates the Laplace transform. This transfer function for Case 1 is zero, so the extent to which Case 2 differs from Case 1 depends upon the extent to which the ratio of v_1 to v_2 differs from one, which is a form of the model fidelity index I_D. This index is applicable to the gain error as a function of frequency but the phase angle which is a function only of τ. However, if we define τ with respect to a reference component, in this case component 2, it also is a function of I_D as follows:

$$(1.7\text{-}14) \qquad \underline{/G(j\omega)} = -\tan^{-1}(\tau\omega)$$

$$\text{where} \quad \tau = \frac{Sh\rho_2}{F}\frac{1}{\left(\frac{v_1}{v_2} - 1\right)x_1 + 1}$$

At this point it should come as no surprise that the integral of the absolute error (IAE) also differs from zero as a function of I_D. This shows, that for this simple example at least, the same index can be used to characterize all of the measures of model fidelity. Further, this index is simple to evaluate *a priori* . Finally, almost all of the measures are directly

proportional to I_D. So, for example, if the dynamic modeling errors are not to exceed 10%, say, then I_D must not exceed 1.1.

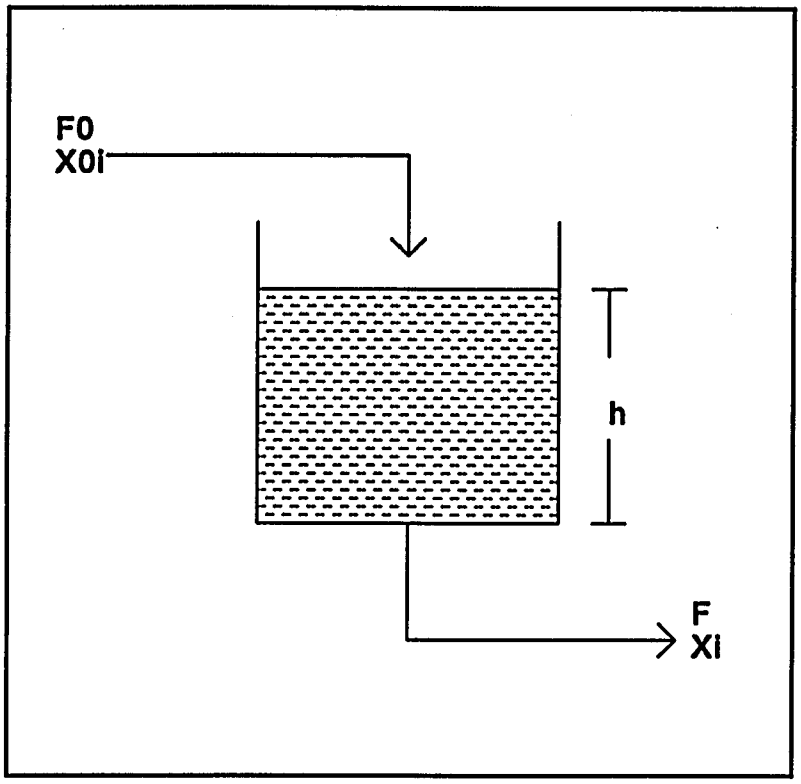

Figure 1-1. Mixing Tank

CHAPTER TWO. SINGLE-STAGE SYSTEMS

EFFECTS OF VAPOR-LIQUID EQUILIBRIUM MODELS ON FIDELITY

2.1 Introduction

It is well-known that a considerable fraction of the total computation time required for process simulation, both steady-state and dynamic, is required for the evaluation of thermo-physical properties and vapor-liquid equilibrium (VLE) relationships. For example, one of the major flash and distillation algorithms, the inside-out method (Boston 1974, 1978, 1980) was developed to minimize the need for these evaluations. In this chapter the choice of VLE models for the evaluation of K-values is examined with respect to its impact on the fidelity of single-stage systems, specifically, a flash drum.

In general, three types of VLE models are used for the evaluation of K-values:

1) Both phases assumed to be ideal.

The liquid is assumed to be an ideal solution and the vapor an ideal gas. K-values are calculated from Raoult's Law.

2) Vapor phase ideal, liquid phase non-ideal.

It is assumed that deviations from nonideality in the liquid phase can be represented by an activity coefficient model. In this work the Wilson Equation (Reid 1987) is used.

3) Both phases non-ideal.

For this situation an equation of state such as that of Redlich-Kwong (Reid 1987) is used to evaluate all deviations from ideality. For various reasons this case was not

included in the present study. First, most equilibrium staged systems are not operated at conditions where there are significant deviations from ideal behavior which cannot be adequately represented by an activity coefficient model. (One important exception involves the vapor phase association involving organic acids, for instance.) Second, for the systems studied in this work, the Redlich-Kwong-Soave (RKS) Equation gave such a poor representation of the VLE behavior that one would probably not choose to use it under any circumstances. Third, cubic equations such as the RKS have multiple roots. While there are well-developed procedures for determining which are the correct roots for the vapor and liquid phases (Gosset 1986; Gundersen 1982), these require additional computations over and above the calculation of the roots themselves.

In all early dynamic simulations only the ideal physical properties models were employed for the reasons discussed in the previous chapter. In recent years, more rigorous models have been used to improve simulation fidelity but at the cost of increased computation time. For example, in a flash simulation of the water-methanol-ethanol system, the real time factor (RTF) is 140 with a simple non-ideal VLE model (Wilson Equation) while it is 194 with an ideal VLE model on a DECstation 3100. (The difference is probably larger since version of the DYSIM simulator on which this was run has a fairly high fixed overhead.) One would also expect the difference to increase with number of components since the computational burden of evaluating the Wilson Equation increases approximately with the square of the number of components.

On the other hand, it should be clear that the more non-ideal the system is, the larger

the error will be from using an ideal VLE model. Thus it is important to know when the use of a non-ideal VLE model is justified. To determine what the trade-offs are, fifteen different systems were examined, ranging from nearly ideal to very non-ideal. The basic data characterizing these systems, namely, binary pair infinite dilution activity coefficients and azeotropic compositions where applicable, are given in Table 2.1 (See Section 2.3). The focus of this effort is to develop simple rule-of-thumb to determine when one should use the non-ideal VLE models instead of the ideal VLE model in flash drum simulations. Later on we will examine to what extent this rule-of-thumb also applies to multi-staged systems.

2.2 Literature Review

1) Dynamic Flash Drum Models

Given the fact that flash drums are a common and widely used item of chemical processing equipment, very little attention is given in the literature to their dynamic behavior. Their steady-state behavior is, of course, covered in detail in every text on equilibrium stage separation operations (Henley 1981 and King 1980, for example) as well as many other places. The modeling is straightforward. Most of the attention is given to (1) identifying the correct degrees of freedom and (2) to solving the resulting set of nonlinear algebraic equations (Boston 1978, for instance).

When it comes to dynamic modeling, Franks (1972) and Luyben (1990) have presented derivations of the basic equations but these have some shortcomings. In

particular, the DAE index problem that arises was not explicitly recognized. For Franks this is entirely understandable since the DAE index problem was just being explored by mathematicians at the time. This did lead, however, to a rather awkward handling of the situation.

Systematic treatment of the problem has been presented both by Ponton and Gawthorp (1991) and by Asbjørnsen (1987). Ponton and Gawthorp begin by formulating the model as two sets of equations, one for the vapor phase and the second for the liquid phase, connected by explicit mass and heat transfer fluxes. These equations are essentially those presented in Chapter One. They then combine these to produce an equilibrium stage model in which the vapor and liquid phases are combined. They discuss the index problems that can arise, in particular when implicit control of the liquid or vapor holdups is imposed on the model. Their derivation is slightly marred by the use of a dynamic "enthalpy" balance, a common occurrence in the chemical engineering literature as pointed out by Denn (1986).

2) Vapor-Liquid Equilibrium Models

In the simulation of equilibrium staged systems such as a flash drum, physical properties calculations are of primary concern, especially the selection of the appropriate vapor-liquid equilibrium (VLE) model. In dynamic simulation, which VLE model is selected depends on various factors, namely, that it be reliable, accurate, and not require excessive computational effort to evaluate. The status of VLE models at the time is extensively covered by Reid and Prausnitz (1987). More recently Mathias (1994) discussed a number of thermodynamic property model. He listed several equations of state and pointed out the

industrial perspective. These have been widely used for hydrocarbon systems. The well-known cubic equations of state, such as those of Redlich-Kwong-Soave and Peng-Robinson, were published in 1970's. More recently Martin(1979), Gosset(1986), and Stryjet(1986) have studied the mixing rules in order to improve VLE prediction. Gundersen(1982) discussed the implementation of cubic equations of state in flash calculation routines. Shah(1994) derived a quartic equation of state to increase the accuracy of prediction. Angel and coworkers(1986) provided the results of prediction of vapor liquid equilibria of different systems by seven equations of state. Most of them can predict the behavior of VLE properties with reasonable accuracy. So far those kinds of VLE models do a good job when the systems are close to the ideal solutions, e.g., hydrocarbon systems.

Another class of VLE models is based on activity coefficients. Activity coefficient correlations such as Van Lar, Margules, and Bonham, all prior to 1941, have had a long history of use in VLE calculations. Wooley(1989) and Bradani(1991) have evaluated the feasibility of evaluating activity coefficient model parameters from infinite dilution activity coefficient data. The Wilson correlation published in the 1960's marked a major advance in in VLE modeling. Holmes and Van Winkle(1970) compared and summarized four popular correlations with a series of useful data and concluded that the Wilson correlation is the best one among the four for doing ternary systems. Though many types of equations of state were published later and people pay more attention to them currently, for convenience and accuracy, the Wilson correlation still plays an important role in VLE calculations for non-ideal systems.

As already mentioned, in either dynamic or steady-state simulation, it is well-known that properties calculations consume a major part of the required CPU time. Usually, the more accurate the model, the more CPU time it uses. Leesley(1977) pointed out that the major cost in computer time for process simulation is incurred by the generation of K-values. Boston(1972) put forward the inside-out concept to avoid using a complex property model at all integration steps. Barrett(1979), Chimowitz (1983, 1984), Macchietto(1986) and Hillestad(1989) have presented so-called local thermodynamic approximations to save dynamic simulation CPU time. With this method, they can avoid using the original complicated VLE model at each dynamic step, using instead a simple approximation, either a linear or a simple curve, which must be updated based on a error estimate. For this purpose, a regression routine must be prepared to get a simplified thermodynamic models; an interface must be prepared to control the switch between property models; and error criteria must be prepared for that switch.

The principal disadvantage of applying local thermodynamic models is that additional information must be stored. For example, each component on each tray in a distillation column requires a distinct set of data that includes the parameter vector, the covariance matrix and the curvature matrix. Sorlie (1992) pointed out that as much as 80% of computer CPU time may be spent calculating properties. Substituting for rigorous thermodynamic property calculations with local approximations in dynamic flash algorithms gives roughly a 20% saving in computer CPU time. The local model saves computer time but it also introduces an additional source of error into the simulation. Still, it is a very attractive method in multicomponent and multistage process simulation with complicated

thermodynamic models.

3) The DAE Index Problem

As previously mentioned, dynamic models for equipment such as flash drums involve both algebraic and differential equations. In solving them simultaneously, one faces an index problem. Petzold(1982), Gallun(1982), Byrne(1988), Gani(1993), among others, have discussed this problem and methods for dealing with it. As a definition, the index is equal to the number of times one must differentiate the set of algebraic equations with respect to time in to obtain continuous differential equations for all unknown variables. Index zero problems are much easier to solve numerically than those with index one. Indices greater than one are very difficult to solve. Ponton(1991) and Gani(1993), Luyben(1992), and Berber(1993) analyzed situations where flash simulations incur an index of more than one and provided some algorithms to avoid a higher index. To add proper new equations is one method to deduce higher index. That the algebraic equations and the ordinary differential equations are solved separately during function evaluation, as procedures, is another possible method.

2.3 Procedure

In the previous chapter, it was possible to derive analytically relationships between various model fidelity errors and a model fidelity index. Further, the form of the model fidelity index resulted directly from the analysis. A similar approach to the flash drum is not possible. Instead, a more empirical approach must be taken. This is due in part to the

increased complexity of the model equations. That there is no explicit solution of the model equations even for the steady-state further complicates the analysis. Therefore, the various model fidelity errors have been evaluated by simulation and a model fidelity index chosen based on physical considerations.

The model fidelity evaluations were done for each of eleven binary systems and four ternary systems. These systems were chosen to represent a wide range of VLE behavior from nearly ideal to highly nonideal. Three of the binary systems and one ternary form azeotropes. The major indicator of nonideality that was used in the selection of this systems was the extent to which the infinite dilution activity coefficients differed from unity.

The VLE data for these systems, both Antoine Equation coefficients for vapor pressure and the interaction coefficients for the Wilson Equation, were taken from the compendium assembled by Holmes and Van Winkle (1970). The systems chosen are given in Table 2.1.

Table 2.1 VLE Characterization of Systems Studied

Binary Systems (1/2)	Infinite Dilution Activity Coefficients (1 in 2)	(2 in 1)	Relative Volatilities	Index A
Non-azeotropic:				
Methanol/Ethanol	0.99	0.97	1.62	0.588
Benzene/n-Heptane	1.36	1.76	1.65	0.948
Acetone/Ethanol	1.89	1.95	1.86	0.999
Acetone/Water	14.3	5.00	3.73	2.664
Methanol/Water	2.90	1.70	3.50	1.656
Acetone/Chloroform	0.48	0.52	1.38	0.201
Acetone/Methanol	1.85	1.96	1.36	0.851
Acetone/Benzene	1.66	1.48	2.20	1.024
Azeotropic:				
Methanol/Chloroform	7.90	2.62	1.34	1.875
Ethanol/Water	7.72	3.08	2.19	2.041
Ethanol/Benzene	7.60	4.40	1.25	1.627
Ethanol/n-Heptane	24.3	16.3	2.22	2.450
Additional Systems for Ternary Studies:				
Acetone/Carbon Tetrachloride	2.60	2.21	1.94	1.198
Benzene/Carbon Tetrachloride	1.10	1.14	1.13	0.482
Ternary Systems				
Methanol/Ethanol/Water				1.257
Acetone/Methanol/Chloroform				0.685
Ethanol/Benzene/n-Heptane				1.558
Acetone/Benzene/Carbon Tetrachloride				0.839

Azeotropic Compositions:

Azeotrope 1/2/3	Composition (Mol fractions)	Temperature (deg C)	Pressure (Atm)
Methanol/Chloroform	0.6500/0.3500	53.50	1.0
Ethanol/Water	0.8943/0.1067	78.15	1.0
Ethanol/Benzene	0.4480/0.5520	68.24	1.0
Ethanol/n-Heptane	0.3320/0.6680	58.68	1.0
Acetone/Methanol/ Chloroform	0.226/0.397/0.377	57.50	1.0

As mentioned earlier, the only VLE models to be considered are those for ideal systems and those described by the Wilson Equation. Equations of state such as the Redlich-Kwong-Soave were ruled out as being inappropriate for the systems being studied. This is substantiated in Figs. 2-2 through 2-4 where the predictions of activity coefficients for the two models are compared with actual data (Perry 1984). The failure of the RKS Equation for the ethanol water system is dramatic. Even for the nearly ideal system of n-hexane and 1-hexene, the difference is noticeable at low concentrations.

Based on initial simulations, particularly of the steady-state, a procedure for evaluating model fidelity errors was developed. It was found that errors for each system varied with its feed composition. Further, the composition at which the maximum error occurred differed from system to system. Thus, a scan had to be performed for each system in order to determine the maximum error that could occur for that system. Frequency domain errors were then evaluated for each system using the feed composition that gave the maximum steady-state errors.

The choice of the index was made by trying several forms that seemed appropriate based on physical reasoning. The one that gave the best correlations of the various model fidelity was determined by visual inspection of the various model fidelity error graphs. This is discussed in more detail in Section 2.5.

2.4 Flash Process Simulation Modeling

In this section the model equations for a flash drum operating with a single liquid phase are developed from the basic equations derived in Chapter 1. The flash drum is shown diagramatically in Fig. 2-1. A multicomponent feed is flashed. If the drum has a cross-section area S and a tangent-to-tangent height l_D, then the component mass balance and energy balance equations are, respectively,

$$\frac{d[Sl\rho_L x_i]}{dt} = F_{L0}x_{0i} - Lx_i + \eta_i, \quad i=1,...,nc \tag{2.4-1}$$

$$\frac{d[Sl\rho_L U_L]}{dt} = F_{L0}H_{L0} - LH_L + \sum_{j=1}^{nc}\eta_j h_j^* + q_{VL} + q_{in} \tag{2.4-2}$$

where l the liquid level in the drum, η_i is the rate of mass transfer of component i from vapor phase to the liquid phase, q_{VL} is the rate of heat transfer from the vapor phase to the liquid phase, and q_{in} is the rate of heat input to the liquid phase from external sources (such as a heating coil), and h^*_i is the partial molal enthalpy of the ith component crossing the vapor-liquid interface.

A similar set of equations can be written for the vapor phase, namely,

$$\frac{d[S(l_D-l)\rho_V y_i]}{dt} = F_{V0}y_{0i} - Vy_i - \eta_i, \quad i=1,...,nc \tag{2.4-3}$$

$$\frac{d[S(l_D-l)\rho_V U_V]}{dt} = F_{V0}H_{V0} - VH_V - \sum_{j=1}^{nc}\eta_j h_j^* + q_{in} \tag{2.4-4}$$

If it is assumed that the rates of heat and mass transfer between the vapor and liquid phases

are very high, this is tantamount to assuming that the two phases are in thermodynamic equilibrium. This amounts to assuming that $y_i = K_i x_i$ and $T_V = T_L = T$.

Adding Eqns. 2.4-1 and 2.4-3 gives a composite component material balance for both phases, namely,

$$\frac{d(S[l\rho_L + (l_D - l)\rho_V K_i]x_i)}{dt} = F_0 z_i - (VK_i + L)x_i \tag{2.4-5}$$

while adding Eqns. 2.4-2 and 2.4-4 gives a composite energy balance, namely,

$$\frac{d(S[l\rho_L U_L + (l_D - l)\rho_V U_V])}{dt} = F_0 H_0 - VH_V - LH_L + q_{in} \tag{2.4-6}$$

Finally, an equilibrium constraint must be imposed. In this case it is that the liquid phase be at its bubble point, or,

$$\sum_{i=1}^{nc} K_i x_i - 1 = 0 \tag{2.4-7}$$

Eqn. 2.4-7 is algebraic and the set of model equations 2.4-5 through 2.4.7 are a set of DAE's of Index One. Differentiating Eqn. 2.4-7 with respect to time gives

$$\sum_{j=1}^{nc} (K_j + x_j \frac{\partial K_j}{\partial x_j}) \frac{dx_j}{dt} + \sum_{j=1}^{nc} x_j \frac{\partial K_j}{\partial T} \frac{dT}{dt} + \sum_{j=1}^{nc} x_j \frac{\partial K_j}{\partial P} \frac{dP}{dt} = 0 \tag{2.4-8}$$

The next step is to reduce Eqns. 2.4-5, 2.4-6, and 2.4-8 to first-order form in the state

variables. This is not a straightforward exercise given the complexity of the holdup Jacobian. This hurdle is generally surmounted by assuming that the capacitance of the vapor phase for both mass and energy is negligibly small compared to that of the liquid. The following analysis will demonstrate under what circumstances this assumption is warranted. First, consider the assumption with respect to mass. To so this, consider a flash drum which is operated isothermally and at constant pressure. Then Eqn. 2.4-5 becomes

$$(2.4\text{-}9) \qquad \varphi_i \frac{dx_i}{dt} = F_0 z_i - (VK_i + L)x_i$$

$$where \quad \varphi_i = S[l\rho_L + (l_D - l)\rho_V]$$

We can define a time constant $\tau_i = \dfrac{S[l\rho_L + (l_D - l)\rho_V K_i]}{L + VK_i}$ which will be different for each

component. Note that if K_i is small, i.e., $K_i << 1$, $\tau_i \rightarrow Sl\rho_L/L$. This is just the liquid phase residence time, a result to be expected for components that are essentially non-volatile. Similarly, for $K_i >> 1$ (component essentially non-condensable), $\tau_i \rightarrow S(l_D - l)\rho V/V$. As to be expected, th is just the vapor phase residence time. Now, flash drums are generally operated half full of liquid so that $l = l_D - l$ with a nominal liquid phase residence time on the order of five minutes. Unless the pressure is extremely high, the vapor phase residence time will be one to two orders of magnitude smaller. Only if K_i is very large, say 100 or greater, will the vapor phase capacitance approach that of the liquid. So, unless non-condensable gases are present in the feed, the vapor phase capacitance for a flash drum can be neglected with respect to mass holdup up. (This matter is dealt with in more detail in the next chapter.)

To determine whether or not the vapor phase can be neglected with respect to the energy balance, consider Eqn. 2.4-6. If we neglect the effects of composition and pressure on the internal energy U of each phase, then the ratio of the vapor phase capacitance to that of the liquid for a drum half full is merely $R = \frac{\rho_L c_{pL}}{\rho_V c_{pV}}$. Some typical values are as follows:

	ρ_L	c_{pL}	c_{pV}	R	
Component	(kmol/m^3)	(kcal/kmol-K)		at 1atm	at 10 atm
Water	55.4	17.8	8.1	0.0002	0.0029
Hexane	7.5	50.7	24.6	0.0023	0.0225
Ethanol	17.1	37.7	17.8	0.0010	0.0096

For the compounds examined, up to 10 atm, the vapor phase capacitance is no more than about 2% of that for the liquid.

We can conclude that unless the pressure is very high or the drum is operated with a large vapor volume compared to the liquid volume, that the vapor phase capacitance can be neglected with respect to the energy balance. The same is true with respect to the mass balance expect for components that are essentially non-condensable.

Neglecting the vapor phase capacitance allows simplification of Eqns. 2.4-5 and 2.4-6 to:

$$(2.4\text{-}10) \qquad \frac{d[Sl\rho_L x_i]}{dt} = F_0 z_i - (VK_i + L)x_i, \quad and$$

$$(2.4\text{-}11) \qquad \frac{d[Sl\rho_L U_L]}{dt} = F_0 H_0 - VH_V - LH_L + q_{in}$$

Some further simplifications can be introduced by noting that for a liquid, $U_L \approx H_L$ and that, based on the analysis of the previous chapter, the variation of density can be neglected under most circumstances. This second simplification also allows us to concentrate on the model fidelity effects of various K-value models without confusing these with other physical properties effects.

Before proceeding to a final simplification of the flash drum model, we need to specify the operating mode for the drum. That which is most natural is open-loop, namely, that the flow-rates leaving the drum are specified as functions of time, say, by the action of suitable control valves. This is the mode that would be employed if one were analyzing or designing the control system. However, unless the flow rates are exactly balanced, the drum pressure and liquid level will vary. As with the physical properties, these variations may confuse the interpretation of results. Therefore, it was decided to use an implicit control mode in which both perfect pressure and level control are assumed. This mode is quite often employed in dynamic simulation of entire processes, being applied to minor items of equipment whose control is well-understood and generally fast compared to the more important items of equipment.

Incorporating these additional simplifications to Eqns. 2.4-7 and 2.4-8 gives

$$(2.4\text{-}12) \qquad Sl\rho_L \frac{dx_i}{dt} = F_0 z_i - (VK_i + L)x_i, \quad and$$

$$(2.4\text{-}13) \qquad Sl\rho c_{pL} \frac{dT}{dt} = F_0(H_0 - H_{0L}) - V\Lambda - q_{in}$$

$$where \quad c_{pL} = \sum_{j=1}^{nc} x_j c_{pLj}$$

$$H_{0L} = \sum_{j=1}^{nc} z_j h_{Lj}(T) \quad and$$

$$\Lambda = \sum_{j=1}^{nc} K_j x_j (h_{Vj}(T) - h_{Lj}(T))$$

An overall mass balance is given by summing with respect to i over Eqn. 2.4-12

$$(2.4\text{-}14) \qquad V + L - F_0 = 0$$

Applying the dynamic bubble point constraint of Eqn. 2.4-8 to Eqns. 2.4-12 and 2.4-13 gives

$$(2.4\text{-}15) \qquad aV + bL = cF_0$$

$$where\ a = \sum_{j=1}^{nc} [(K_j + x_j \frac{\partial K_j}{\partial x_j}) K_j x_j + \frac{\Lambda}{c_{pL}} x_j \frac{\partial K_j}{\partial T}],$$

$$b = 1 + \sum_{j=1}^{nc} x_j^2 \frac{\partial K_j}{\partial x_j} \quad and$$

$$c = \sum_{j=1}^{nc} [(K_j + x_j \frac{\partial K_j}{\partial x_j}) z_j + \frac{(H_0 - H_{0i})}{c_{pL}} x_j \frac{\partial K_j}{\partial T}]$$

Eqns. 2.4-14 and 2.4-15 must be solved simultaneously for V and L. This completes the development of the basic model equations for the flash drum.

As mentioned previously, two VLE models were chosen for this study. Actually, a third, pseudo-ideal, was examined briefly as an example of local thermodynamic models.

Let us consider the characteristics of each model.

1) Ideal.

The ideal K-value model is based on the assumption of ideal solution behavior in both the vapor and liquid phases. Knows as Raoult's Law, it is merely the component vapor pressure divided by the flash system operating pressure. This model is the simplest K-value model, being a function of only the system temperature and pressure. For that reason it is widely used for preliminary design. Functionally it is given by:

$$(2.4\text{-}16) \qquad K_i = \frac{P_i^{\circ}(T)}{P}$$

2. Pseudo-Ideal

This is a local thermodynamic model which uses a constant value of an activity coefficient to adjust an ideal K-value to the correct value at specific operating point. This eliminates the steady-state error at that point but otherwise does little to improve model fidelity. Functionally, it is given by

$$(2.4\text{-}17) \qquad K_i = \frac{\gamma_i^s P_i^{\circ}(T)}{P}$$

where γ^s_i is the activity coefficient of the ith component at the specific operating point. Obviously, to use this model, one must have the means for evaluating γ^s_i. The limitations of this model are illustrated in Fig. 2-5 which shows the step response of a flash drum to a step change in feed flow rate. γ^s_i was evaluated at the intial steady state using the results from the Wilson model. There is an significant error in flash temperature at the intial steady state

between the ideal model and the Wilson (approximately 2 K) but none between the pseudo-ideal and the Wilson. At the new steady state, there is a significant difference, one which is larger than that between the ideal and Wilson. For this and similar reasons, further evaluation of the pseudo-ideal K-value model was abandoned.

3. Non-ideal (Wilson)

A non-ideal K-value is calculated from:

$$K_i = \frac{\gamma_i(X,T)P_i^{\circ}(T)}{P} \qquad (2.4\text{-}18)$$

γ_i is the activity coefficient of the ith component and is a function of both composition and temperature. For the well-known Wilson Equation this relationship is given by:

$$\ln\gamma_i = 1 - \ln[\Sigma_{j=1}^{n} X_j\Lambda_{ij}] - \Sigma_{k=1}^{n}\frac{X_k\Lambda_{ki}}{\Sigma_{j=1}^{n} X_j\Lambda_{kj}} \qquad (2.4\text{-}19)$$

$$\textit{where} \quad \Lambda_{ij} = \frac{v_j^L}{v_i^L}\exp[-\frac{(\lambda_{ij}-\lambda_{ii})}{RT}]$$

2.5 Fidelity Results for Vapor-Liquid Equilibrium Models

In this section the various model fidelity measures are evaluated by comparing the performance of the flash drum for both the Ideal K-value and the Wilson K-value VLE models. To start, consider two systems. The first is acetone and water, a system that is highly non-ideal (as indicated by the infinite dilution activity coefficients listed in Table 2.1) but non-azeotropic. The second is ethanol and benzene, somewhat less non-ideal but a

system that is azeotropic. It is instructive to look at the behavior of these two systems in both the frequency and time domains. The response of the flash temperature to a 10% increase in feed flow rate is shown in Fig. 2-5 for the acetone/water system. The temperature decreases since the heat input remains constant in spite of the increase in throughput. We see that (1) there is a significant difference of about 2 K between the initial steady-state temperatures predicted by the Ideal and Wilson VLE models and (2) there is also a significant difference in the static gains for the two models. The result for the Ideal K-value model is slightly larger (0.15 K) than that for the Wilson model.

In the frequency domain, Bode plots are shown for the response of the outlet (flash) temperature to the inlet (feed) temperature. That for acetone/water is shown in Fig. 2-6 while that for ethanol/benzene is shown in Fig. 2-7. The difference for between the phase and gain curves using the Ideal model and the Wilson model are significant for the acetone water system, about 5 dg (decilogs) for the gain and 10 degrees for the phase angle. The differences are much more pronounced for the ethanol/benzene system. The static (zero frequency) gain is about 8 dg and becomes progressively larger as the frequency increases. The maximum phase angle error exceeds 35 degrees, which is quite large considering that the phase angle can only vary between zero and 90 degrees. Very large fidelity errors appear to be characteristic of azeotropic systems.

1. Fidelity Index Development

It was not possible to derive a fidelity index for the flash drum directly from the

model equations. Instead, one had to be determined empirically. To do so requires considering the factors that contribute to non-ideality. Referring to Eqn. 2.4-18, we can see that the main elements which effect the components' K-values are the activity coefficients for the system and their vapor pressures. The activity coefficient determines the degree of the component's non-ideality in that system. But the activity coefficient is a function of composition and question arises as to what composition should be used for its evaluation. Since, for most systems, the activity coefficient is a maximum at infinite dilution, it was decided to use the infinite activity coefficients as one component of our model fidelity index. If an activity coefficient correlation, such as the Wilson Eqn., is available, the infinite dilution activity coefficients can be easily and directly calculated. For instance, for the Wilson Eqn., the expression for this coefficient is

$$(2.5-1) \qquad \gamma^0_i = EXP(1-\Lambda_{ji}-\ln[\Lambda_{ij}])$$

Alternatively, infinite dilution activity coefficients are relatively easy to measure. If necessary, these can be used to estimate the parameters in activity coefficient models with considerable utility and success (Wooley 1989).

So, the infinite dilution activity coefficient is a simple and useful measure of a system's non-ideality. When the system is ideal, γ^0_i is one. The further from one γ^0_i is, the more non-ideal the system. Therefore, the deviations of flash results between the Ideal and Wilson VLE models should be a function of the infinite dilution activity coefficients and their ratio.

It was also found that the component's vapor pressures are another element factor that must be considered. Again, to keep things simple, we chose to use the ideal relative volatility for each pair in a multicomponent system. So, the various indices that were tested are functions of both the infinite dilution activity coefficients (at 323^0 K) and the relative volatilities from Ideal K-value model. Various combinations of these parameters were tested to see which gave the best correlation of the various model fidelity measures. First, an index Aij was developed for binary systems of components i and j. The one that was found to work best is

$$(2.5-2) \qquad Index\, A_{ij} = \ln[\frac{\gamma_{max}}{\gamma_{min}}(\gamma_i + \gamma_j)\alpha_{ij}]^{1/2}$$

Here, γ_{max} is the larger of the two activity coefficients and γ_{min} is the smaller. Note that the minimum value this index can have is 0.35 (system ideal and a relative volatility of unity).

An index for a ternary mixture was then developed based on the binary pair indices for the three binary pairs in the mixture. Again, after some experimentation, the following was found to work best.

$$(2.5-3) \qquad Index A_{1,2,3} = (A_{1,2}A_{1,3}A_{2,3})^{1/3}$$

2. Model fidelity correlation

In order to get a rule of thumb that shows the differences between Ideal and Wilson flash results for different degrees of system non-ideality, eleven binary systems and four

ternary systems were evaluated. The infinite dilution activity coefficients in these systems range from 0.5 to 24 (See Table 2-1).

A flash drum was designed to handle a feed flow rate of 14,000 kg/hr with approximately a third to half of this being flashed to vapor. The drum was designed to have a liquid residence time of 10 min. The diameter was calculated so that the vapor velocity was 80% of flooding (Wankat 1988, Henley and Seader 1981). The details of the design and the steady-state performance for one of the systems studied are given in Appendix A.

There are a wide range of conditions for which the fidelity measures can be evaluated. These include feed composition and temperature, operating pressure, and heat input. Time constraints precluded searching the entire operating space. Therefore the search was standardized to some extent. The flash pressure was always one atm and the feed temperature 300K. The heat input was adjusted so that approximately a third to a half the feed was flashed to vapor.

The steady state accuracy was then determined for two variables of interest, namely, the vapor flow rate and the flash temperature. What were searched for are the maximum deviations for each variable as a function of feed composition. The following feed compositions were evaluated for each binary system: 0.1, 0.3, 0.5, 0.7, and 0.9. These results are shown in Figs. 2-8 (Temperature) and 2-9 (Vapor Flow Rate). Both errors appear to correlate reasonably well as functions of the index A.

In the frequency domain, the following was done. The relative errors in steady state gain and phase angle were determined using the feed composition that gave the maximum steady-state errors in temperature and vapor flow rate. The error in phase angle was determined at the frequency at which the phase using the Wilson model is -45 degrees. This was not necessarily the maximum phase angle error (refer to Fig. 2-7) but a standardized way of determining the phase angle error. Typical steady-state gain errors are shown in Figs. 2-10 through 2-12 which are for responses of flow rate to feed rate, the flash temperature to feed temperature, and the vapor flow rate to feed composition respectively. As can be seen, the errors for most of the systems fall on or near the straight lines. The agreement is reasonable for values of the index less than 1.5; the scatter becomes greater at higher values. Most of the points that show the most pronounced deviations are for systems which form azeotropes.

Phase angle errors are shown for two responses, liquid composition to feed composition in Fig. 2-13 and flash temperature to feed temperature in Fig. 2-14. These are the least convincing of the various model fidelity correlations. However, many of the points lie between the two lines drawn on each plot. These are the non-azeotropic systems. Those points which show major deviations are all for mixtures involving azetropes. As is the case for steady-state gain, the phase angle results are reasonably well-behaved for index values less than 1.5.

The important question is whether or not these results can be used to guide the choice of VLE model for dynamic simulation. From the standpoint of credibility, the steady-state errors are the most important. If our criterion is a steady-state temperature error of less than,

say, 5 K, then if the index for the mixture exceeds 1.0, the Wilson model (or whatever the appropriate activity coefficient model is) should be used. If our criterion is a relative error in vapor flow rate of less than, say, 5%, the critical value of the index is about 1.3. If our criterion is a maximum relative error in steady-state gain of less than 20%, then, for the three gains shown in Figs. 2-10 through 2-12, the critical value of the index is about 1.0. For a phase angle error criterion of 10 degrees, the critical value of the index is about 1.5. Another consideration is the fact that the scatter in many of these error correlations becomes significant for values of the index greater than 1.5. It seems clear therefore that no matter what the values of the various error criteria are that one is willing to accept, a non-ideal VLE model should be used whenever the index exceeds 1.5.

2.6 Conclusions

There are a number of conclusions that can be drawn from the work reported in this chapter.

(1) If the flash feed contains no components with extremely high relative volatilities, the vapor phase holdup can be neglected with no steady-state and negligible dynamic error.

(2) It is possible to develop an index that can be evaluated *a priori* which provides a useful guide to the choice of VLE model to use in flash calculations. One such index is given by Eqn. 2.5-2 for binary systems and 2.5-3 for ternary mixtures. (The question arises as to what is an appropriate index for multicomponent mixtures with more than three components. The recommendation, untested at this point, is to use the ternary index

evaluated for the three most significant components present in the feed.)

(3) For reasonable values of the various error criteria, both steady-state and dynamic, the critical value of the index is 1.0 for deciding whether or not to use the Wilson or other non-ideal VLE model. Under no circumstances should the Ideal VLE model be used for an index value greater than 1.5. If the system contains azeotropes, then a non-ideal VLE model should be used.

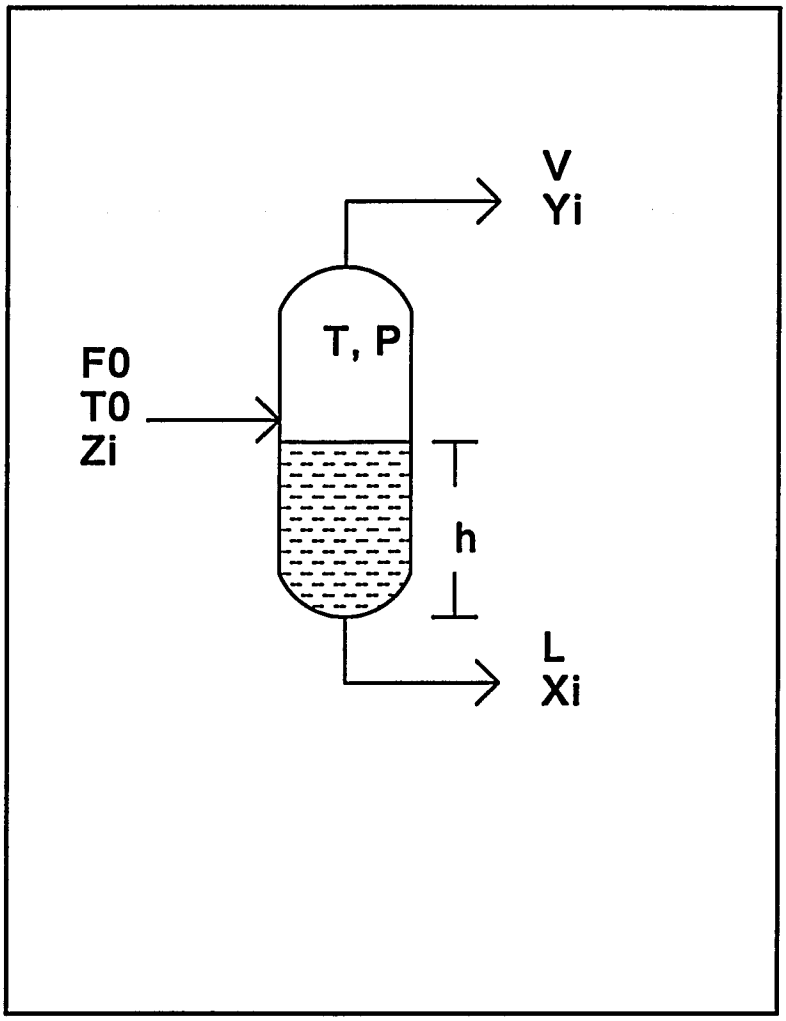

Figure 2-1. Flash Drum

Figure 2-2. Activity Coefficient Models

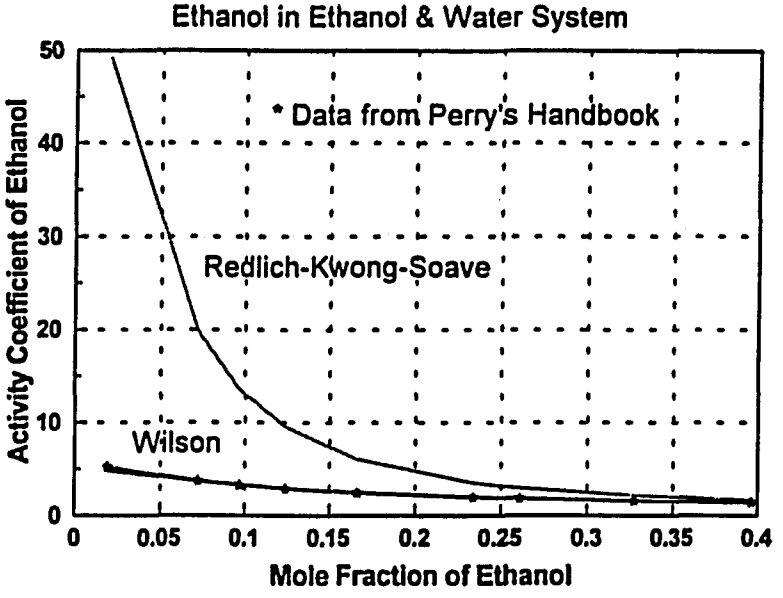

Figure 2-3. Activity Coefficient Models

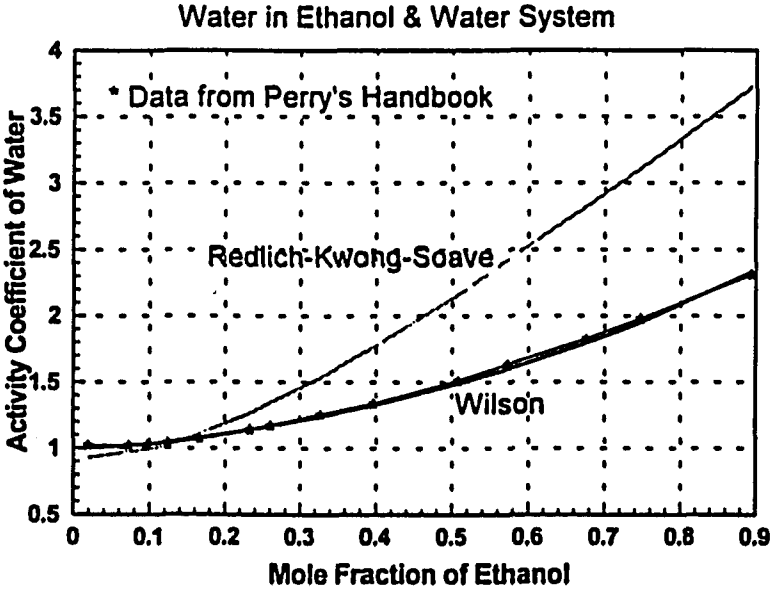

Figure 2-4. Activity Coefficient Models

n-Hexane in n-Hexane & Hexene-1 System

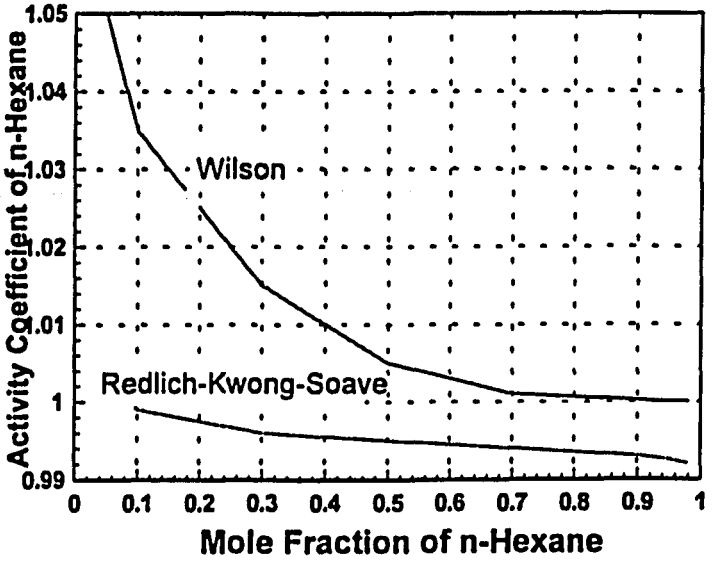

Figure 2-5. Response of Tout to a 10% Step Increase in Fin

Acetone and Water System

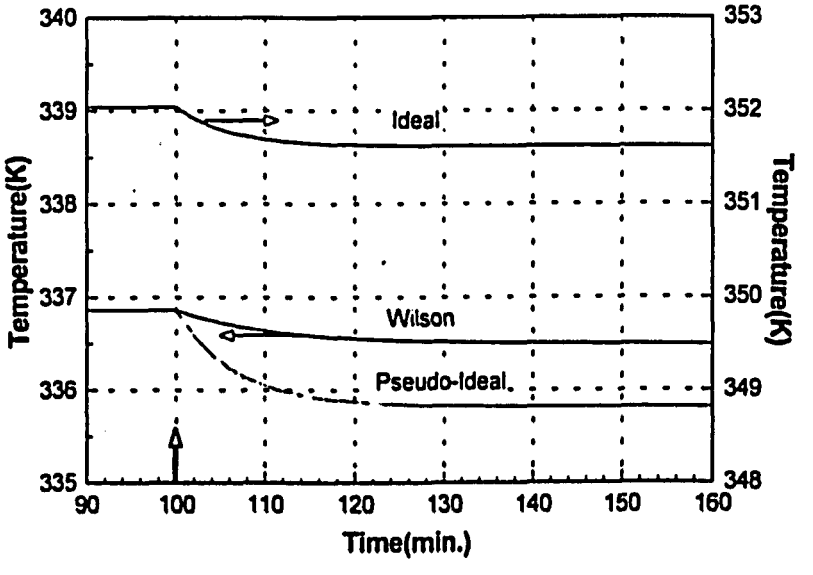

Figure 2-6. Frequency Response of Tout/Tin

Acetone and Water System(feed a/w=5/5)

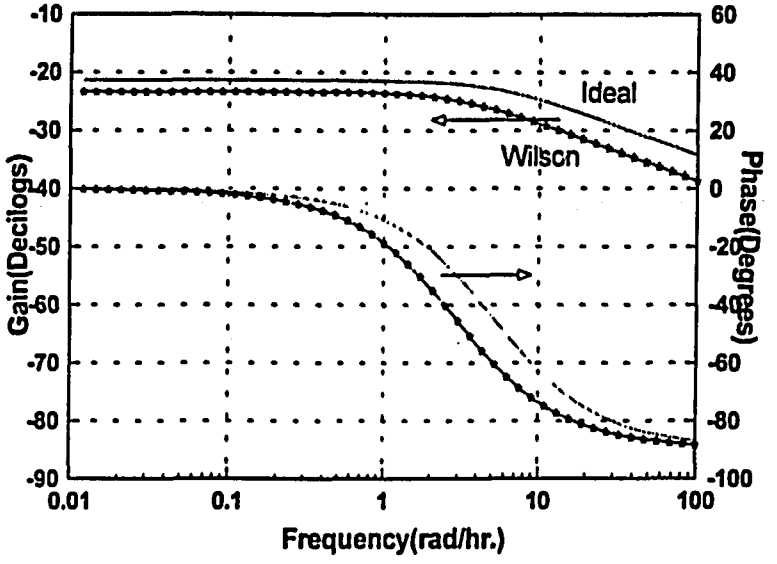

Figure 2-7. Frequency Response of Tout/Tin

Ethanol and Benzene System(feed e/b=1/9)

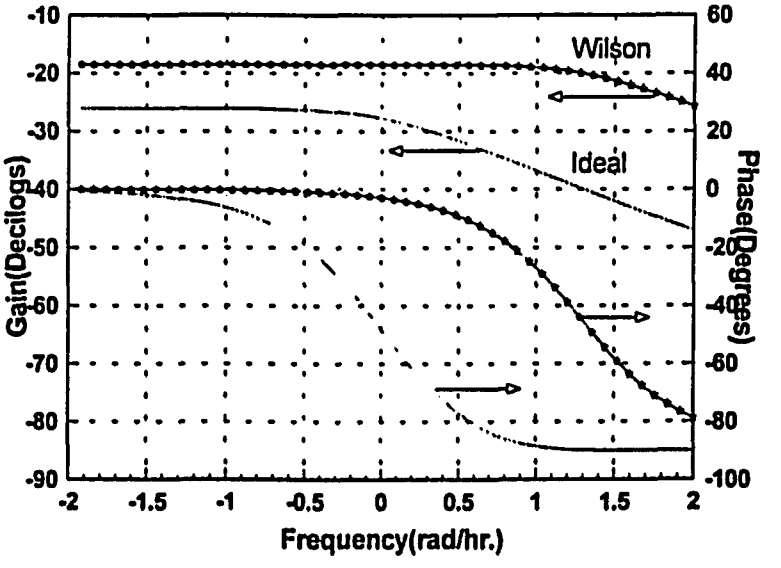

Figure 2-8. Steady-State Temperature Errors

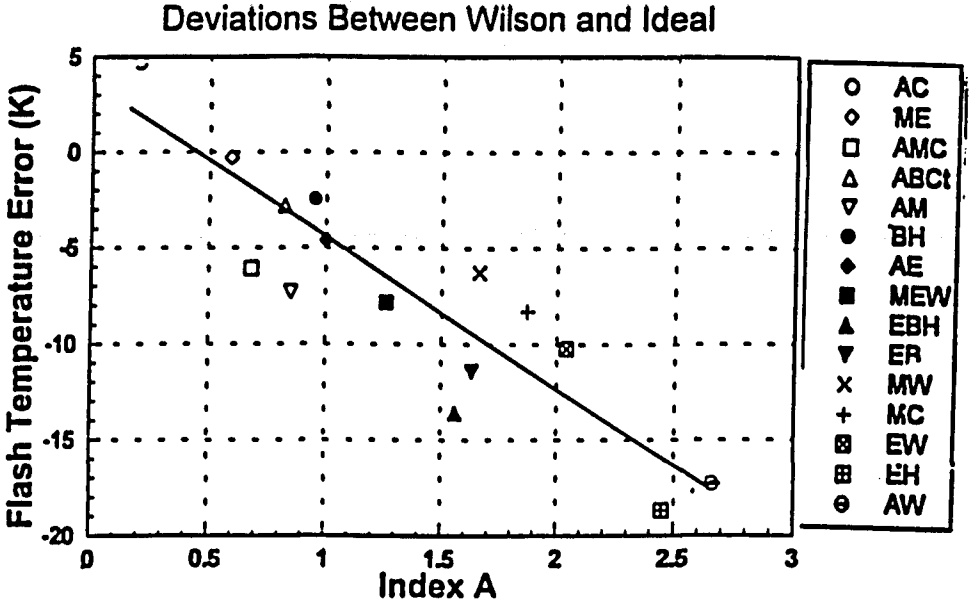

Figure 2-9. Steady-State Vapor Flow Rate Relative Errors

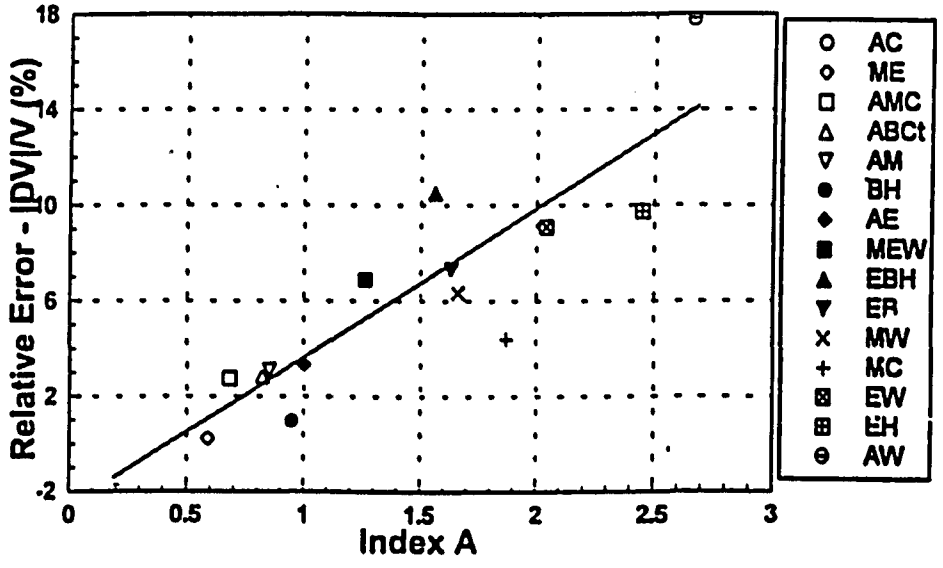

Figure 2-10. Steady-State Gain Error of Vout/Fin

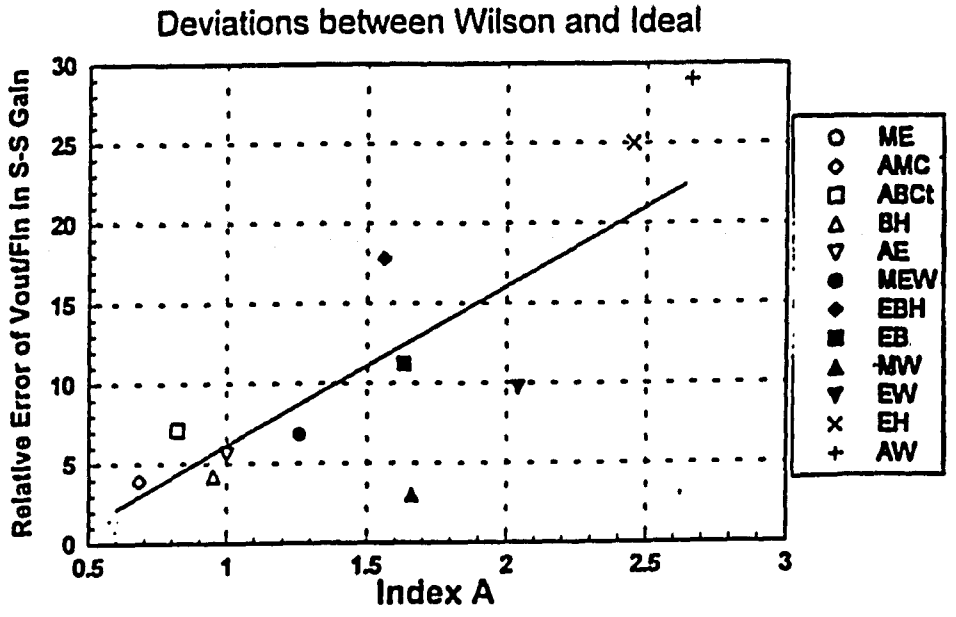

Figure 2-11. Steady-State Gain Error of Tout/Tin

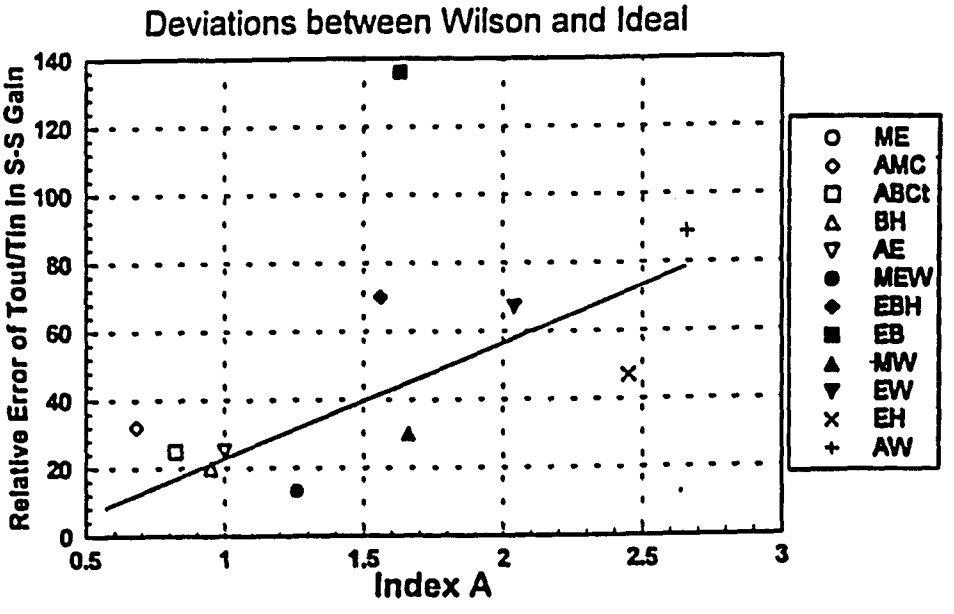

Figure 2-12. Steady-State Gain Error of Vout/X1in

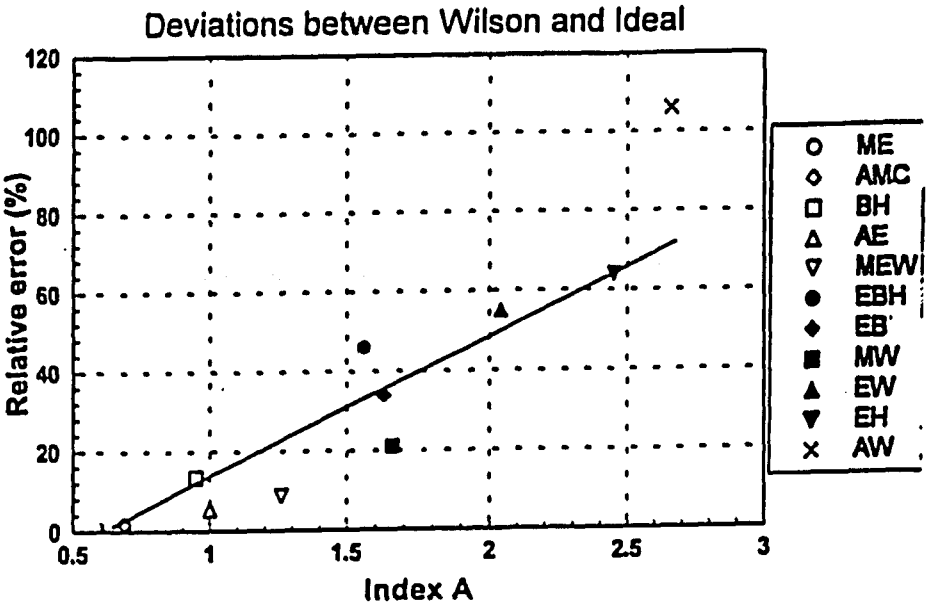

Figure 2-13. Phase Angle Error of X1out/X1in

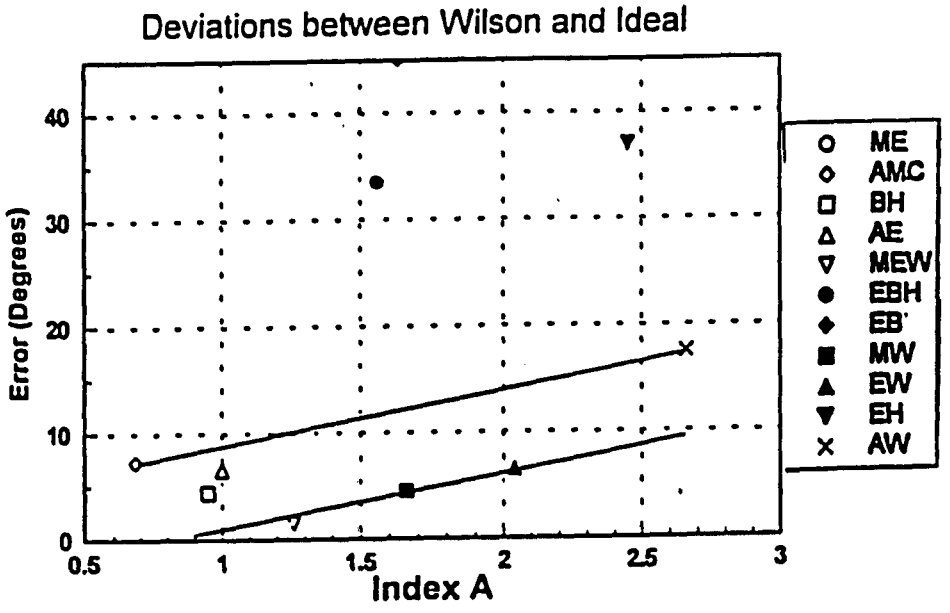

Figure 2-14. Phase Angle Error of Tout/Tin

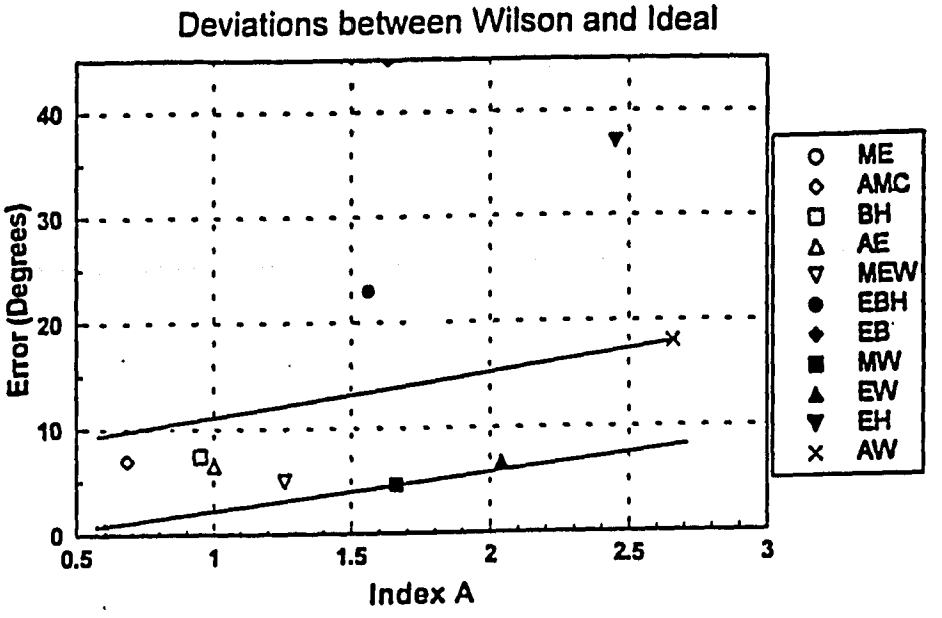

CHAPTER THREE. MULTISTAGE SYSTEMS.
EFFECT OF MODEL STRUCTURE ON FIDELITY

3.1 Introduction

In this chapter we turn our attention to multistage systems with the intent of examine the choices of model structure on fidelity. The question arises as to how accurately the dynamics of gas absorbers and distillation columns must be modeled in order to give an acceptable representation of the overall column dynamic performance. Specifically, to what extent must the dynamics of the individual stage be modeled with respect to overall performance?

Staged separation devices, especially distillation columns and gas absorbers, are widely used in the chemical and petro-chemical industries. Distillation columns constitute a significant fraction of the capital investment in chemical plants and refineries around the world. The operating costs of distillation columns are often a major part of the total operating costs of many processes. And it is well known that better control can be a major contributor to improved energy utilization. This is the rationale for examining the dynamic modeling of staged systems in detail.

A number of problems arise in the modeling and simulation of staged separation operations:

1) There are many choices to be made in modeling, both structural details and the

physical properties characterization. The standard model found in much of the literature (Franks 1972, Luyben 1990, and Grassi 1992, to cite a few) is based on the assumptions that the each tray can be modeled as a single well-mixed stage, that the dynamic response of the liquid and vapor flow rates to changes in reflux rate and reboiler heat input are very fast compared to the composition and temperature dynamics, that the liquid holdup dynamics in the downcomers can be either neglected entirely or lumped with the active tray holdup, and that the tray efficiency is 100%. Further, all but the most recent models presume perfect pressure control.

2) There are large number of differential and algebraic equations (DAEs), which results in an index problem.

3) The ordinary differential equations (ODEs) are stiff in most staged systems.

4) The condition number (sensitivity to modeling errors) of staged separation systems is usually very large (10^5 or more).

In this chapter we look primarily at effects of structural modeling in simple gas absorbers; in the next we test these results and those of the previous chapter on distillation models.

Our reference model is a dynamic version of that originally developed by Kremser (1930) for the steady-state design of gas absorbers over sixty years ago. In spite of its simplicity, it is still very useful for the design and analysis of many gas absorbers and liquid-liquid extractors. It is also very useful for this phase of our investigation in that it allows us to isolate the effects of structure without having to simultaneously consider energy balance and VLE effects.

3.2 Literature Review

There is a substantial literature concerning our topic, especially concerning staged separation process modeling, VLE property modeling, and simulation algorithms. The VLE models have been discussed in the Chapter Two.

The structural modeling of distillation and related staged separation equipment has received extensive coverage in the literature. Most of the work done prior to 1975 was incorporated in the rather substantial distillation dynamic modeling effort undertaken by Royal Dutch Shell (Rademaker 1975). Work on distillation modeling at DuPont began in the late 1950's and has proceeded ever since. The early models are given in the book by Franks (1972); more recent work is discussed by Tyreus (1992). What can be considered the standard model is presented in various texts, that of Luyben (1990) being a typical example. Only recently have models been developed which attempt to model the dynamics realistically. Lundstrom et al. (1993) presented a distillation column model based on a foam model of the vapor-liquid contact on the tray and included the effects of tray hydraulics and pressure dynamics. A similar model, but one which is based on a mass transfer rate model rather than a tray efficiency has been developed by Kooijman (1995). Dynamic tray efficiencies are back-calculated and shown to vary substantially during transients.

A second topic that has received considerable attention is the integration of the model equations. Many integration methods and strategies have been developed for ordinary differential and algebraic equations. Cameron (1988) suggested the Adaptive Runge-Kutta

algorithm. Ranzi(1988) pointed out in his paper: "There is a general agreement in recent literature that implicit integrators, especially involving backward differentiation formulas, are highly effective and reliable for the dynamic simulation of distillation columns." Grassi (1992) states that Euler integration works well for solving the distillation models that were developed in his chapter. These different opinions tell us that the selection of integration algorithms is not completely understood. Also Ranzi(1988) pointed out in the same paper mentioned above: "On the contrary, there is little knowledge about the effects of the simplifying assumption made in attempting to solve the whole set DAEs."

As mentioned above, staged separation modeling concerns two main parts: column or tray structure modeling and property modeling, especially, the vapor liquid equilibrium modeling. The development of approximate or simplified models for complex, high-order systems such as distillation column is a continuing effort. From MaCabe and Thiele (1925) to Underwood and etc.(1940's), staged process models were simple and done without computers. These models are still used for initial column design. Dynamic simulation of multi-stage, multi-component separation operations was first achieved in 1960's. The early dynamic models were transplanted from steady-state models. The holdup Jacobian of the models was simplified to a diagonal matrix and generally the dynamic terms in the energy balance were eliminated. See, for instance, Franks(1972), Holland(1983), and Luyben(1990). So-called rigorous dynamic models for dynamic simulation came in the 1970's. Then Gani (1989,1992) and Eckert (1994) considered more detailed dynamic equilibrium models which included even weeping, flooding, and entrainment. They proposed an extended model for continuous dynamic simulation.

The equilibrium stage assumption has been used in steady-state distillation column simulation for many years and is described in most of the chemical engineering textbooks, such as Henley(1981) and Wankat(1988). For steady-state simulation, it works well and, as a result, has been transplanted to dynamic modeling. In recent years, the non-equilibrium staged model has received more and more attention. Biardi (1989) and Taylor(1994) have developed non-equilibrium stage models. In Kooijman and Taylor's (1995) recent paper, they pointed out that the equilibrium model should not be used for dynamic simulation although the equilibrium stage assumption is still widely applied in dynamic simulation. Though more detailed models of distillation column have been developed, some simplified models are still in use. This is because simplified models allow the behavior of distillation process to be better understood and are needed in process computer system for large process simulations, optimization and advanced regulatory controls.

Currently, several different levels of models for distillation columns are used for simulation:

a) Pinto and Biscaia (1988) used a model with only the component balance.

b) Wong(1991), Drozdowicz (1988), Cook (1987) considered hydraulic dynamics.

c) Luyben (1990) used the same model as in b), but treated the energy equation as a algebraic equation. For this model, Ranzi (1988) and Gani(1986) presented some comparisons to show the importance of the proper evaluation of the time derivatives of enthalpy in the column and suggested that it be kept in the model.

d) Gani (1986) and Rovaglio (1990) consider hydraulic and pressure dynamics. Gani considered downcomer dynamics also. Some refer to this as a rigorous model.

e) Krishnamurthy and Taylor (1985) started non-equilibrium stage modeling in 1980's. Grottoli (1991) worked on a model for a real tray absorption column. Both of them used non-equilibrium stage models in their steady-state simulation. Recently, Kooijman and Taylor (1995) developed a non-equilibrium distillation column model for dynamic simulation and pointed out that the back-computed Murphree tray efficiencies are not constant over time. This is a direct challenge to the traditional equilibrium stage assumption in dynamic staged simulations.

For a complicated simulation object like a distillation column, it is reasonable that different modeling simplifications have been presented to describe dynamic behavior of distillation column. Most of these models will be discussed in our later study. Comparing the study of staged column structure modeling, published studies of model fidelity are incomplete and unsystematic. Some papers provide comparisons of different models. For example, Levy(1969) compared some column models. He tried to provide an idea of what were the differences between those models. Faced with so many different levels, different descriptions and different complexities in modeling, we are trying to evaluate them by the model fidelity concept and trying to develop a set of rules of thumb to guide process engineers in the choices of staged separation dynamic models for simulation and control.

3.3 Components of Model Structure

In this section we outline the components of model structure that are of interest in this study. These will be evaluated in this Chapter using a simple model of an isothermal

gas absorber. Since neither the energy balance nor a non-ideal VLE model are involved, this allows us to focus on the structural aspects without any confusion from physical properties models.

Five models are to be considered:

1. Basic Model (Reference model)

This is the simplest possible model. It is dynamic version of the Kremser steady-state model.

2. The Weir Model

The liquid flow rate dynamics associated with the tray outlet weir are added to the basic model.

3. The Downcomer Model

The mixing dynamics of the tray downcomers are added to the basic model.

4. The Pressure Model

The basic model with pressure dynamics;

5. The Non-equilibrium Tray model

A Murphree tray efficiency is used to take into account tray efficiency.

In detail, what are examined are:

1. The effect of vapor phase holdup.

2. The effect of liquid flow rate dynamics (weir effect).

3. The effect of downcomer dynamics.

4. The effect of pressure dynamics.

5. The comparison of an equilibrium-stage model with a rate-limited stage model.

All of above tests have been done for the gas absorber study.

The following types of studies were done:

1. Dynamic simulation for each model, in particular, step responses.

2. Linearization of each the model to obtain transfer functions and frequency domain Bode Plots. Because of the large number of equations involved, this analysis was done mainly through the state space matrix using MATLAB for the calculations.

3. Analysis of both the time and frequency domain results to provide guidance in the choice of models. Where appropriate, model fidelity indices were developed to correlate the fidelity errors of various absorber models.

3.4 Gas Absorber Model Equations

A ten equilibrium-stage sieve tray column was designed for absorbing dilute acetone mixed in air by fresh water. The operation is countercurrent and isothermal. The absorber is shown schematically in Fig. 3-1. The details of an individual tray are shown in Fig. 3-2. The details of the design are given in Appendix B. The following is a description of the model equations derived for the various models mentioned in the previous section.

The simplest model used here for simulating gas absorber behaviors is based on Kremser model (1930) with following assumptions:

1. The components being absorbed are dilute in both the gas and liquid phases. Further, the gas and liquid are at same temperature and the heat of absorption effects are negligible. This allows one to assume that the total vapor and liquid flow rates do not vary from tray to tray and the column is isothermal.

2. The vapor-liquid equilibrium of the dilute components being absorbed (or stripped, as the case may be) is assumed to be ideal. Subscritial components thus obey Raoult's Law while supercritical components can be handled using a Henry's Law coefficient.

3. The liquid is incompressible and perfectly mixed on each tray. Downcomer holdup is lumped with tray holdup. Vapor holdup at each tray is neglected. The column pressure is constant.

Various important factors are added to Kremser model in order to make the model more realistic. These include vapor holdup, weir effect, downcomer effect, pressure dynamics, and rate-limited tray behavior. In this work, the final absorber model considers non-equilibrium behavior, weir effect and pressure dynamics. The following are the five models for the gas absorber which have been discussed above:

1. The Kremser model: (Model #1)

This model considers the component mass conservation on each equilibrium stage.

$$\varphi_n \frac{dX_n}{dt} = VKX_{n-1} - (VK+L)X_n + LX_{n+1} \qquad (3.4\text{-}1)$$

where $\varphi_n = \Phi_T \rho_l \epsilon_l$

2. Weir model (Model #2)

The gas absorber we designed above is a sieve tray column. Hydraulic dynamics play a role in multi-stage column dynamic simulation. The Francis formula is used to add the flow-over-the-weir effect to the Kremser model. The Francis formula for sieve tray with

segmental weir is:

$$q = 3.33 l_w (h_{ow})^{1.5} \tag{3.4-2}$$

A total mass balance on the nth tray gives

$$\frac{d\varphi_{Tn}}{dt} = L_{n+1} - L_n \tag{3.4-3}$$

where $\varphi_n = \Phi_T \rho_l \epsilon_l$

and $\epsilon_l = (h_w + h_{ow})/h_T$

where h_w is the weir height, h_{ow} is the liquid height over the weir, and h_T is the tray spacing. Then Model #2 becomes:

$$\varphi_n \frac{dX_n}{dt} = VKX_{n-1} - (VK + L_{n+1})X_n + L_{n+1}X_{n+1} \tag{3.4-4}$$

$$\Phi_T \rho_l \frac{dL_n}{dt} = 556\, L_n^{1/3}(L_{n+1} - L_n)$$

3. Downcomer model (Model #3)

Model #3 includes the downcomer dynamics. The liquid on a tray is divided into two parts: One third is in downcomer while the other two thirds is on the tray which has contact with the vapor when it passes through the liquid. This model is

$$\varphi_n \frac{dX_n}{dt} = VKX_{n-1} - (VK + L)X_n + LXd_n \tag{3.4-5}$$

$$\Phi_d \rho_l \frac{dXd_n}{dt} = L(X_{n+1} - Xd_n)$$

4. Pressure dynamics model (Model #4)

Model #4 includes the effects of liquid flow rate and pressure dynamics. The derivation is from the pressure drop through each sieve tray.

$$\varphi_n \frac{dX_n}{dt} = V_{n-1}KX_{n-1} - (V_nK + L_{n+1})X_n + L_{n+1}X_{n+1} \quad (3.4\text{-}6)$$

$$\Phi_T \rho_l \frac{dL_n}{dt} = 556\, L_n^{1/3}(L_{n+1} - L_n)$$

$$\frac{\Phi_V}{RT}\frac{dP_n}{dt} = (V_{n-1} - V_n)$$

$$where \quad \rho_{vn} = \frac{P_n}{RT}$$

5. The rate limited stage model (Model #5)

This non-equilibrium model is the same as the Model #4 but the Murphree (Emv) stage efficiency is included.

$$\varphi_n \frac{dX_n}{dt} = V_{n-1}Y_{n-1} - V_nY_n - L_{n+1}X_n + L_{n+1}X_{n+1} \quad (3.4\text{-}7)$$

$$\Phi_T \rho_l \frac{dL_n}{dt} = 556\, L_n^{1/3}(L_{n+1} - L_n)$$

$$\frac{\Phi_V}{RT}\frac{dP_n}{dt} = (V_{n-1} - V_n)$$

$$E_{mvn} = \frac{Y_n - Y_{n-1}}{KX_n - Y_{n-1}}$$

The Models #1, #2, #3, and #4 are based on the equilibrium stage assumption. All of them have same steady-state solution but different dynamic responses when a disturbance occurs. Model #5 is nearer to real stage behavior.

3.5 Fidelity Results

The Kremser model is very popular and well-understood. For that reason it was chosen as our reference model. For the more complex models, the relative errors between the new one and the reference model are examined. The condition numbers of the process Jacobians and stiffness ratios of the models are also determined.

In the absorber studies, five model choices are studied.

1. The effect of vapor phase holdup

In most stage models, the vapor phase holdup is neglected. We study under what circumstances this neglect results in significant errors in dynamic simulations. If the vapor holdup is included, the total tray holdup term is

$$\varphi' = \Phi_T(\rho_V\epsilon_V K+\rho_L\epsilon_L) \qquad (3.5-1)$$

If the vapor holdup is neglected, the holdup term is

$$\varphi = \Phi_T\rho_L\epsilon_L \qquad (3.5-2)$$

Eqn. 3.5-2 is chosen as our reference model. Two indices are explored. Index S uses the stripping factor as the index, one which is familiar to engineers in regard to absorber operation.

$$(3.5\text{-}3) \qquad Index\ S = S = \frac{VK}{L}$$

Another index is suggested by the ratio of the component vapor phase capacity to the liquid phase capacity at equilibrium, i.e., (vapor holdup*K value/liquid holdup).

$$(3.5\text{-}4) \qquad Index\ R = \frac{\rho_V \epsilon_V K}{\rho_L \epsilon_L} = \frac{\phi_V \rho_V K}{\phi_L \rho_L}$$

The numerator in Eqn. 3.5-4 is what we have neglected in the total holdup term in the basic model. The denominator is the liquid part of the total holdup. Index R relates the ratio of the neglected vapor holdup to the liquid holdup.

In frequency domain, the responses of Yout and Xout to Yin, Vin, Lin, and Xin with different indices are examined. When the index is small, i.e., Index S is 0.9, both cases of all the responses almost overlap. A typical case is shown in Fig.3-3. As the index increases, the deviations between the two models cases increases gradually. Figs. 3-3 to Fig.3-5 show the frequency response of Yout to Yin as the Index S goes from 0.9 to 9.0, then to 90. These deviations are reasonable because we neglect only 2% of holdup when Index R is 0.9, but 18% when Index R is 9, and 68% when Index R is 90. The same tendency can be found in the time domain. Fig. 3-6 shows the deviation due to neglecting vapor holdup for S=9. Without the vapor holdup, the response of Yout to a 10% step change in Yin clearly leads the dynamic response that includes the vapor holdup. This lead increases with the Index S from 0.9 to 90.

In general, the vapor density is much less than the liquid density so that the

numerator of the Index R is much smaller than the denominator in Eqn. 3.5-4. But the volume of the liquid phase on a stage is usually considerably less than the volume of vapor phase. If vapor-liquid equilibrium constant K is also very big, the numerator of Index R becomes important. Then the vapor phase is not negligible. Both time domain and frequency domain responses were examined in order to show the fidelity relationships. In the frequency domain the fidelity of phase angle errors (degrees) of Yout/Yin to Index R is shown on Fig. 3-7. In the time domain, the relative error in the time required to achieve 63% of steady-state in response to a step change is shown as a function of Index R in Fig. 3-8. From that figure, we can see when the Index R is less than 0.05, the relative error is less than 5%. When the Index R is 0.2, the relative error is 15%.

This examination points out that neglecting vapor holdup in dynamic simulation of a vapor-liquid equilibrium stage is reasonable when the index is not very big, for example, in our case Index R less than 0.05 or Index S less than 2. Otherwise, this neglect would result in a larger error in the dynamic response.

2. The effect of liquid flow rate dynamics

The liquid flow rate leaving a tray is a function of the height of liquid above the tray outlet weir. However, as shown by Eqn. 3.4-4, if the liquid flow rate onto a tray changes, the outlet flow rate does not follow it instantaneously. Model #2 includes the liquid flow rate dynamics. In the frequency domain, the most largest fidelity error is seen in the response of Xout to Lin. This is shown in the Bode Plot of Fig. 3-9. The error is negligible at low

frequencies, in this case less than 0.1 rad/min. However the error becomes very large at high frequencies. The question is why. For the base case (Model #1) the system is essentially first order in its overall behavior. Thus the phase angle is asymptotic to -90 degrees at high frequencies. This is true regardless of the number of stages in the absorber and is typical of flow rate forcing of many types of equipment including heat exchangers and plug flow reactors. However, it is only true when the flow rate changes instantaneously throughout the equipment. Including the weir effects decouples the flow rate dynamics from stage to stage. This can also be seen from the transfer function analysis presented in Appendix C. The overall order of the Model #2 response increases with the number of stages while that for Model # 1 does not.

In the time domain, Yout responses to step changes of Yin, Vin, Lin, and Xin were examined. There is a obvious delay in Model #2 in response to a step change in Lin compared to the Kremser (Model #1). Clearly, the improvement of Model #2 to the Kremser model is limited to the responses of Xout to Lin and Yout to Lin. Further analysis is presented in the comparison of the reference model and Model #4.

3. The effect of downcomer dynamics

The effect of downcomer dynamics were evaluated primarily in the frequency domain. Two approaches were used, namely, 1) examination of the analytical transfer functions for absorbers containing two and three stages (the transfer functions become too unwieldy beyond this) and 2) Bode Plots calculated from the state-space matrices.

The transfer functions are derived and analyzed in Appendix C. It is clear that the biggest impact is on the response of Xout to Xin. For Model #1 this response is on the order of the number of trays in the column. For Model #3 the order doubles. This not surprising. For the liquid phase each tray is basically a well-mixed tank in which some mass transfer takes place. So the liquid phase response of Xout to Xin looks like a series of well mixed tanks, the number of tanks being the number of trays N_T. The only difference between this model and a simple cascade of well-mixed tanks is that the gain is less than one due to the mass transfer due to the mass transfer. Each downcomer is also a well-mixed tank but one in which no mass transfer takes place. So, for Model #3, the liquid phase now looks like a series of 2 N_T well-mixed tanks.

Bode Plots were prepared using Matlab. Selected results are shown in Figs. 3-10 through 3-12. Fig. 3-10 shows the response of Xout to Lin. Unlike the response of Model #2 in Fig. 3-9, the fidelity errors for Model #3 for the same operating conditions are relatively small and, for all practical purposes can be ignored.

In Model #3 it has been assumed that the downcomer is well-mixed. The question arises as to how much the response would differ if the downcomer were in plug flow. The real situation is somewhere inbetween. So, a second version of Model #3 was evaluated based on a deadtime model for the downcomers. These results are shown for the response of Xout to Xin in Figs. 3-11 and 3-12, the difference between the two being in the value of the stripping factor S. At low frequencies (those for which the phase lag is less than -180

degrees), the differences between both versions of Model #3 and Model # 1 are small for S = 0.9. At higher frequencies, the differences become more pronounced, increasing with frequency. For S=9, the phase angle error is quite significant at frequencies well below that at which the Model #1 phase lag reaches -180 degrees. However, a value of S=9 indicates that the component is not being absorbed to any great extent and therefore its dynamic behavior in the liquid phase is probably not of overriding interest. On the other hand, for S = 0.9, this is a component that is essentially being completely absorbed and hence its liquid phase dynamic behavior is certainly of interest.

It is interesting to note that the gain for the plug-flow version of Model #3 tracks that of Model #1 while that for the well-mixed version drops off more rapidly with frequency. This is to be expected since the gain of a plug-flow model is unity for all frequencies. Also to be expected is the fact that the phase angle predicted by the plug-flow version of Model #3 always exceeds that of the well-mixed version, the difference increasing with frequency. However, based on the analysis of the effect of S presented in the previous paragraph, it would seem that the well-mixed version is adequate for most purposes.

4. The effect of liquid flow rate and vapor dynamics

Model #4 includes the weir effect and pressure dynamics. These improvements do not affect the responses of Yout and Xout to Yin and Xin very much. But they do affect the responses of Yout and Xout to Lin and Vin. Our studies show Yout/Lin and Yout/Vin with stripping factors from 0.1, 0.9 and 9. Compared with Model #2, the Model #4 has pressure

dynamics. It turns out that the weir effect is significant for Xout/Lin (or Yout/Lin) while the pressure dynamics are so for Yout/Vin (or Xout/Vin). This is not particularly sunrising. The response of Xout/Lin was shown in Fig. 3-9. The effect of pressure dynamics to Yout/Vin is at high frequency but the effect of liquid flow rate to Yout/Lin is at both low and high frequency. Roughly, the deviations of Yout/Vin increase with increasing stripping factor, while the deviations of Yout/Lin decrease. This is because the effect of liquid flow rate decreases when the stripping factor increases. In the time domain, clear delays exist in the Yout responses to Vin and Lin step changes. The significant point in this model is that the pressure dynamics make the stiffness ratio if this model significantly large. This problem is discussed in Chapter Five.

5. Comparison of the ideal tray, or equilibrium-stage, model with the actual tray, or rate-limited stage model

The question arises as how to handle multi-staged systems when the tray efficiency is not 100%. One can model such systems by including the tray efficiency in the model, thereby converting the overall model from ideal trays to actual trays. This is relatively straight forward as our version, Model #5, derived earlier, demonstrates. Doing so, however, increases the size of the model since, in general, the number of actual trays required for a given separation is greater than the number of ideal trays. Thus, if a particular column requires 20 ideal trays but 40 actual trays, the number of ODE's required will be increased by a factor of two.

For simple multi-staged systems, such as the Kremser absorber model, there is a simple relationship in steady state between the ratio of the actual number of trays required to number of ideal trays and the Murphree tray efficiency. This is shown in Fig. 3-13 for various values of the stripping factor. Using this figure we can see, for instance, if the Murphree efficiency is 50%, and stripping factor is 0.75, 22 trays are needed instead 10 equilibrium stages for the same separation.

The question is now whether something similar can be done for the dynamic model. If we use the relationship shown in Fig. 3-13, we can determine the number of ideal trays required to preserve steady-state accuracy. However, it is obvious that this will distort the dynamics if the actual tray holdup is used since the total holdup in the column will be reduced by the ratio of ideal to actual trays. One possibility is to increase the holdup on each of the ideal trays so as to preserve the total holdup in the column.

This approach was examined and the results are shown in Figs. 3-14 through 3-16. Fig. 3-14 shows the frequency response of Xout to Lin. The result for a column containing 22 non-equilibrium stages is very close to that for 10 ideal stages (Murphree efficiency is 50%, stripping factor is 0.75). From this it looks like the ideal tray approximation is sufficient if actual tray holdup is prorated. However, when we look at the response of Xout to Xin, shown in Fig. 3-15, we see that fidelity error becomes quite large at high frequencies. However, if we only interested in the response below the critical frequency (where the phase angle is - 180 degrees), the error appears to be acceptable. However, if the flow-over-the-weir model is used instead, one can see from Fig. 3-16 that, unlike Fig. 3-14, there is a

significant difference between the two models even below the critical frequency.

3.6 Conclusions

1. Vapor phase holdup will not clearly affect the dynamic simulation when the indices R and S are small. In general, some absorption and most distillation cases meet this criterion.

2. Liquid flow rate dynamics cannot be neglected if acceptable fidelity errors out to the critical frequency are required. The bigger the stripping factor, the smaller the error.

3. Unless very high fidelity is required, downcomer dynamics can be neglected. The downcomer holdup should be lumped with the active tray holdup. If the downcomer dynamics must be included, the well-mixed model should be adequate.

4. The ideal stage assumption is reasonably good if the tray holdup is prorated to give the total holdup for both ideal and actual trays for simple Kremser model. Otherwise, non-ideal tray model is recommended.

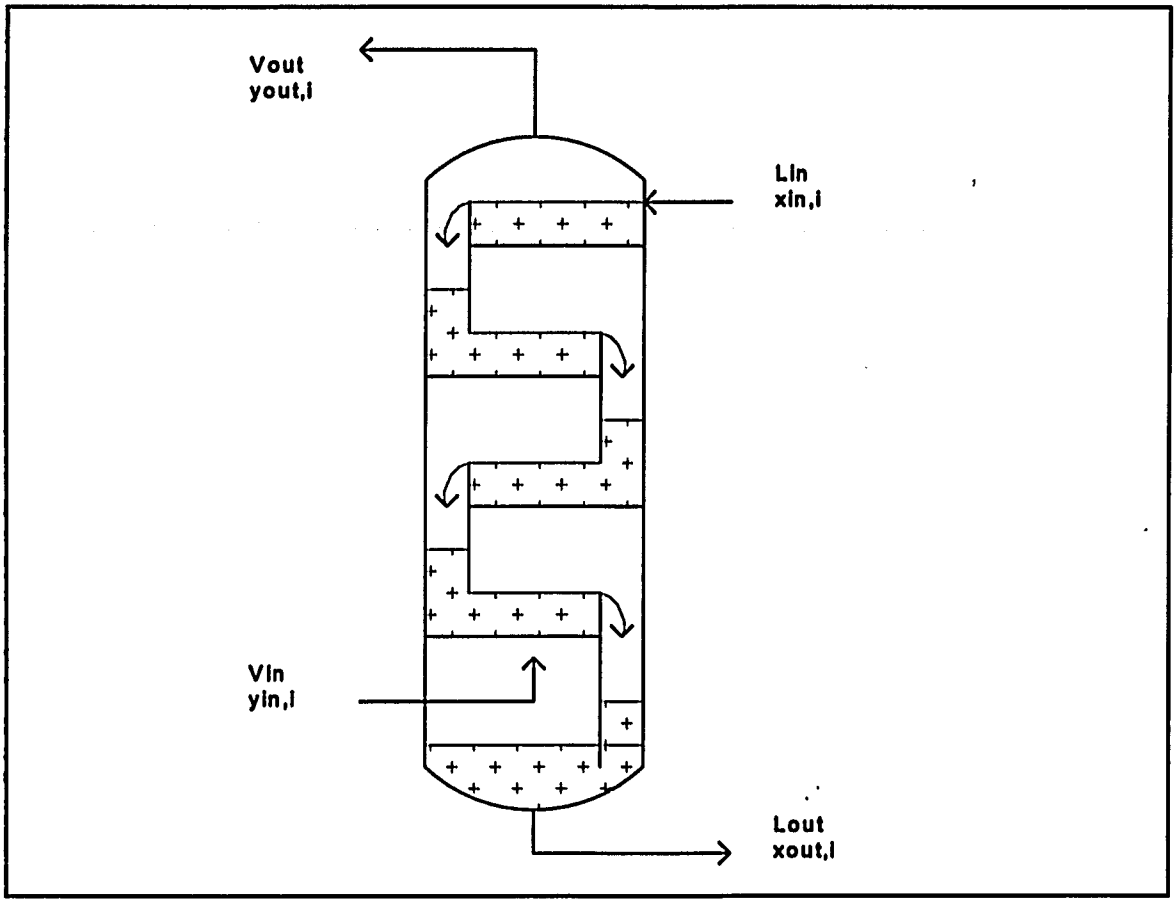

Figure 3-1. Gas Absorber

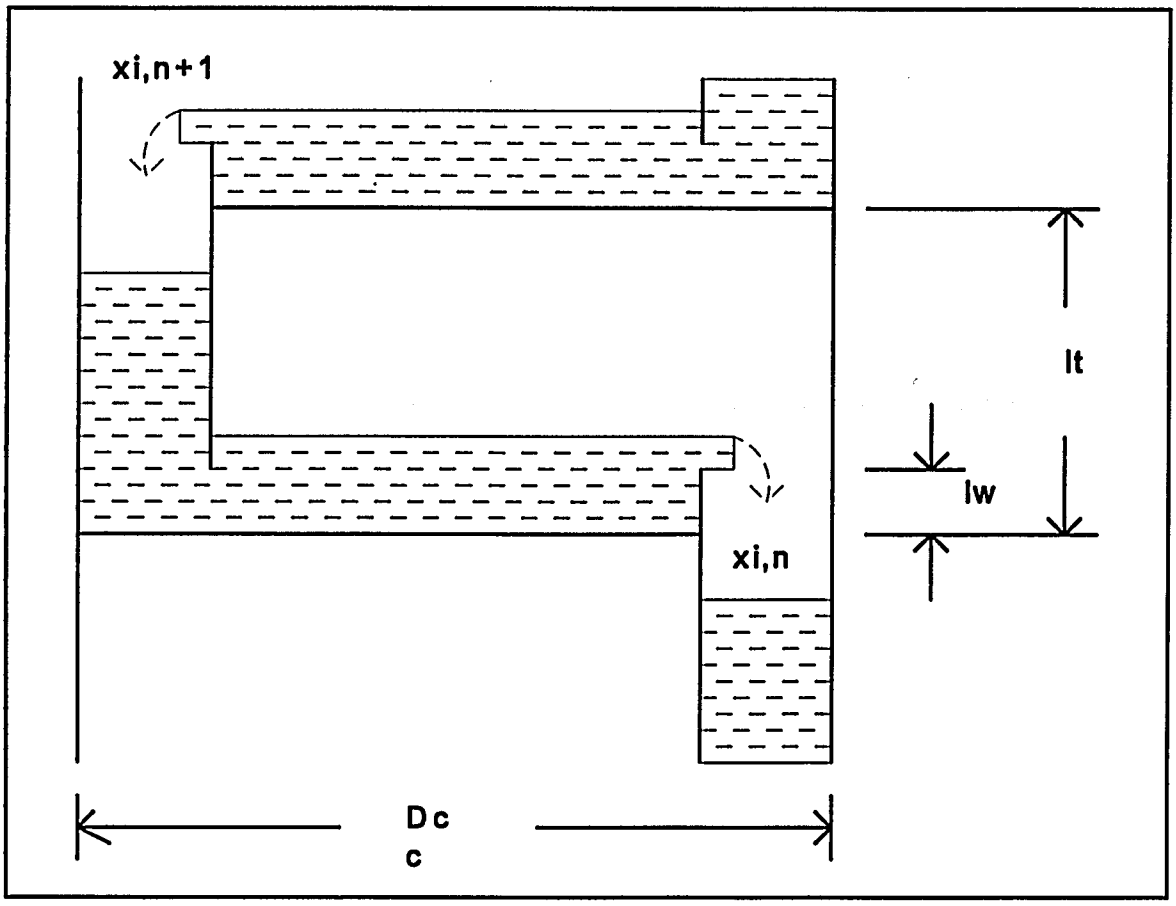

Figure 3-2. Tray Details

Figure 3-3. Absorber-Response of Yout to Yin

Effect of Vapor Phase Holdup(S=0,9)

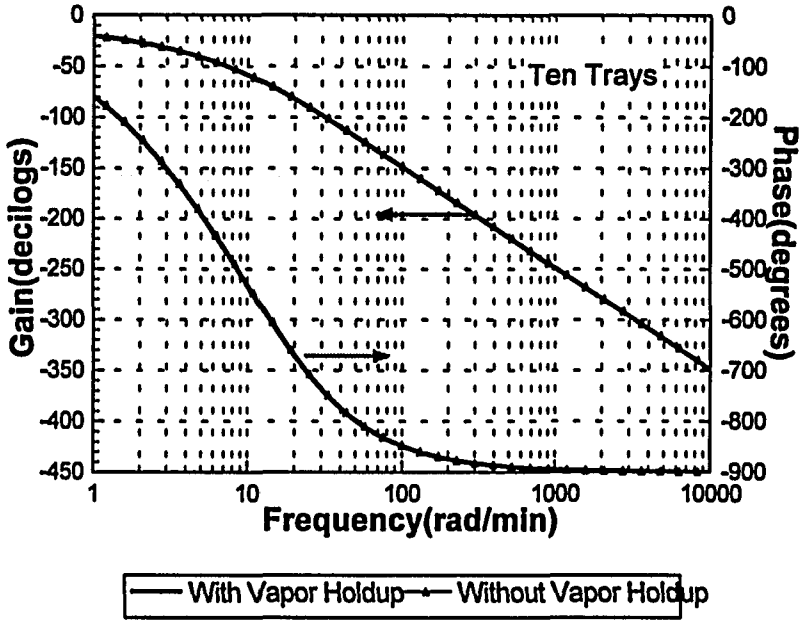

Figure 3-4. Absorber-Response of Yout to Yin

Effect of Vapor Phase Holdup(S=9)

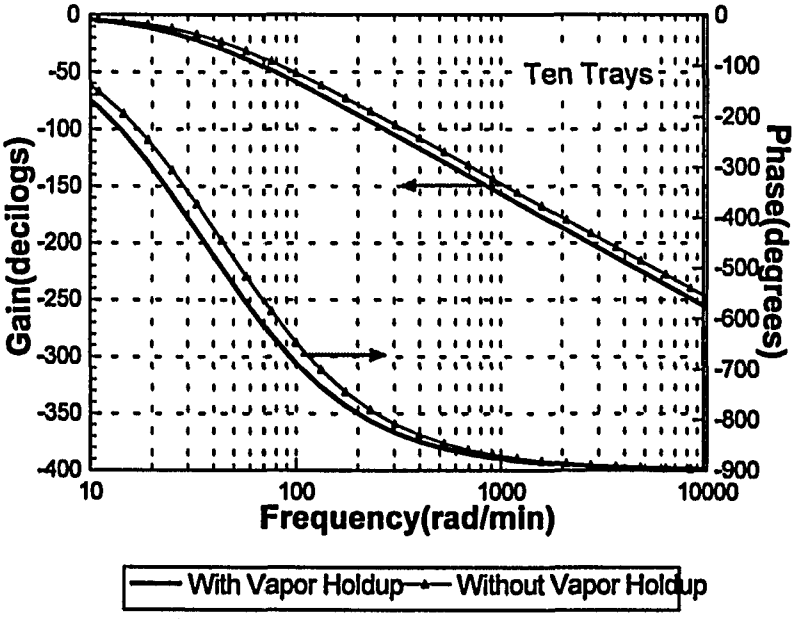

Figure 3-5. Absorber-Response of Yout to Yin

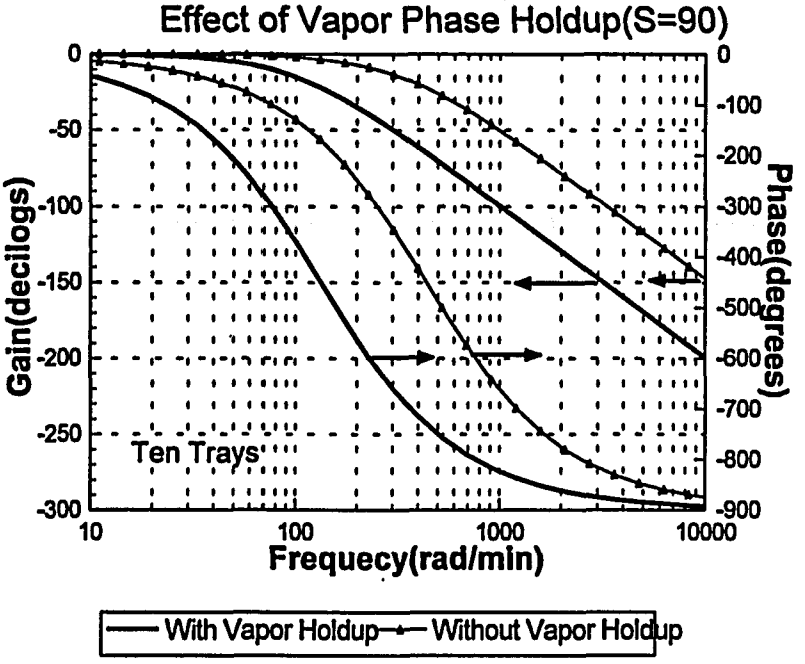

Figure 3-6. Absorber-Response to 10% Yin Step

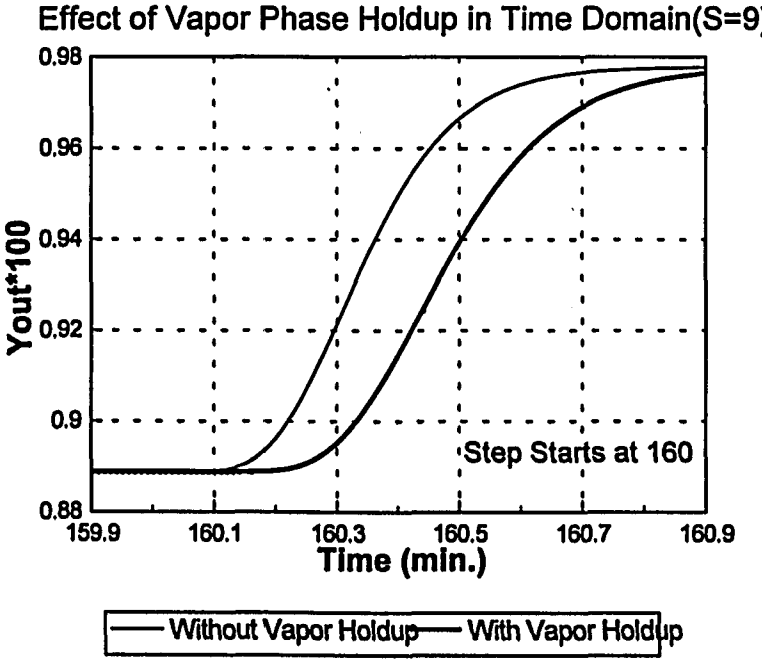

Figure 3-7. Absorber-Effect of Vapor Holdup

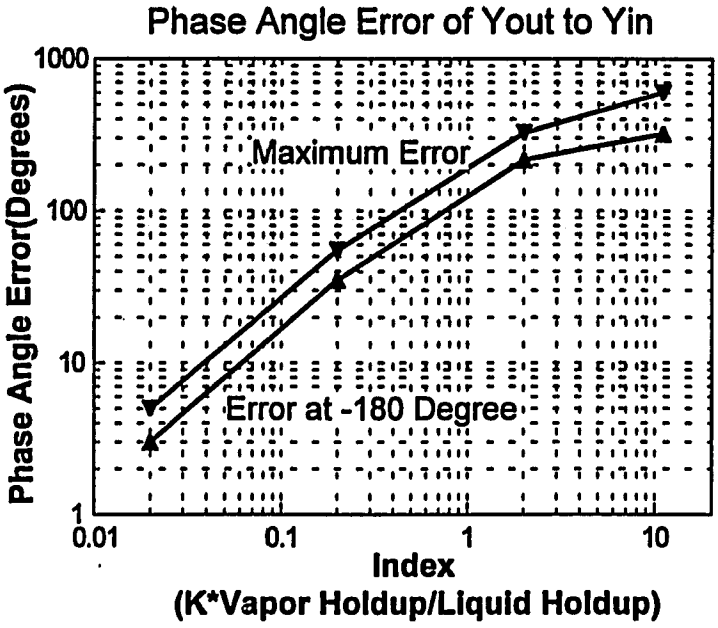

Figure 3-8. Absorber-Effect of Vapor Holdup

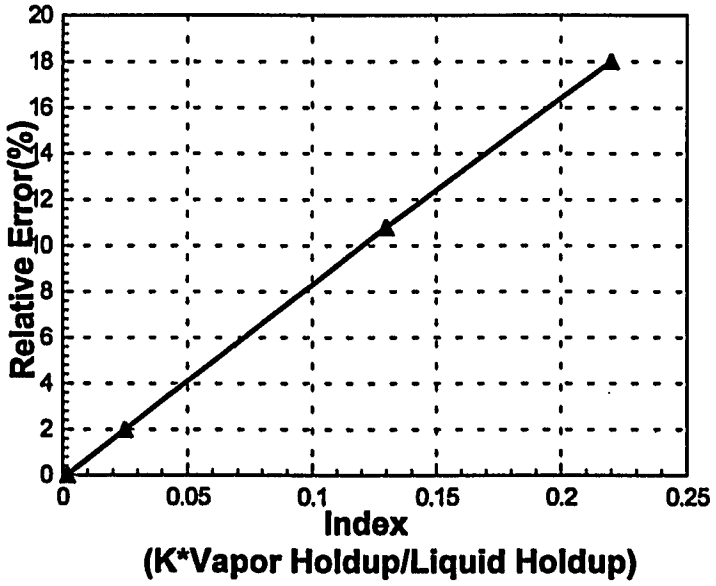

Figure 3-9. Absorber-Response of Xout to Lin

Effect of Liquid Flow Rate Dynamics(10 Trays, S=0.9)

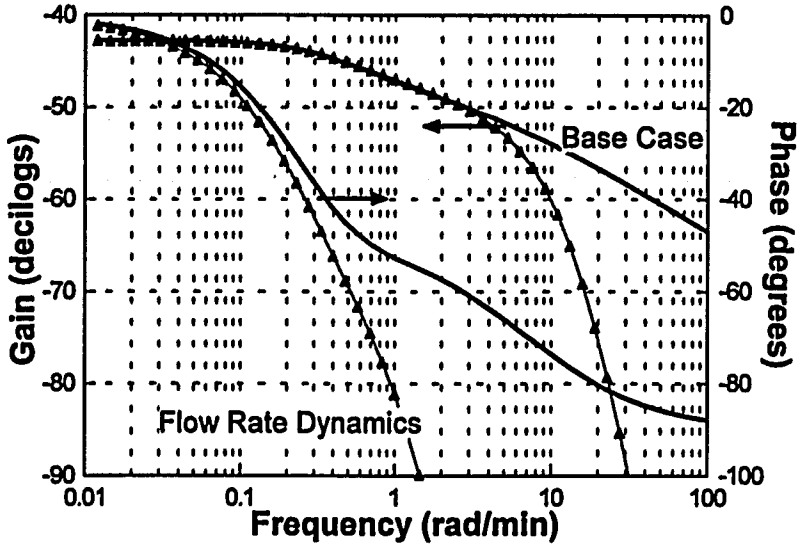

Figure 3-10. Absorber-Response of Xout to Lin

Effect of Downcomer Dynamics(10 Trays, S=0.9)

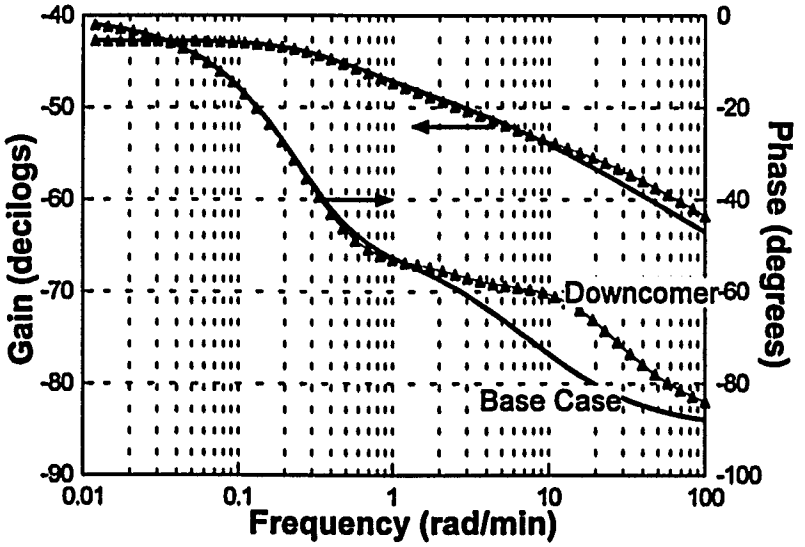

Figure 3-11. Absorber-Response of Xout to Xin

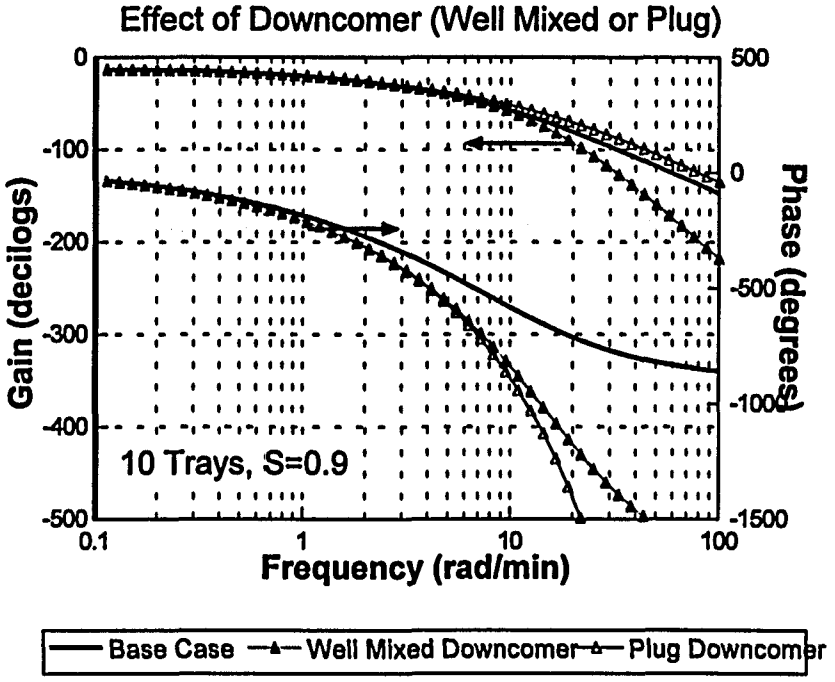

Figure 3-12. Absorber-Response of Xout to Xin

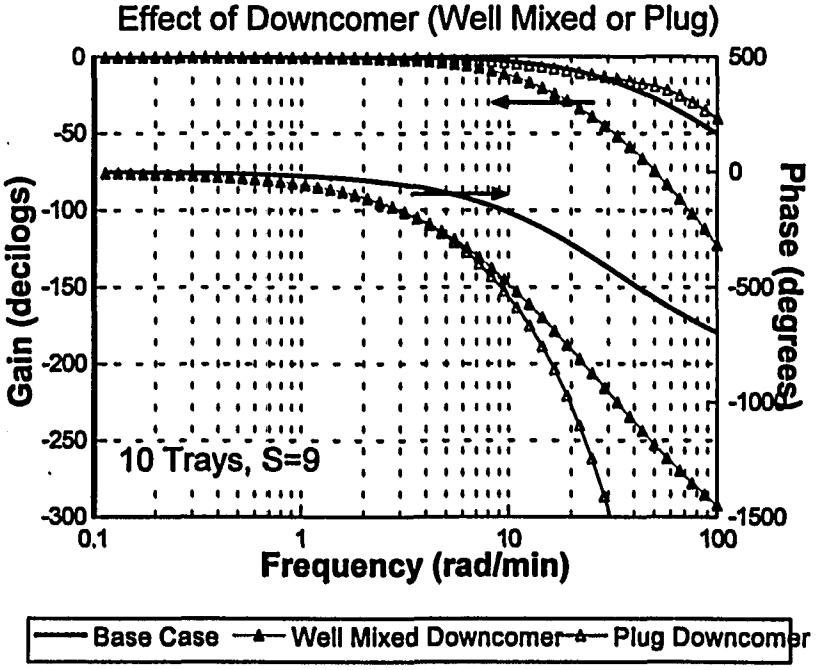

Figure 3-13. Absorber-Trays vs. Efficiency

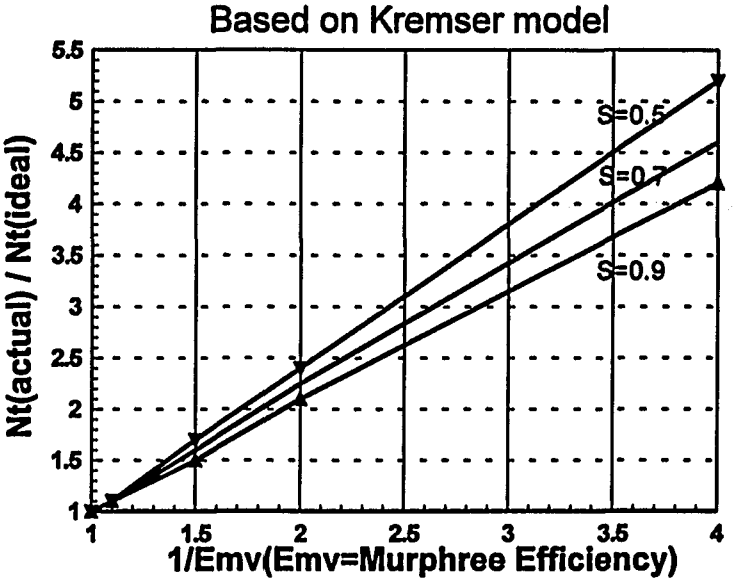

Figure 3-14. Absorber-Response of Xout to Lin

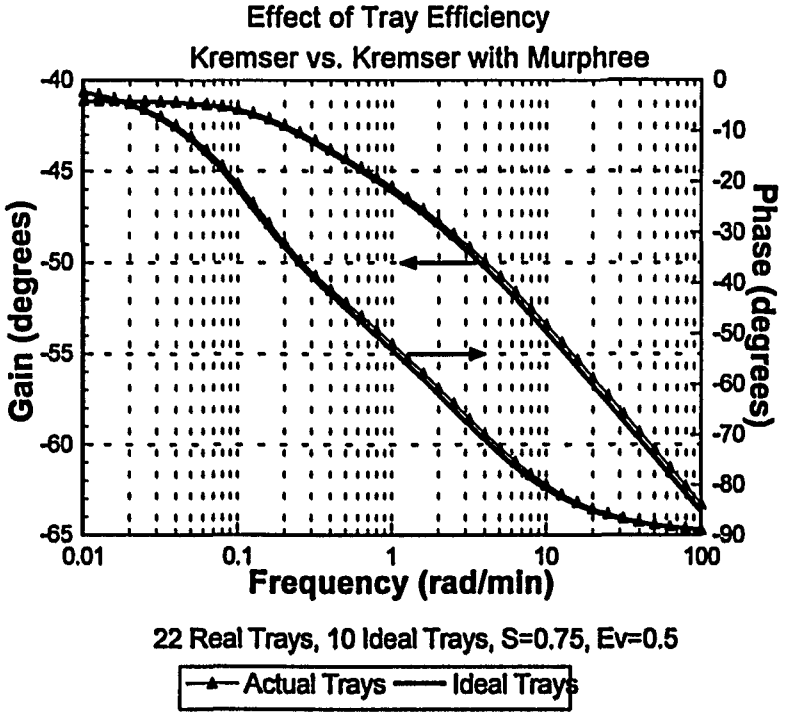

Figure 3-15. Absorber-Response of Xout to Xin

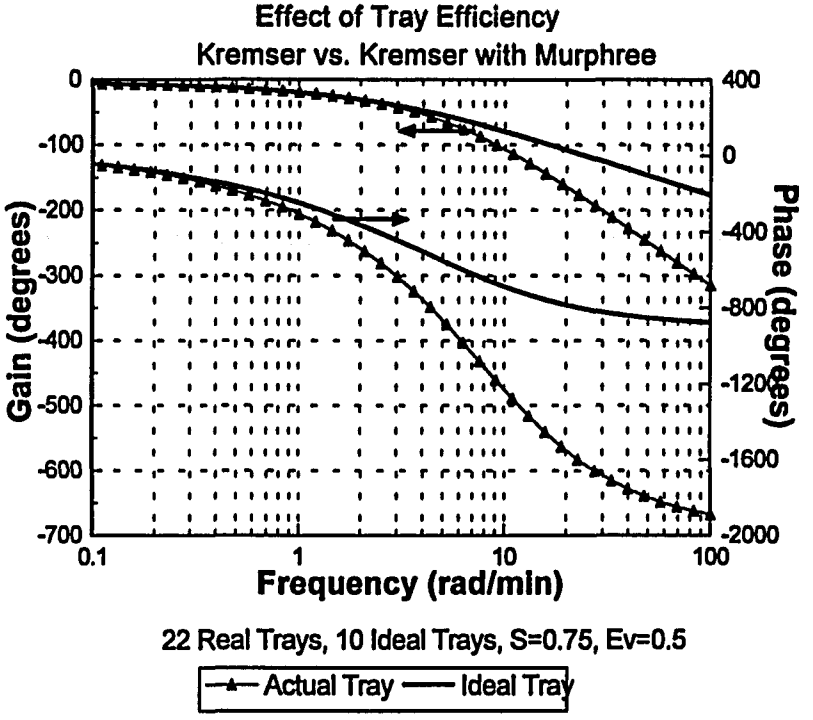

Figure 3-16. Absorber-Response of Xout to Lin

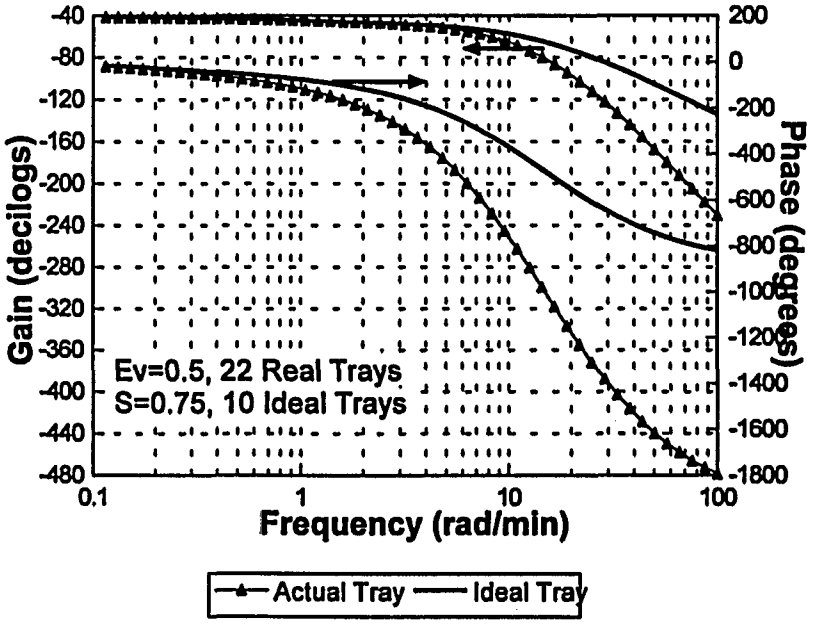

CHAPTER FOUR. FIDELITY EFFECTS IN DISTILLATION MODELS

4.1 Introduction

In the last two chapters, we developed some useful guidelines regarding the choice of VLE models and model structure for multi-staged systems. In this chapter these guidelines are put to the test. We evaluate them using a complex staged separation process, namely, distillation. Compared to the structure of a gas absorber, the structure of a distillation column is more complicated. A distillation column is composed of not only the staged column body, but also a condenser, a reflux drum, a bottom sump, and a reboiler. One feed or several feeds separate the column into different sections: rectifying and stripping sections.

Two cases are considered. The first is a distillation column modeled under the assumption of constant molal overflow (CMO). This simplifying assumption has been used since the 1920's. It is widely used as the basis for column design and initial simulation and is still widely accepted as one notes referring to the more recent textbooks on the subject (Henley and Seader 1981, Wankat 1988). This CMO assumption is based on the fact that the molar heats of vaporization of the two species in a binary system are quite often nearly equal; and that heats of mixing, stage heat losses, and sensible heat changes of both liquid and vapor are negligible or offset each other. Then every mole of condensing vapor vaporizes exactly one mole of liquid. For many system this assumption causes no significant errors in a section of equilibrium stages. But it greatly simplifies distillation simulation and design.

This distillation model will be referred to as the CMO model. Our reason for studying its model fidelity aspects is that the CMO model decouples VLE model effects from those that might be caused by energy balance effects. The second model to be studied is the so-called rigorous model in which the energy balance is included for each tray.

4.2 Literature Review

Most of the relevant literature that is applicable was been discussed in the previous chapter. It is summarized here for convenience. Most of the early work on distillation modeling can be found in the Shell compendium by Rademaker et al (1975). Early versions of dynamic multicomponent are described in the books by Franks (1972) and Luyben (1990). These are rigorous models but are based ideal VLE and enthalpy relationships and contain few, if any, structural details. More recently rigorous models have been reported by Ranzi *et al* (1988) and Rovaglio *et al* (1990). An up-to-date review of rigorous modeling and simulation is given by Grassi (1992). The most recent and most realistic dynamic distillation models have been reported by Jacobsen and Skogestad (1994) and Kooijman and Taylor (1995). These are based on a foam model of the mass transfer action taking place on each stage.

Two other aspects of dynamic distillation modeling which are somewhat outside the scope of the present work are batch distillation and approximate models. Both have a large literature; only a brief summary will be given here. Batch distillation, by its vary nature, must be modeled as a time-varying operation. It is only in recent years when good integration

algorithms have become available for stiff systems, that useable batch distillation programs have become available. One example is the BATCHFRAC program commercially available from ASPEN Technology. In recent years attention has been focused the various aspects of design such as optimal reflux policies and the effective use of slop cuts. Much of this work is described in the recent article by Muher and Luyben (1992).

Given the complexity of distillation column modeling and the great expense in the earlier years of doing anything approaching rigorous simulation, much effort has been spent to develop approximate dynamic models for distillation. One of the earliest efforts in this area is the work of Weigand et al (1972). The current state of the art can be found in the article by Papadourakis and Rijnsdorp (1992).

4.3 Constant Molal Overflow (CMO) Distillation Models

In this section we develop the model equations for the distillation column models based on the assumption of constant molal overflow (CMO). Additional assumptions required for this model are:

1. The vapor and liquid phases are at equilibrium on each stage. The liquid is incompressible and perfectly mixed. The vapor holdup at each tray is negligible. The pressure on each tray is constant.

2. The liquid holdups in the bottom sump and in the reflux drum are constant. The

reboiler is an ideal stage. The overhead condenser is a total condenser without dynamics. The downcomer holdup is lumped with tray holdup in the basic model.

3. The vapor and liquid flow rates across the feed tray are determined by the thermal condition of the feed. Any change in feed flow rate or reflux flow rate is transmitted instantaneously throughout the column. For simplifying later calculations, a saturated liquid feed is used in this study. Most of these assumptions are commonly made for most distillation models published in the literature.

There are still two degrees of freedom in the CMO distillation simulation model. We have chosen to specify the reflux flow rate (LT) to the top tray and the boil-up vapor rate (VB) from the reboiler. The withdrawal rates of the distillate (D) and the bottom product (B) are set by material balances respectively.

The main goal is to examine model fidelity using the CMO distillation model, particularly the effects of the downcomer and flow over the weir. Three models have been with this in mind.

1. The basic CMO model

This model considers the component mass balances and the vapor-liquid at the bubble points at all trays. The component mass balance equations is given by

$$\Psi_n \frac{dX_{n,j}}{dt} = V_{n-1}K_{n-1,j}X_{n-1,j} - (V_nK_{n,j} + L_n)X_{n,j} + L_{n+1}X_{n+1,j} + F_nZ_{n,j} \qquad (4.3-1)$$

The assumption, equilibrium between the vapor and liquid leaving the tray, has been made in the above equation.

(4.3-2) $$Y_{n,j} = K_{n,j}X_{n,j} = K_{n,r}\alpha_j X_{n,j}$$

At equilibrium the liquid on each tray must be at its bubble point.

(4.3-3) $$\Sigma_j K_{n,r}\alpha_j X_{n,j} - 1 = 0$$

Since the energy balance is being ignored due to the CMO simplification, the above equation can be solved for Kn,r (the reference component K-value) directly. In this

(4.3-4) $$K_{n,r} = \frac{1}{\Sigma_j \alpha_j X_{n,j}}$$

simulation the K-value is no longer a constant.

The remaining parts of the distillation column are the condenser and the reboiler. Assuming a total condenser and a reflux drum of constant holdup Ψ_D, a component mass balance for the reflux drum is

(4.3-5) $$\Psi_D \frac{dX_{D,j}}{dt} = V_{NT}K_{NT,j}X_{NT,j} - L_j X_{D,j}$$

Assuming a reboiler and a column base of constant holdup Ψ_R, a component mass balance for the reboiler is

$$(4.3\text{-}6) \qquad \Psi_R \frac{dX_{R,j}}{dt} = L_1 X_{1,j} - (V_R K_{R,j} + B) X_{R,j}$$

In this section, both the vapor and liquid flow rates are assumed to be instantaneous functions of time. After the reflux flow rate LT(t) and the boiled up vapor rate VB(t) specified, the other flow rates for a single feed(F) to a n stage column are given by:

Vn = VB (vapor flow rate at any nth tray)

Ln = LT (liquid flow rate above feed tray)

Ln = LT + F (liquid flow rate below feed tray, including feed tray)

D = VB - LT (distillate flow rate)

B = F + LT - VB (bottom product flow rate)

2. The CMO with liquid flow rates dynamics model

This model comes from the basic model but includes the weir effect, which is determined by Francis weir formula. This formula has been discussed in the gas absorber part in the Chapter Three. The weir effect makes the liquid flow rates change from tray to tray when the reflux flow rate changes. For the staged column, weirs do play an important role, delaying liquid flow rates changing through the column. The main part of this model is composed of total mass balances and component mass balances in ODEs. The C_L is the function of the liquid density and the column geometry.

$$(4.3\text{-}7)\quad \Psi_n \frac{dX_{n,j}}{dt} = V_{n-1}K_{n-1,j}X_{n-1,j} - (V_nK_{n,j} + L_n)X_{n,j} + L_{n+1}X_{n+1,j} + F_nZ_{n,j}$$

$$\frac{dL_n}{dt} = C_L L_n^{(1/3)}(L_{n+1} - L_n + F_n)$$

Eqn. 4.3-7 and Eqns 4.3-2 to 4.3-6 comprise the liquid flow rates dynamics model. The vapor flow rates are still assumed to be instantaneous function of time. After LT(t) and VB(t) specified, the other flow rates for a single feed to stage nt are given by:

Vn = VB (vapor flow rate at any nth tray)

D = VB - LT (distillate flow rate)

B = L1 - VB (bottoms flow rate)

3. The CMO with downcomer model

This model includes downcomer dynamics. One fourth of the liquid on the tray in the basic model is assigned to the downcomer and does not interact with the vapor phase that passes though the tray. Now the mass balance equations become:

$$(4.3\text{-}8)\quad \Psi_n \frac{dX_{n,j}}{dt} = V_{n-1}K_{n-1,j}X_{n-1,j} - (V_nK_{n,j} + L_n)X_{n,j} + L_{n+1}Xd_{n,j} + F_nZ_{n,j}$$

$$\Phi_D \rho_L \frac{dXd_{n,j}}{dt} = L_n(X_{n+1,j} - Xd_{n,j})$$

Eqn. 4.3-8 and Eqns. 4.3-2 to 4.3-6 comprise the downcomer CMO model. In this model, both the vapor and liquid flow rates are assumed be instantaneous functions of time. After LT(t) and VB(t) are specified, the other flow rates for a single feed (F) to an N- stage are determined in the same manner as in the basic CMO model.

The advantage of CMO distillation model is relatively simpler than rigorous model. The mass balance equations become linear algebraic equations in the steady-state simulation:

$$(4.3-9) \qquad A_j X_{i,j-1} + B_j X_{ij} + C_j X_{i,j+1} = D_j$$

Aj, Bj, Cj, and Dj are calculated by feed, vapor, liquid flow rates and K values on each tray. This model can be solved by the Thomas algorithm by backward substitution.

4.4 Fidelity Results for CMO Distillation

Three CMO models are listed above, basic CMO model, CMO with flow rate dynamics over weir, and CMO with downcomer dynamics. Both time domain and frequency domain responses have been determined. Usually, the temperature profile is not calculated for the CMO model. In this part three comparisons of composition step responses are prepared.

1. The effect of liquid flow rate over weir:

Fig. 4-2 shows the weir effect when the reflux flow rate experiences a step change. The response of the distillate composition is slightly delayed. The effect is much more pronounced for the bottom product composition. This is shown in the frequency domain the Bode Plot. of Fig. 4-3. There are large differences in gain and phase well before the critical frequency is reached even though both start from the same steady-state gain.

2. The effect of downcomer dynamics:

Fig. 4-4 shows the downcomer effect when the reflux flow rate experiences a step change. The response of the distillate composition is slightly delayed. In frequency domain, those deviations is smaller also. Fig. 4-4 shows the difference in gain and phase angle. This result is consistent with that from the absorber studies.

3. The effect of different K value models

When the relative volatilities are estimated from ideal K-value model, the composition profiles plots shown in Figs. 4-6 and 4-7 are clearly different from those estimated from the Wilson K-value model for the methanol, ethanol and water system. It is clear that property models play an important role in the dynamic simulation of distillations as well as for flash drums.

The advantage of CMO distillation model is its simplicity of calculation. But the CMO model is not as accurate as the rigorous model. This is illustrated in the next section.

4.5 Rigorous Distillation Models

The rigorous distillation model is composed of total mass balances, component mass balances, energy balances and bubble point equations, which some people call the Summation Equations. After the vapor flow rate leaving the reboiler and reflux flow rate to the top tray are specified, the vapor and liquid flow rates, the composition of the liquid and the equilibrium temperature at each tray can be solved out by these equations. This is a

nonlinear model, including algebraic equations(AEs) and ordinary differential equations(ODEs). The total mass balances, component mass balances, energy balance equations are ODEs but the Summation Equations are AEs. These equations comprise an index problem if they are solved simultaneously. In this simulation, at each time the algebraic equations are solved first and then the ordinary differential equations are solved for that time step.

Other than that the liquid and vapor flow rates now change from tray to tray, the assumptions for this model are the same as for the CMO model.

There are still two degrees of freedom in this distillation simulation. The reflux flow rate (LT) to the top tray of the column and the boiled up vapor rate (VB) from the reboiler are specified. In this part our main purpose is to examine the effect of weir, because this effect is very important in the absorber and CMO distillation studies. Two models are prepared in this part.

1. The basic rigorous model

This model assumes that the liquid level at each tray is constant. The entire model is given by a group of ODEs and a group of AEs. The ODEs are:

$$(4.5\text{-}1)\qquad \Psi_n\frac{dX_{n,j}}{dt} = V_{n-1}K_{n-1,j}X_{n-1,j}-(V_nK_{n,j}+L_n)X_{n,j}+L_{n+1}X_{n+1,j}+F_nZ_{n,j}$$

$$\Psi_n Cp_L\frac{dT}{dt} = V_{n-1}(HV_{n-1}-HL_{n-1})-V_n(HV_n-HL_{n-1})+L_{n+1}(HL_{n+1}-HL_{n-1})$$

$$+ F_n(HF_n-HL_{n-1})-\Psi_n\Sigma_j hl_{n,j}\frac{dX_{n,j}}{dt}$$

The AEs are:

$$(4.5\text{-}2)\qquad V_{n-1} - V_n - L_n + L_{n+1} + F_n = 0$$

$$\Sigma_j K_{n,j}X_{n,j} - 1 = 0$$

The equilibrium assumption between the vapor and liquid leaving the tray is applied to the above model. The liquid and vapor flow rates are calculated from the above AEs. Wilson and Ideal K value models are used for the distillation simulation.

2. The basic rigorous with liquid flow rate dynamics model

This model includes the weir effect. The total mass balances equation become ODEs that are AEs in the basic rigorous model. The C_L in the mass balances equation is the function of the liquid density and the column geometry. The ODEs of the model are:

$$(4.5\text{-}3)\qquad \Psi_n\frac{dX_{n,j}}{dt} = V_{n-1}K_{n-1,j}X_{n-1,j}-(V_nK_{n,j}+L_n)X_{n,j}+L_{n+1}X_{n+1,j}+F_nZ_{n,j}$$

$$\Psi_n Cp_L\frac{dT}{dt} = V_{n-1}(HV_{n-1}-HL_{n-1})-V_n(HV_n-HL_{n-1})+L_{n+1}(HL_{n+1}-HL_{n-1})$$

$$+ F_n(HF_n-HL_{n-1})-\Psi_n\Sigma_j hl_{n,j}\frac{dX_{n,j}}{dt}$$

$$\frac{dL_n}{dt} = C_L L_n^{(1/3)}(L_{n+1} - L_n - V_n + V_{n-1} + F_n)$$

The algebraic equations of the model are:

$$\Sigma_i K_{n,i} X_{n,i} - 1 = 0 \qquad (4.5\text{-}4)$$

In this model, the liquid flow rate from tray to tray have a dynamic process though the column. In both of above model options, the vapor flow rates are obtained from the derivations of the summation equations.

$$\Sigma_i K_{n,i} \frac{dX_{n,i}}{dt} + \Sigma_i X_{n,i} \partial \frac{K_{n,i}}{\partial T_n} \frac{dT_n}{dt} = 0 \qquad (4.5\text{-}5)$$

Both Ideal and Wilson K value models are used. In the following studies, three combinations are examined, such as basic rigorous distillation model with ideal K-value model, basic rigorous distillation model with Wilson K value model, and weir rigorous distillation model with ideal K value model.

4.6 Fidelity Study Results for Rigorous Distillation

The rigorous distillation model provides more detailed information than does the CMO modes. It provides not only the composition at each tray, but also the temperature profile, liquid and vapor flow rates and K-value profiles from tray to tray. This model is no longer too complex and difficult to solve with current computers.

1. The effect of liquid flow rate over weir:

Figs. 4-8 and 4-9 show the weir effect when the reflux flow rate is subjected to a step change. The responses of the distillate composition and temperature are obviously delayed

because of flow rate dynamics over the weir. This delay is as long as twenty to thirty minutes for the top temperature or composition. In frequency domain we usually examine the responses of bottom variables to the reflux flow rate. Fig. 4-10 shows the large difference in gain and phase. This result is consistent with that from the absorber studies.

2. The effect of different K value models

When the K values are estimated from either Ideal K-value model or the Wilson K-value model, the deviations of the composition profiles and the temperature profile are illustrated on Figs. 4-11 through 4-14 for the methanol, ethanol and water system. The maximum temperature deviation exceeds 15 K. The maximum relative error in composition is more than 100%. This is not a strongly non-ideal system according to our correlation in Chapter Two. It is obvious that the VLE model plays an important role in the dynamic simulations.

The relative volatility profiles are plotted on Fig. 4-15 and Fig. 4-16 for a ternary system, methanol, ethanol and water. Fig. 4-15 is for the methanol/ water pair and 4-16 for the ethanol/water pair. The differences of relative volatilities are the basic differences between the two K-value models. For example, for the ethanol and water system, when the Ideal K- value model is used, the relative volatilities on different stages are nearly constant, ranging only from 2.22 to 2.31 with a geometric-mean value 2.25. When the Wilson K- value model is used, the relative volatilities on different stages vary significantly from 1.36 to 12.7 with a geometric-mean value 2.86. From this point of view, a constant relative volatility can be used only for ideal systems without significant errors. A further examination

of vapor and liquid flow rate profiles through the distillation column are illustrated in Figs. 4-17 and 4-18. The differences are significant for the vapor flow rate.

From the dynamic responses, after a reflux flow rate step change, the temperatures and compositions at both distillate and bottom product are very different. They start at different steady states and then follow different response trajectories. This is shown in Figs. 4-19 through 4-22.

4.7 Comparison of CMO and Rigorous Distillation Models

A comparison of the CMO and rigorous distillation models is quite interesting. Figs. 4-23 and 4-24 show the steady state composition profiles using the ideal K-value model. Both composition profiles are quite close. Only few points show clear deviations. It means that the CMO model can predict ideal system separations fairly well. This result explains why the CMO model has been used for such a long time. But the profiles are not so close when the Wilson K-value model is applied as shown in Figs. 4-25 and 4-26. Though the top and bottom compositions are quite close, the interior profiles differ significantly.

From the dynamic response point of view, it is not that easy to compare these two models because they start from different steady state values. But we can see the difference in both dynamic trajectories and different incremental changes in the final values. This is shown for the same step change in reflux flow rate, an increase of 6% in Figs. 4-27 and 4-28. The CMO model gives sharper and bigger dynamic responses.

4.8 Conclusions

A number of conclusions can be drawn from the results of this chapter. First and foremost is that the model fidelity results determined for simple systems such as the flash drum (Chapter Two) and the isothermal gas absorber (Chapter Three) carry over to the more complex distillation column systems. Second, the CMO distillation model should not be used unless the underlying VLE is close to ideal.

One point should be noted. The results for the downcomer model show only small and acceptable fidelity errors for responses to reflux flow rate. This is consistent with the results of Chapter Three. However, the situation will probably not be the same for changes in feed composition. Unfortunately, time constraints did not permit evaluation of this response. Prudence dictates, therefore, that if significant feed composition changes are anticipated, the downcomer dynamics should be included.

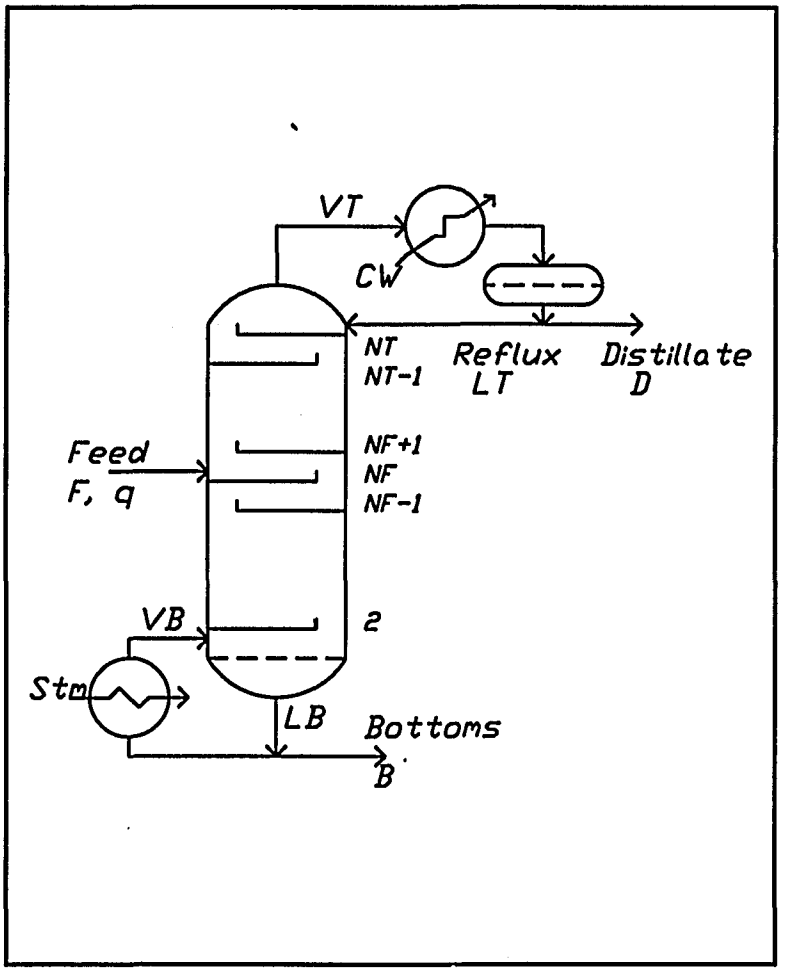

Figure 4-1. Distillation Column

Figure 4-2. CMO Column Model-Effect of weir Dynamics

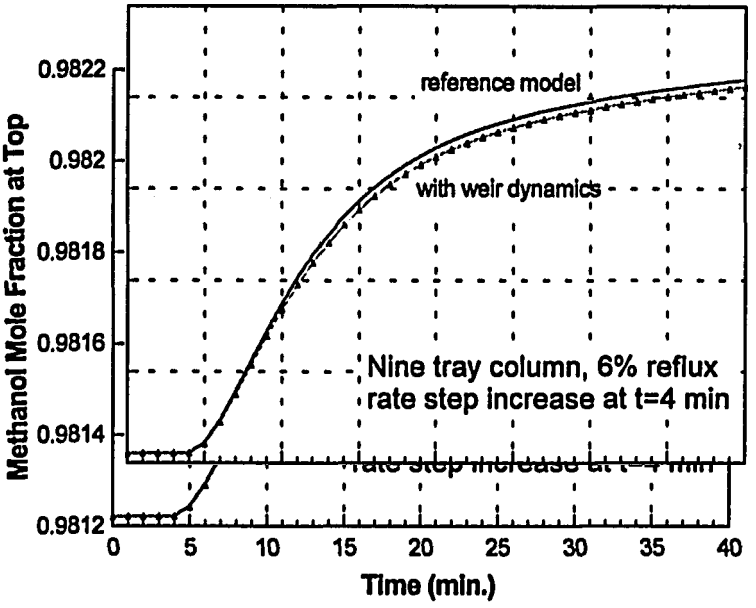

Figure 4-3. CMO Column Model-Effect of Weit Dynamics

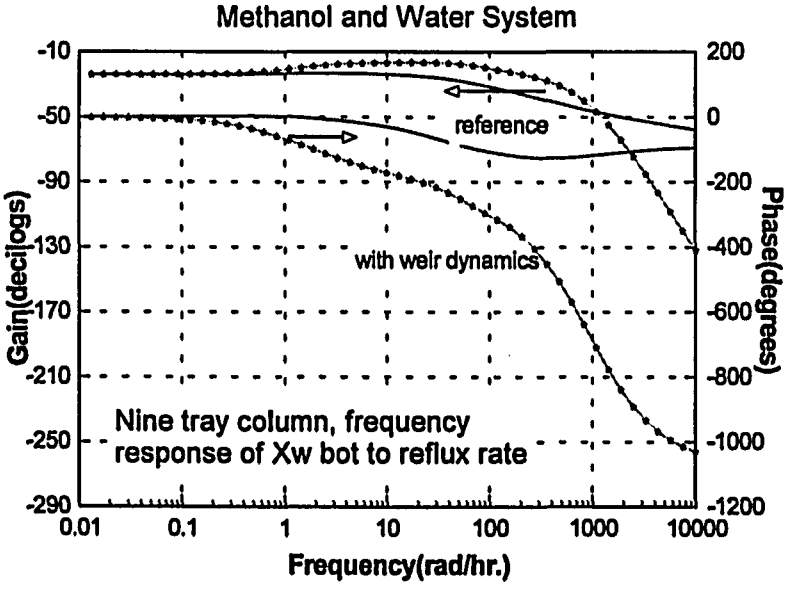

Figure 4-4. CMO Column Model-Effect of Downcomer Dynamics

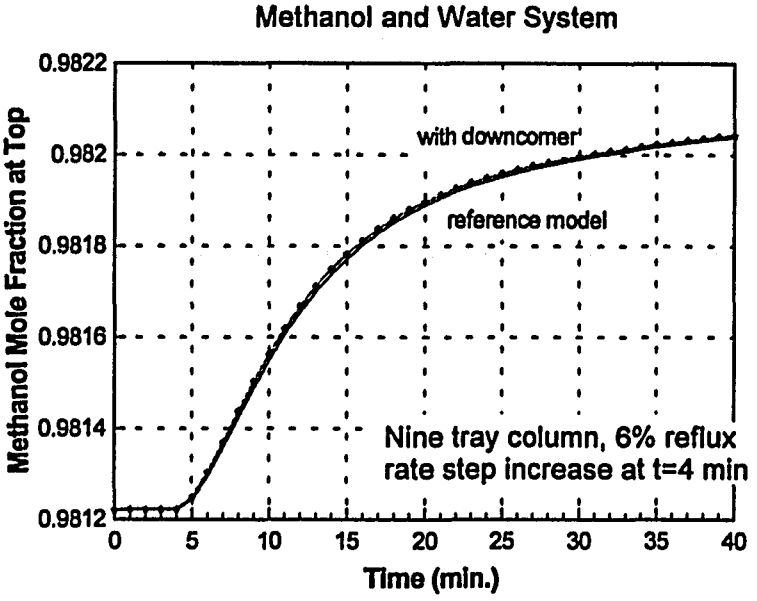

Figure 4-5. CMO Column Model-Effect of Downcomer Dynamics

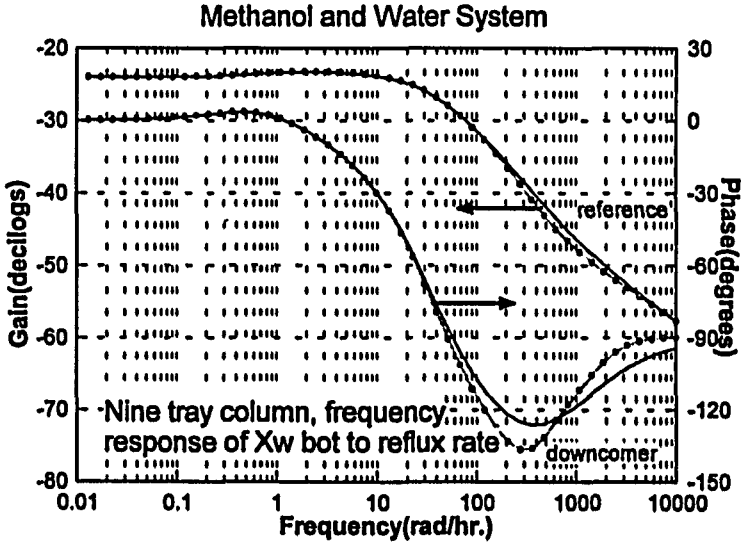

Figure 4-6. CMO Column Model-Effect of VLE on Composition

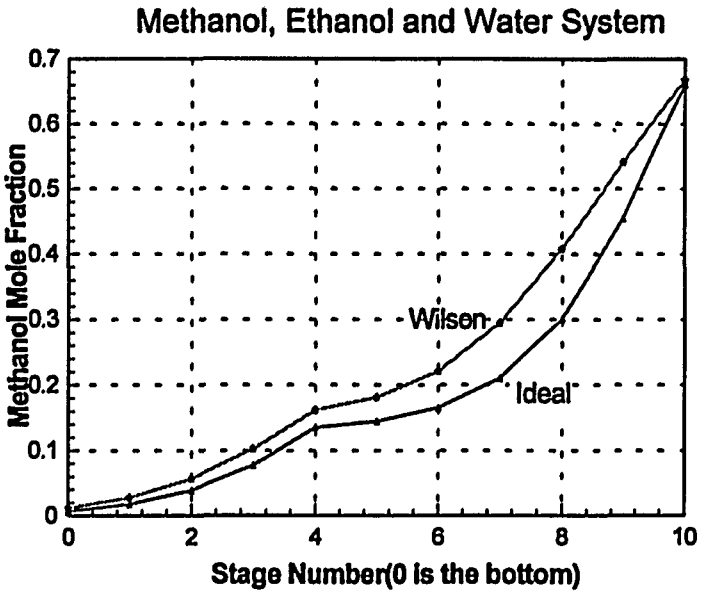

Figure 4-7. CMO Column Model-Effect of VLE on Composition

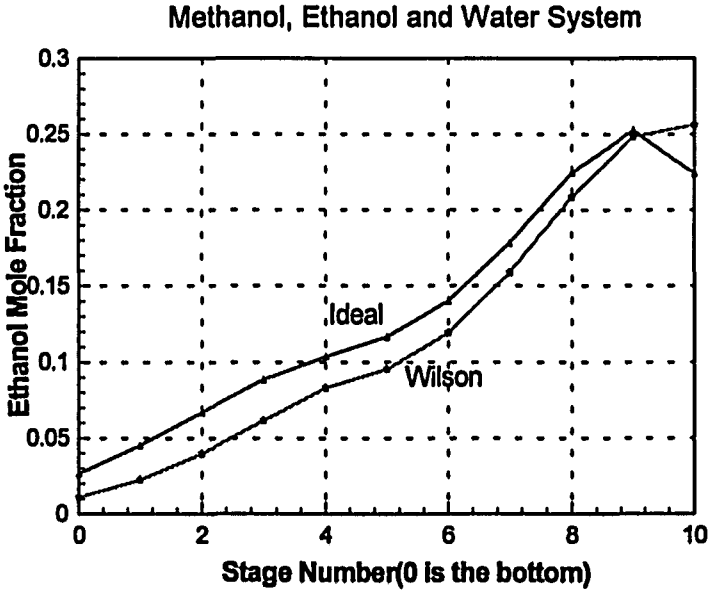

Figure 4-8. Rigorous Column Model-Effect of Weir on top Composition

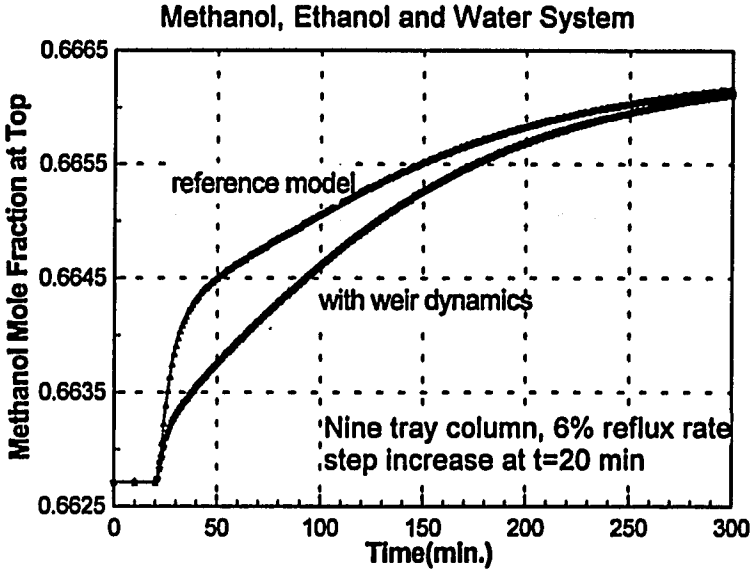

Figure 4-9. Rigorous Column Model-Effect of Weir on Top T

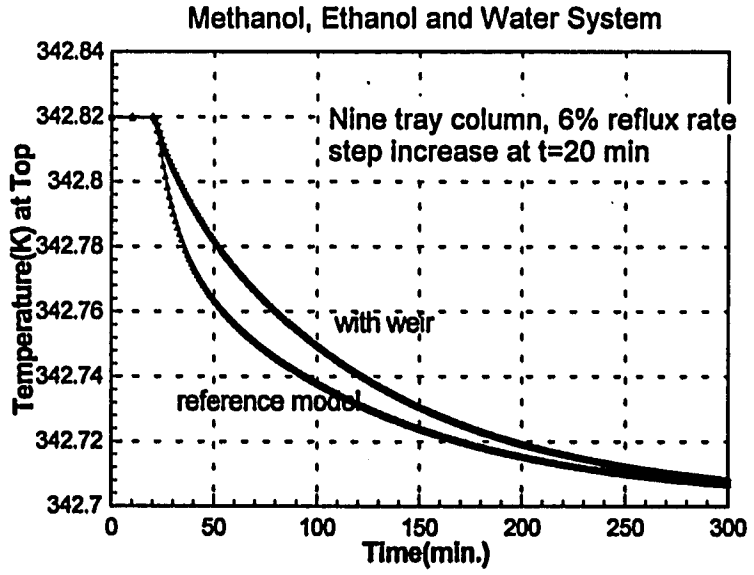

Figure 4-10. Rigorous Column Model-Effect of Weir Dynamics

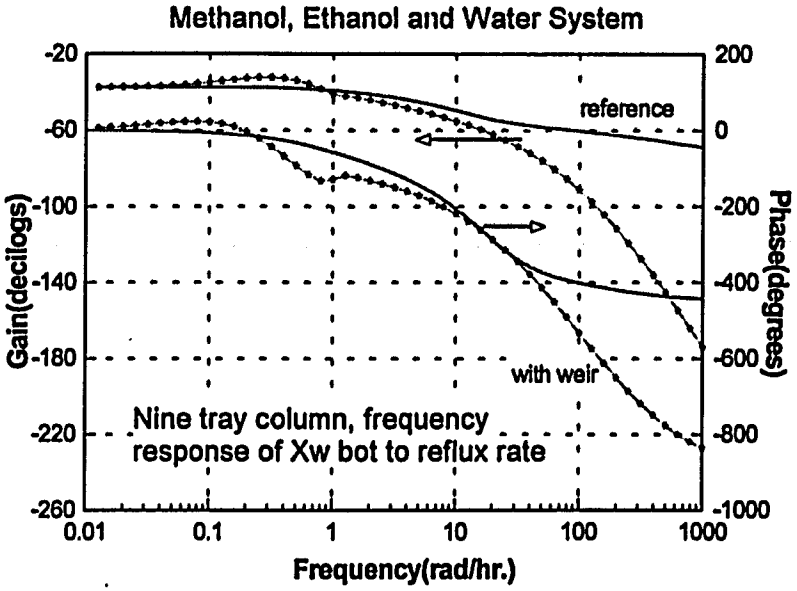

Figure 4-11. Rigorous Column Model-Effect of VLE on Composition

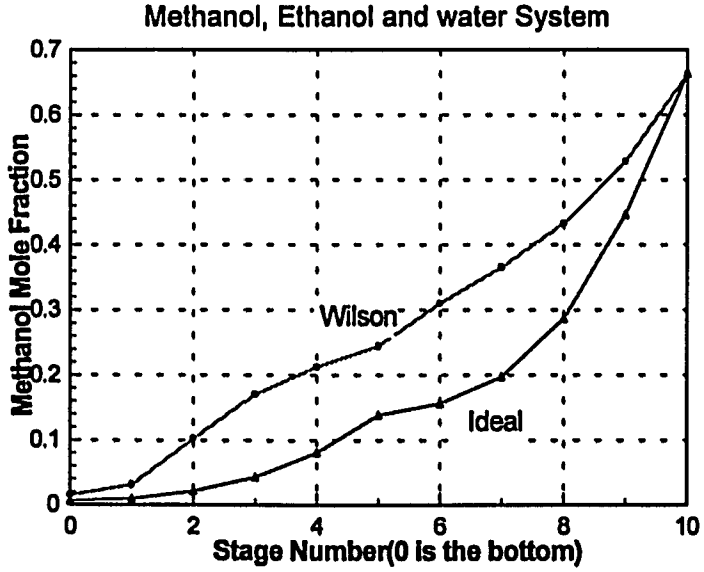

Figure 4-12. Rigorous Column Model-Effect of VLE on Composition

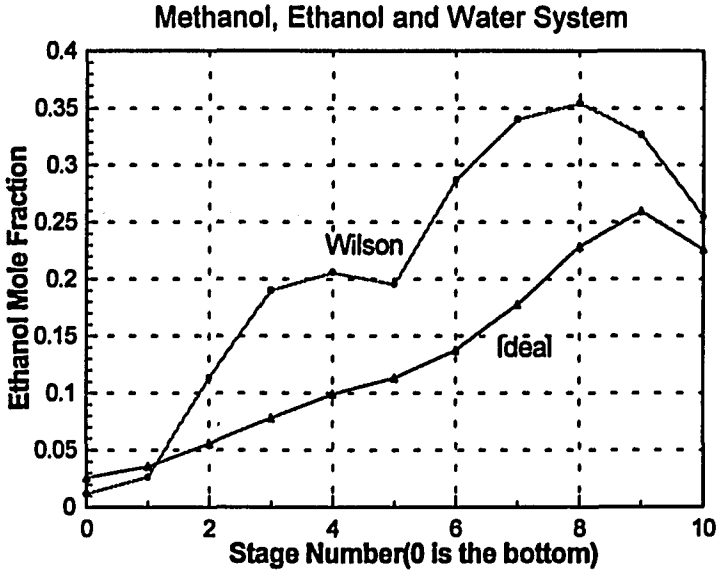

Figure 4-13. Rigorous Column Model-Effect of VLE on Composition

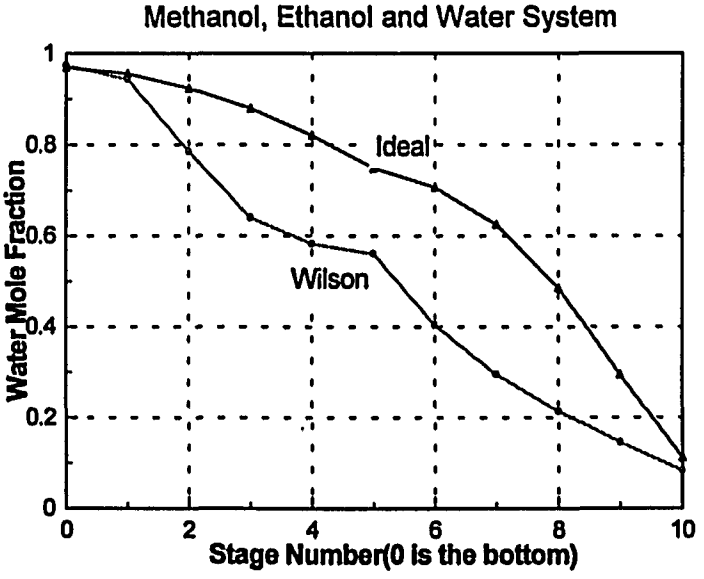

Figure 4-14. Rigorous Column Model-Effect of VLE on Temp.

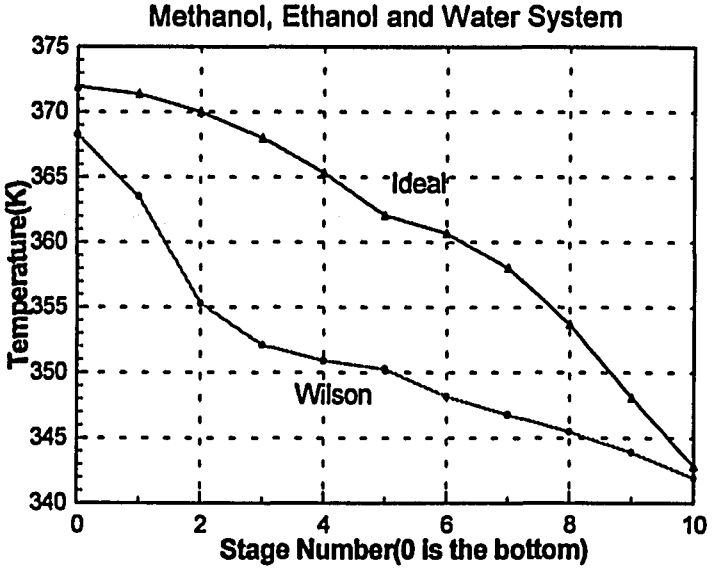

Figure 4-15. Rigorous Column Model-Effect of VLE on Volatility

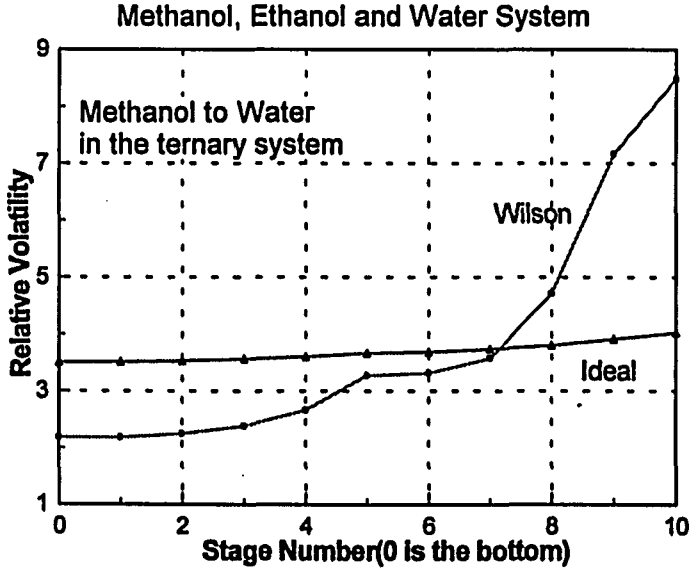

Figure 4-16. Rigorous Column Model-Effect of VLE on Volatility

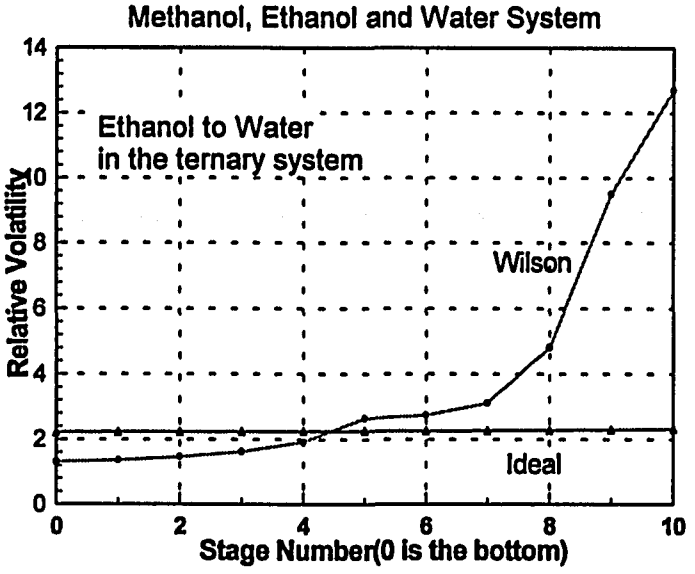

Figure 4-17. Rigorous Column Model-Effect of VLE on Flow Rate

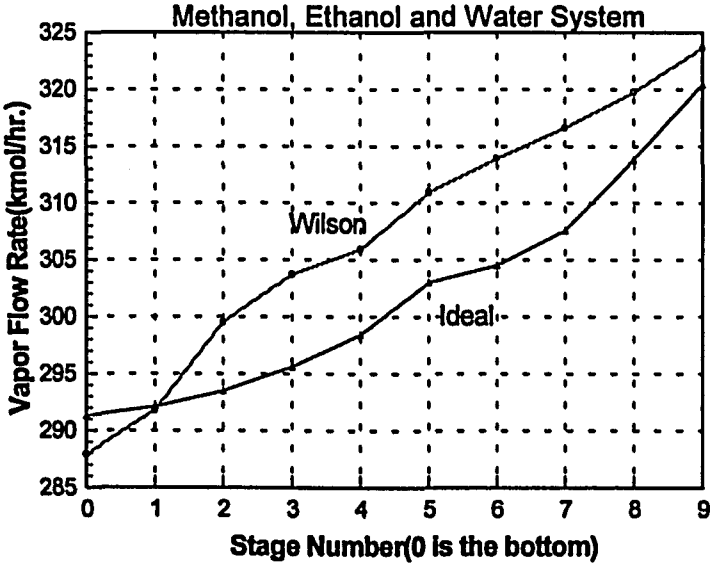

Figure 4-18. Rigorous Column Model-Effect of VLE on Flow Rate

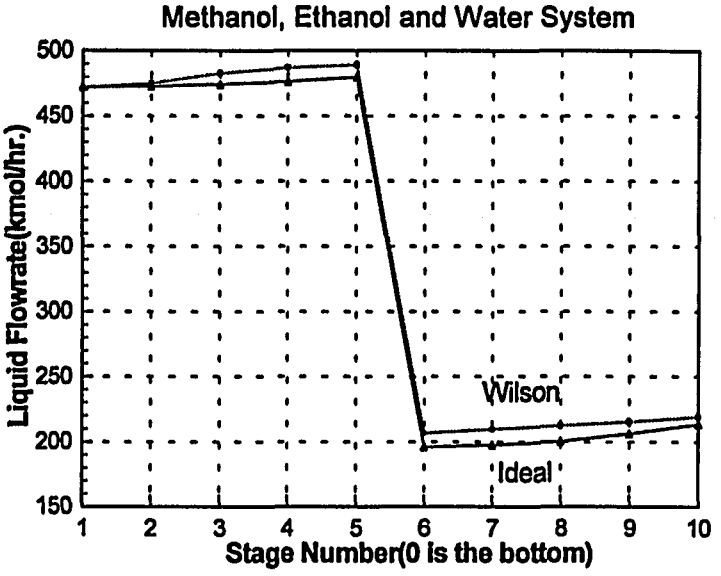

Figure 4-19. Rigorous Column Model-Effect of VLE on T bot

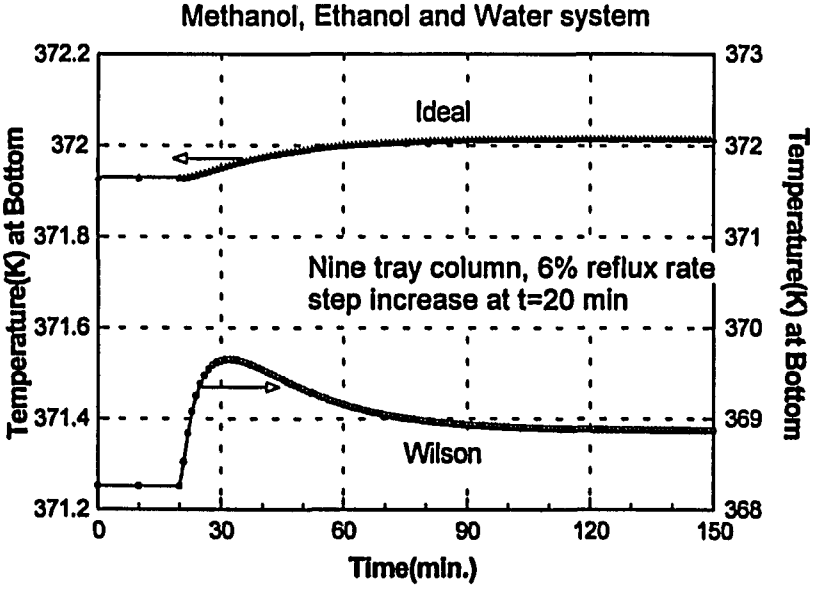

Figure 4-20. Rigorous Column Model-Effect of VLE on Composition

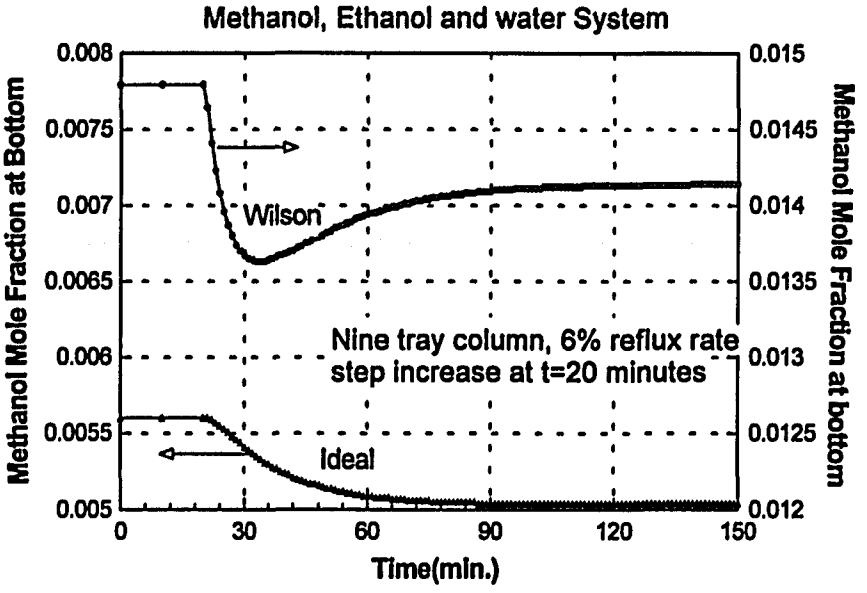

Figure 4-21. Rigorous Column Model-Effect of VLE on Composition

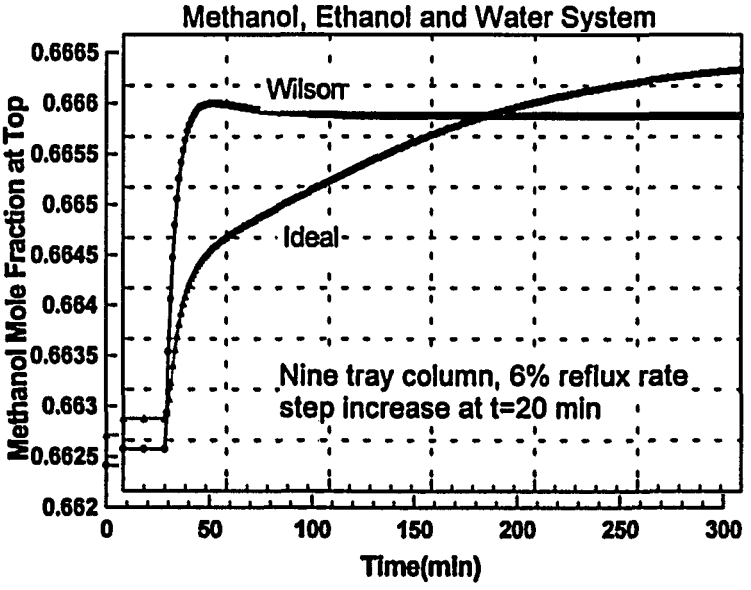

Figure 4-22. Rigorous Column Model-Effect of VLE on Temp.

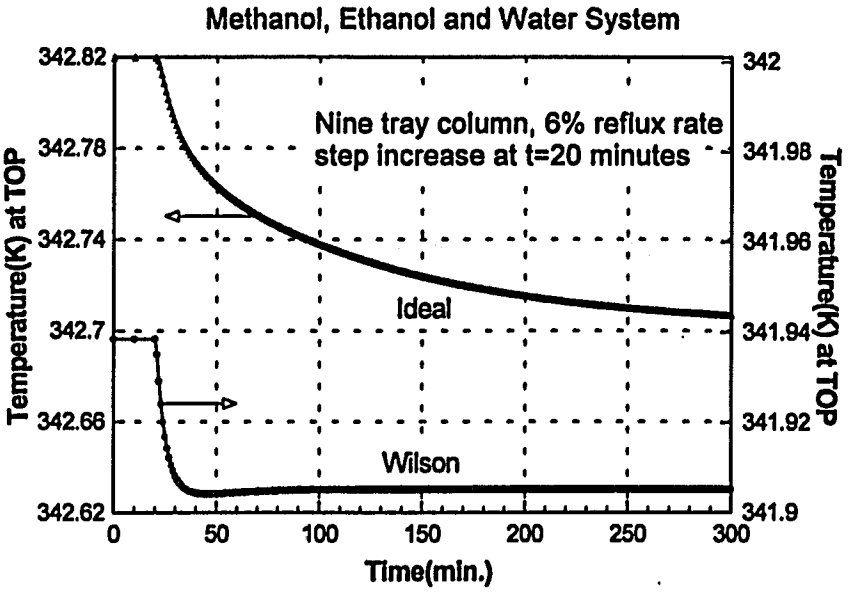

Figure 4-23. Rigorous & CMO-with Ideal K Model

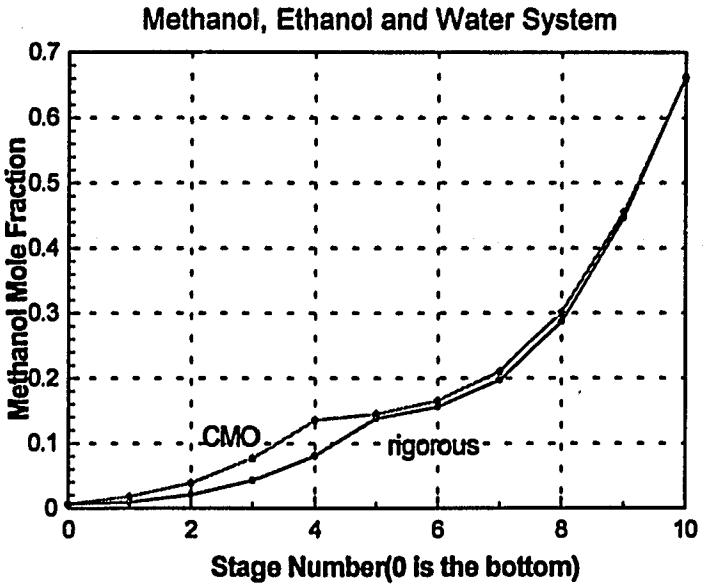

Figure 4-24. Rigorous & CMO-with ideal K Model

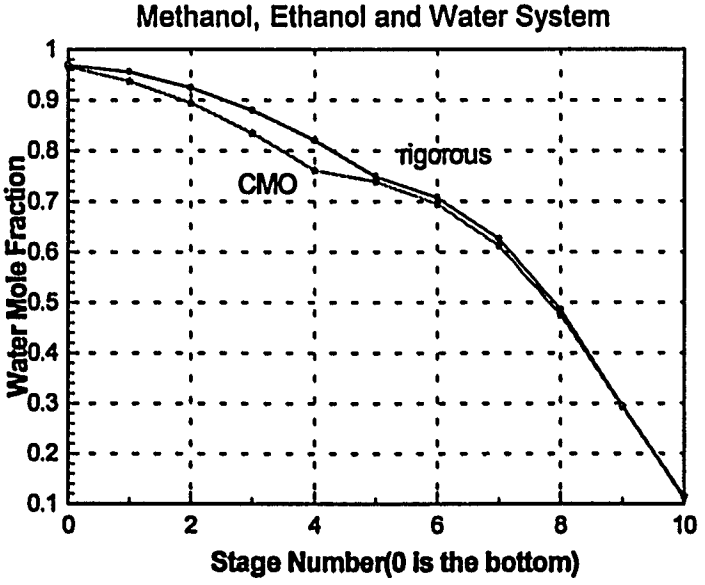

Figure 4-25 Rigorous & CMO-with Wilson K Model

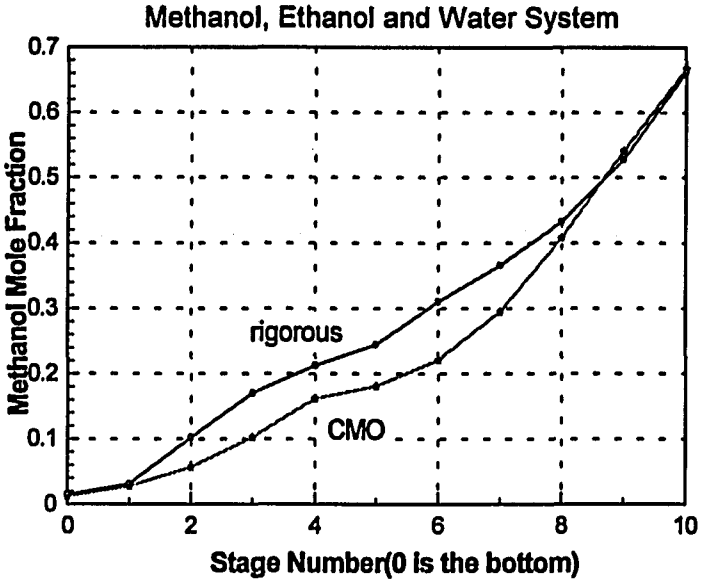

Figure 4-26. Rigorous & CMO-with Wilson K Model

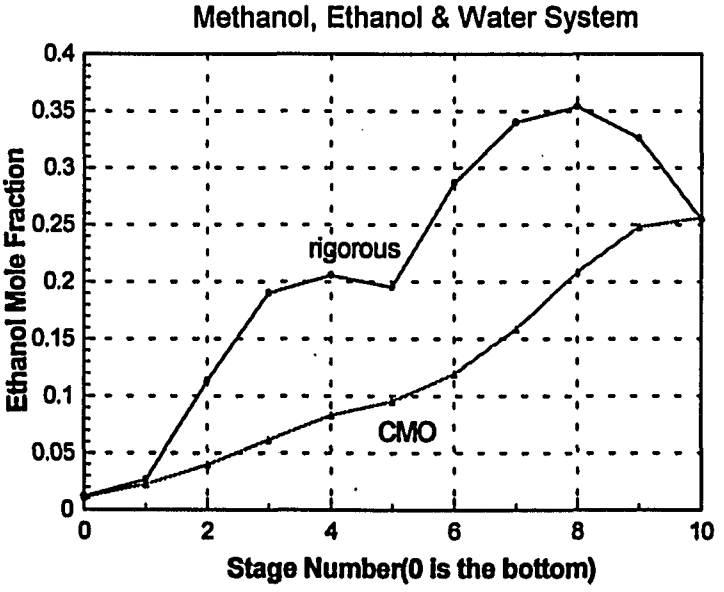

Figure 4-27. Rigorous & CMO-Response to Reflux Rate Change

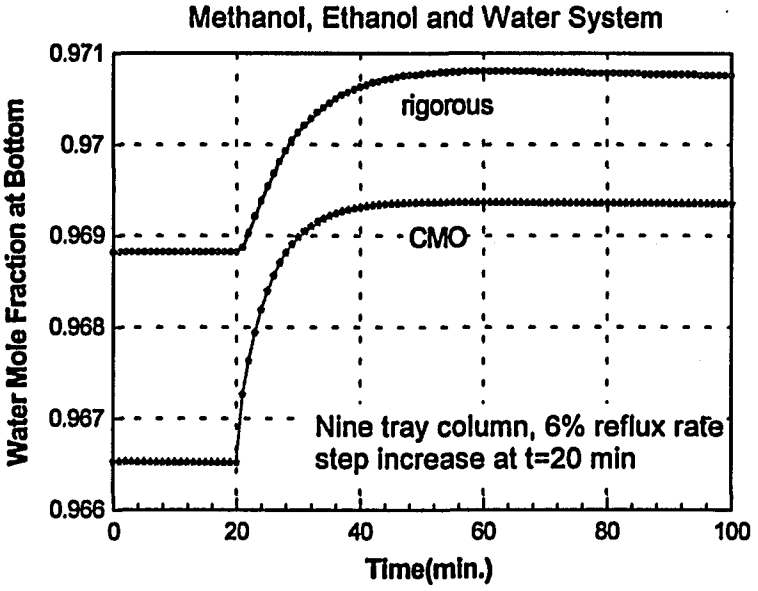

Figure 4-28. Rigorous & CMO-Response to Reflux Rate Step Change

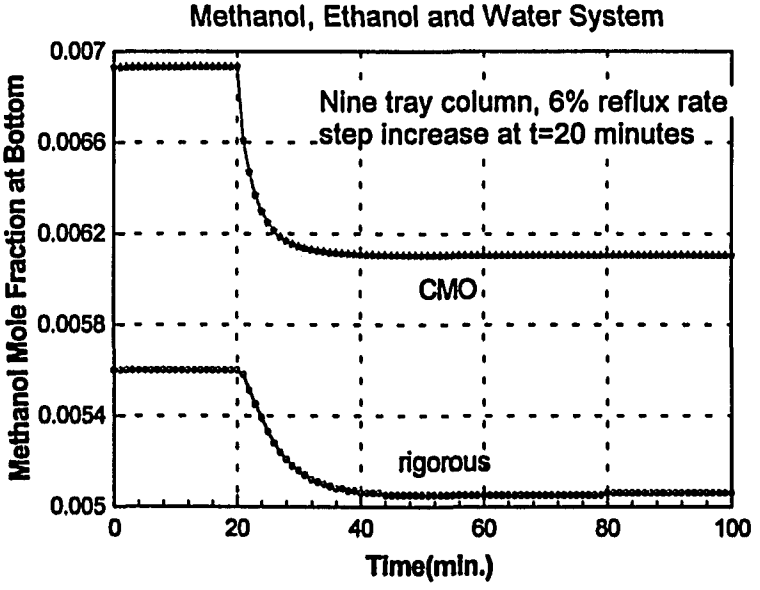

CHAPTER FIVE. EFFECTS OF MODEL COMPLEXITY

In the previous three chapters the effects of physical properties models and model on model structure were evaluated. In this chapter we turn the effects these factors have on model complexity or, in other words, the price that must be paid for a given level of model fidelity.

Some of the effects are obvious. For instance, if one chooses to include the downcomer mixing in a distillation column model, the number of ODE's that must be solved is doubled. The CPU time requirements are not, however, since the right-hand-sides of the ODE's for the downcomer are much simpler than those for the tray itself. If one chooses to use the Wilson Equation for VLE rather than Raoult's Law, the CPU requirements are also increased. What is not so obvious is the effect of model complexity on the difficulty of integrating the model ODE's as measured by the stiffness ratio or on the sensitivity of the models to modeling error as measured by the condition number.

Before proceeding, let us review the what is required of integration methods for ODE's. The selection of such methods is an important part of dynamic simulation. In this selection one must consider accuracy, the robustness, and CPU time. In our simulation work, three different integration sources were used. These are the well known methods of Euler and Runge-Kutta as well as the LSODE package. Before we compare the different integration methods, let us briefly introduce LSODE (Livermore Solver for Ordinary Differential Equations). It provides two integration methods, one or the other of which must

be chosen *a priori* by the user. These are Adams predictor-corrector method for non-stiff problems and the method of Gear based on Backward Differentiation Formulas (BDFs) for stiff problems. There are several Method Flags (MF) for either non-stiff or stiff problems. Some of them are examined with our simulations. These are listed in Table 5-1.

Table 5-1. Method Flags in the LSODE Package

MF	Mathematical Methods
10	Implicit Adams is used and the Jacobian matrix is not used
20	BDFs is used and the Jacobian matrix is not used
21	BDFs is used and user-supplied full Jacobian matrix is used
22	BDFs is used and internally generated Jacobian matrix is used
23	BDFs is used and internally generated diagonal Jacobian matrix is used

In order to illustrate the general application of Lsode, a simple ODEs is prepared with the initial values: X1(0) = 1, X2(0) = 0.

$$(5-1)\quad \frac{dX_1}{dt} = 999998X_1 + 199998\,X_2$$
$$\frac{dX_2}{dt} = -999999X_1 - 199999\,X_2$$

The stiffness ratio of the above ODEs is 100000. Some CPU times for same simulation time interval with different choices of MF are listed on Table 5-2. One advantage of the LSODE package is that different MF's may be applied to different problems. The methods for MF=21 and MF=22 save considerable CPU time in this stiff problem.

Table 5-2. Different CPU Times with Different Method Flags

MF	No. of STEPs	No. of FCNs	No. of JACs	CPU Time(sec.)
10	1995728	2081991	0	426
20	----	----	0	330
21	179	209	26	2.0
22	196	292	28	2.2

Here STEPs refers to the number of integration steps required; FCNs, the number of right-hand-side function evaluations required; and JACs, the number of Jacobian evaluations required. The CPU time is that for a DECstation 3100.

5.1 Accuracy Analysis for Different Integration Methods

To compare accuracy of Euler, Runge-Kutta and LSODE in dynamic simulation, a simple piping spool piece with a valve is chosen as an example. The time constant of the valve position change is 0.005 hr. The initial value is X(0) = 41.3397.

$$\frac{dX}{dt} = 200\,(70 - X) \qquad (5.1-1) \quad (3)$$

A ten-minute simulation was done using each of the numerical methods described above. The analytical solution is also listed in for comparison. The accuracy for LSODE can be found on the Table 5-3; that for Runge-Kutta and Euler in Tables 5-4 and 5-5 respectively . In Tables 5-6 and 5-7 are shown the effects of step size and tolerance on accuracy using LSODE.

Table 5-3. The Accuracy of LSODE. (MF=10, Tolerances: 10 E-5, CPU time: 10 sec.)

Time(min)	Analytical solution	Lsode	Relative Errors %
0	41.3397	41.3397	0
0.01	42.2792964	42.2793749	-0.00018567
0.05	45.7395798	45.739947	-0.00080281
0.1	49.4639977	49.4646317	-0.00128174
0.5	64.5867686	64.5856299	0.001763055
1	68.9775726	68.9742174	0.00486419
5	69.9999983	69.9999979	0.000000571
10	70	70	0

Table 5-4. The Accuracy of Runge-Kutta. (Step size: 0.0005, CPU time: 101 sec.)

Time (min)	Analytical solution	Runge-Kutta	Relative Errors %
0	41.3397	41.3397	< 10 E-8
0.01	42.2792964	42.2792964	< 10 E-8
0.05	45.7395798	45.7395798	< 10 E-8
0.1	49.4639977	49.4639977	< 10 E-8
0.5	64.5867686	64.5867686	< 10 E-8
1	68.9775726	68.9775726	< 10 E-8
5	69.9999983	69.9999983	< 10 E-8
10	70	70	< 10 E-8

Table 5-5. The Accuracy of Euler. (Step size: 0.0001, CPU time: 127.4 sec.)

Time (min)	Analytical solution	Euler	Relative Errors %
0	41.3397	41.3397	0
0.01	42.2792964	42.2794504	-0.0003642445
0.05	45.7395798	45.7402552	-0.0014766205
0.1	49.4639977	49.4651457	-0.0023208799
0.5	64.5867686	64.5882745	-0.0023315921
1	68.9775726	68.9781412	-0.0008243259
5	69.9999983	69.9999983	0
10	70	70	0

Table 5-6. The Effect of User-Specified Error Tolerance in LSODE (MF=10)

Time (min)	Analytical solution	Tol. =0.00000001	Tol.=0.00001
0	41.3397	41.3397	41.3397
0.01	42.2792964	42.2792966	42.2793749
0.05	45.7395798	45.7395807	45.739947
0.1	49.4639977	49.4639993	49.4646317
0.5	64.5867686	64.5867553	64.5856299
1	68.9775726	68.9775733	68.9742174
5	69.9999983	69.9999984	69.9999979
10	70	70	70

Table 5-7. The Effect of Step Size in LSODE (Tolerances: 10 E-5, MF=10)

Time (min)	Analytical solution	Lsode	Relative Errors %
Step size 0.01			
0	41.3397	41.3397	0
0.01	42.2792964	42.2793749	-0.0001856701
0.1	49.4639977	49.4646317	-0.0012817403
Step size 0.1			
0.5	64.5867686	64.5856318	0.00176011283
1	68.9775726	68.9776058	-0.0000481316
step size 1.0			
5	69.9999983	69.9998517	0.00020942858
10	70	69.9999883	0.000017

We can interpret and summarize the above comparisons as follows.

1. For a simple first order ODE, all numerical results are quite accurate. The errors are less than or near 10^{-5}.

2. The step size for Euler integration method is evaluated according to the absolute stability requirement:

$$-\lambda h \leq 2$$

where the λ is the eigenvalue of the ordinary differential equation and the h is the integration step size. In this example, λ is -12000/min, so that the step size should less than 0.00016

minutes. 0.0001 is chosen as step size here. The step size for Runge-Kutta integration method is difficult to evaluate. In this comparison, this step size is selected as five times as that for Euler integration method, It is 0.0005 minutes. The tolerance in LSODE is 10^{-5}.

3. In Tables 5-3 to 5-5, all show good accuracy, the Runge-Kutta being the best. If the CPU time is examined, LSODE is the best. The CPU for LSODE is 10 seconds, one-tenth of that for Runge-Kutta. The Real Time Factor (RTF) with LSODE is 60; for Runge-Kutta it is 6, while for Euler it is 4.7.

4. The integration errors with Lsode are controlled by a user-specified tolerance that is shown in Table 5-7. Table 5-6 shows how the step sizes effect the results. When the step size is 0.01, the accuracy is better than that from Euler method. When the step size is one, the accuracy is worse than that from Euler method. If the step size is reasonable it does not effect the accuracy requirement. But if the step size is big enough, i.e. 100, in this problem, it interrupts the integration progress. This is because the maximum number of internally defined steps allowed during one call to the LSODE solver is 500 (the default value).

5.2 Timing the Staged Separation Simulations

When we use different integration methods to do different process simulations, it is difficult to say which method is always the best. Examining real time factors (RTF) with different integration methods is one way to evaluate and select an integration method for a particular type of dynamic simulation. As previously mentioned, the RTF is defined as the process time interval simulated divided by the CPU time required for the simulation. The larger the RTF, the less time the simulation takes. Needless to say, the RTF is depends upon the type of computer for the simulation. The results reported here are for a DECstation 3100.

For the fixed step size integration methods, the step size affects the RTF. For adjustable step size integration methods, the tolerance affects the RTF. In order to examine different integration methods, we use the same program (model) with step sizes or error tolerance chosen to give the same accuracy.

Three different simulations are examined as follows: a two-component Kremser absorber, a CMO model distillation column, and a rigorous model distillation column. The process time is 50 minutes with a dynamic response after a input step change. The step size is adjusted so that a maximum error of no more than 10^{-6} between a run made with the selected step size and one half that size is observed. We record both the CPU time for the entire simulation and the loop CPU time required just for the integration loop calculation.

In the two-component Kremser absorber simulation, different relative volatilities,

say 1.5 (stiffness ratio is 70) and 1500 (stiffness ratio is 8000) are examined. The two-component Kremser absorber model is a set of pure, first order ordinary differential equations. It is clear that the RTF is smaller when the stiffness ratio is larger for any integration method. LSODE is intended for this kind of problem. Comparing the RTFs in the Table 5-8, LSODE is the best method in the all three choices. The method of MF = 22 is better than that of MF = 10. It is reasonable because the MF=22 has the aid of Jacobian and is good for the stiff problems. The Runge-Kutta method is better than the Euler method. The RTF of LSODE is more than five times as much as that with Euler method. Comparing the whole CPU time and the loop CPU time, the most time is consumed in the loop integration. The input data collection for the model integration costs only a little time.

Table 5-8. Real Time Factors of Kremser absorber Simulation

Integration Method	Euler		Runge-Kutta		LSODE(MF=10)		LSODE(MF=22)	
Trays	10		10		10		10	
ODE's	20		20		20		20	
Simulation Time(min)	50		50		50		50	
K2/K1	1.5	1500	1.5	1500	1.5	1500	1.5	1500
SR	70	8000	70	8000	70	8000	70	8000
Step Size(min) or tolerance	0.02	2E-5	0.01	1E-4	10 E-6		10 E-6	
Whole CPU Time(s)	14.2	637	16.6	879	2.7	87.8	1.9	3.9
RTF	211	4.7	181	3.41	1111	34.2	1579	769
Loop CPU Time(s)	13.2	636	15.5	978	1.48	86.8	0.9	3

In CMO distillation simulation, five-tray and thirty-tray columns are examined. It is clear that the more trays the column has, the smaller the RTF is with the same integration method. There are two points that are different from the above Kremser absorber simulation. The first is that the RTFs show at almost same level on Table 5-9. The second is that MF=22 is not helpful for this kind of stiff problem of the 30 tray column. The RTF is about one tenth of that with MF=10. The CMO distillation simulation is a stiff problem with a stiffness ratio of 2000. This model involves very non-linear differential equations. After each step of integration, according to the new composition, a new set of K values is recalculated for the next step of integration which interrupts this method and the function of Jacobian matrix in the MF=22. For a thirty tray CMO model, when we use MF=22, there are 10186 integration steps, the FCN is called 738040 times and 7945 Jacobian evaluations are made. Instead for MF=10, there are 10482 integration steps, the FCN is called 19335 times. This result is very different from that in the gas absorber simulation. For a K2/K1=1500 model, when we use MF=22, there are 68 integration steps, there are 401 FCN calls and 16 Jacobian evaluations. Instead for MF=10, there are 86288 integration steps, 157604 FCN calls. In the absorber example, for MF=22, the Jacobian evaluation greatly reduces the FCN evaluation and integration steps.

In this CMO simulation, LSODE with MF=10 is slightly better than the others when the number of trays is lower but Runge-Kutta and Euler are better than LSODE when the number of trays is higher.

Table 5-9. Real Time Factors of CMO Distillation Simulation:

Integration Method	Euler		Runge-Kutta		LSODE MF=10		LSODE MF=22	
Trays	5	30	5	30	5	30	5	30
ODE's	15	90	15	90	15	90	15	90
Simulation Time(min)	50	50	50	50	50	50	50	50
Step Size (min) or tolerance	0.01	0.01	0.05	0.05	10 E-6		10 E-6	
Whole CPU Time(s)	7	15.3	7.5	18	6.7	20.2	6.8	228
RTF	429	197	400	167	448	148	441	13
Loop CPU Time(s)	5.7	14	6.2	16.7	5.5	18.9	5.6	226.7

In the rigorous distillation column simulation, the effect of property models on RTF is examined. Two K value models are used for the distillation simulations: Ideal and Wilson. It is clear that the Wilson model makes the simulation time much longer than the Ideal model. Because of the nonlinearity of the simulated system, methanol, ethanol and water, the step size must be smaller to meet the predetermined accuracy, 10E-6. Euler, Runge-Kutta and LSODE(MF=10) are used. Table 5-10 shows that the Runge-Kutta method performs a little bit better than other methods when the Ideal K value model is used. On the other hand, the LSODE (MF=10) is better than others when the Wilson model is applied.

Table 5-10. Real Time Factors of Rigorous Distillation Simulation:

Integration Method	Euler		Runge-Kutta		LSODE(MF=10)	
Trays	11		11		11	
ODE's	48		48		48	
Simulation Time(min)	50		50		50	
Property Model	Ideal	Wilson	Ideal	Wilson	Ideal	Wilson
Step Size(min) or tolerance	0.025	0.01	0.1	0.05	10 E-6	
Whole CPU Time(s)	197.5	589.7	191	466.4	243.3	309.4
RTF	15.2	5.1	15.7	6.43	12.3	9.7
Loop CPU Time(s)	196.4	588.4	189.7	465.1	242	308.1

From Table 5-8 to table 5-10, the loop CPU time is listed also. The loop CPU time is very close to the whole CPU time. The differences between the two CPU times are one to two seconds in the all three simulations. The main time consumed is in the integration loops. If we consider the time consumed on each ODE equation(short for TCE), the result depends on the complexity of the mathematical models and program structures. In the Kremser model simulation, the TCE is 0.135 seconds for the relative volatility of 1.5 and 0.195 for 1500. In the CMO distillation simulation, the TCE is 0.45 seconds for the five-tray column but 0.17 for the thirty-tray column. In the rigorous distillation simulation, the TCE is 4.0 seconds for the Ideal K value case and 6.4 seconds for the Wilson K value case. The TCE of the bigger size CMO distillation simulation looks to be an exception.

5.3 Considerations in Stiff Absorber Problems

It is well known that the pressure dynamics makes the absorber model #4 and #5 (refer to Chapter three) very stiff. The stiffness ratio and condition number for different absorber models are listed on Table 5-11.

Table 5-11. Stiffness ratio and condition number of different absorber models

	Model #1	Model #2	Model #4	Model #5
Condition No.	13.90	70.25	7.16E4	6.80E5
Stiffness Ratio	13.80	63.10	7.14E4	7.54E5
RTF	5000.	4000.	0.660	0.530

The condition number of the process Jacobians and stiffness ratio of all the above models are examined at S=0.9 and five trays. It is clear that the Model #4 and Model #5 are very stiff problems.

Fig. 5-1 shows the relationship of the stiffness ratio to number of trays and different models(Kremser model and Model #4). With the number of trays increases, the stiffness ratio increases also. The stiffness ratio of Model #4 is much bigger than that of the reference model. The above examinations show that the condition numbers and stiffness ratio increase with the complexity of models.

For most problems, we must consider more than one component being absorbed. For

example, when one absorbs an organic material mixed in air, air can be slightly absorbed in the absorbent also. The absorbed air may be deabsorbed somewhere else in the process and this must be taken into account in modeling the system. In this case, we would like to simulate not only the fate of the main component, but also the fate of the absorbed air. The K-value of air (K2) is much larger than that (K1) of the main component. This situation causes stiffness problems in the dynamic simulation of multi-component absorption.

In multi-component absorption problems, stiffness ratio (SR) is a function of the relative volatility (K2/K1) of components, the stripping factor for the main component, and the number of trays.

We examine the relationships between volatility and number of trays when the main component stripping factor(S1) is fixed to 0.9. As the relative volatility increases, the condition number and stiffness ratio of the model increase very sharply, which is shown in Figs. 5-2 and Fig. 5-3. For a ten-tray gas absorber, if the volatility is 10, the SR is about 120, but if the volatility is 500, the SR increases to 6000.

Further examination shows that not all high volatilities result in a high SR. Fig. 5-4 to Fig. 5-5 show the SR distributions based on Kremser gas absorber model with different main stripping factor(S1), different volatilities(K2/K1), and different number of trays. The interesting results are:

1) Not all large volatilities result in stiff problems unless the main stripping factor (S1) is near one.

2) The stiffness ratio increases very rapidly with increasing volatility or number of trays.

From Fig. 5-4 and Fig. 5-5, we can estimate which problems are non-stiff (SR is less than 50) and which are stiff (SR is bigger than 500). In most gas absorbers, the design is such that S1 is 0.6 to 0.7. So, the problem will be stiff if the other components with high volatilities are present.

The composition profiles for a ten-tray absorber are examined with different stripping factors. From steady-state point of view, when the stripping factor is very small, e.g., 0.01, this component will be absorbed almost entirely in first few trays. (In this example, assume the ratio of vapor flow rate to liquid flow rate is one). When a stripping factor is one, 95% of this component can be absorbed and a clear concentration gradient is there from the bottom tray to the top tray. If a stripping factor is large, e.g., 100, only 1% this component will be absorbed by the first tray and almost there is almost no gradient from tray to tray. So, only when the stripping factor is near one are the composition dynamics distributed over the entire absorber.

From dynamic point of view, when a stripping factor is one, 2.5 seconds of CPU time are required to simulate 200 minutes of real process time at steady-state. It takes 5.2 minutes for the response to a step change to approach 99% of the final steady-state value. But when a stripping factor is 100, we use 45 seconds CPU time to simulate the same real process time. It takes 0.1 minutes for the response to a step change to approach 99% of the final steady-state value. It is clear that the latter costs much more CPU time. But the response is much

sharper than that of the former. In this example, the resident time is 30 seconds with the fixed step Runge-Kutta method.

To avoid and solve stiff problems in multi-component absorption, four methods are recommended:

1) Include the vapor holdup in total holdup to reduce the stiffness ratio.

It was mentioned before that if the K-value is large, the vapor phase holdup can not be neglected. So for components of large volatility, retaining the vapor phase holdup term in the dynamic models can greatly reduce the stiffness ratios. Fig. 5-6 follows the same conditions as Fig. 5-3, but includes the vapor phase holdup in the total holdup term. After including the vapor phase holdup, the SR is clearly reduced. For example, when the volatility is 500, the stiffness ratio is 940 instead of 6000.

2) Approximation of algebraic equation

In fact, the fast response is so fast that we suggest using an algebraic equation to replace the fast response ordinary differential equation. This approximation gives less than 1% relative error after 0.1 minute of dynamic simulation in our example. This alternative can save considerable simulation time. It is suggested that the volatility at which this alternative should be considered is 100.

3) Use different simulation steps

Because the two components do not affect each other, another method is suggested

to do that simulation. We estimate the time constants for both component dynamics. We use smaller integration step for the fast response and then larger integration step for the rest. So we can avoid using small integration steps for whole simulation, and we can save CPU time. However, this approach cannot be used if there is interaction between the components, for instance, if the absorber is nonisothermal.

4) Choose appropriate integration method for stiff problem

As an example, a ten-tray and two-component absorption is illustrated. The real process time is 170 minutes. We examined different situations, such as with or without vapor phase holdup, different volatilities(K2/K1). The run statistics with vapor phase holdup are listed in Table 5-12. The run statistics without vapor phase holdup are listed in Table 5-13.

Table 5-12. RTF with different MF for different stiff problems with vapor phase holdup

K2/K1	SR	MF	#STEPs	#FCNs	#JACs	Time(s)	RTF
50	740	10	474606	870037	0	450	22.7
		20	469705	860416	0	440	23.2
		21	102	123	24	4.3	2372
		22	102	603	24	4.5	2267
500	1700	10	2141256	3925092	0	1990	5.12
		20	2142343	3927279	0	1983	5.14
		21	110	132	25	4.5	2267
		22	110	632	25	4.6	2217

Table 5-13. RTF with different MF for different stiff problem without vapor phase holdup

K2/K1	SR	MF	#STEPs	#FCNs	#JACs	Time(s)	RTF
2	67	10	47059	86104	0	48.5	210
		21	69	86	18	4.0	2550
5	120	21	80	94	18	4.2	2429
50	3000	21	103	124	23	4.5	2267
		22	103	584	23	4.6	2217
500	6200	20	4364134	7998492	0	4120	2.5
		21	112	135	25	4.6	2217
		22	112	635	25	4.7	2170
		23	976	3108	881	5.8	1759

5.4 Conclusions

1. The simple ODE test tells us that all integration methods used above, namely, Euler, Runge-Kutta, and LSODE, can meet the accuracy requirements. LSODE is the fastest and Runge-Kutta gives the best accuracy. Euler can perform at the same level as Runge-Kutta, but takes more time.

2. In real process simulation, the selection of integration methods depends on the model complexities. If the mathematical model is composed of algebraic and differential equations and the differential equation part is very non-linear, LSODE is not the good choice. Runge-Kutta is recommended in this situation. If the differential equation part is linear, LSODE is the best choice, especially for stiff problems.

3. For the absorber problem, the Adams method (MF = 10) does not work for stiff

problems, and the simulation takes a lot of CPU time. Though MF = 20 is a BDF algorithm, there is not much advantage compared with MF=10 for this simulation. But MF=21 and MF=22 are greatly superior to MF=10 and MF=20. There are almost no differences between K2/K1=50 and K2/K1=500, even if vapor phase holdup is neglected. MF=23 has no advantage compared to MF=21 or MF=22. MF=21 looks a little bit better than MF=22. In summary, for multi-component absorber simulations, we can either use an algebraic equation formulation to approximate the stiff ODEs or use MF=21 or MF=22 in the LSODE package to integrate the stiff problems.

Figure 5-1: Absorber Models-Stiffness Ratio vs. Trays

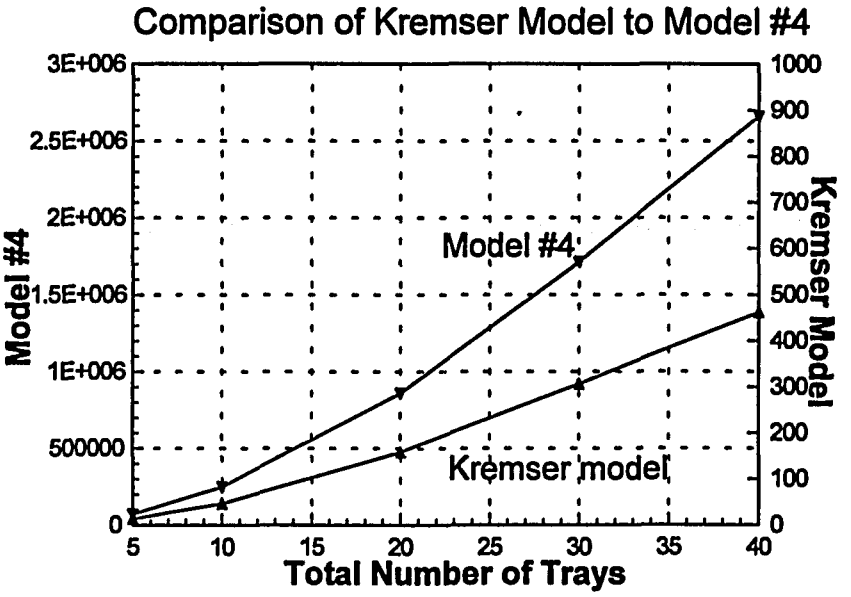

Figure 5-2: Absorber Model-Effect of Volatility

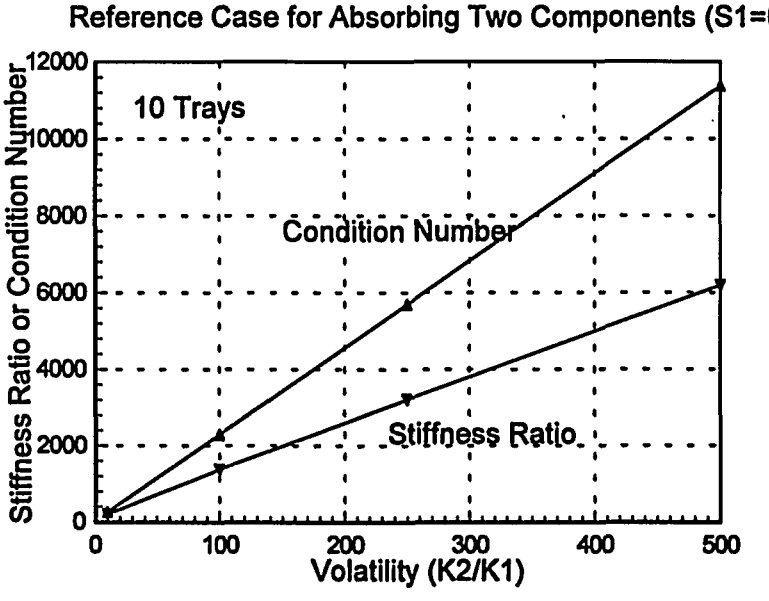

Figure 5-3: Absorber Model-Effect of Volatility

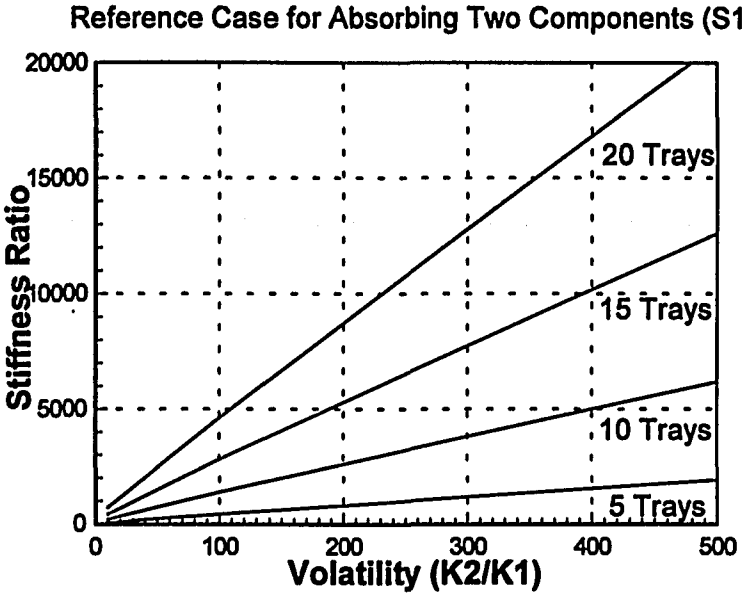

Figure 5-4: Stiffness-Effect of Stipping Factor

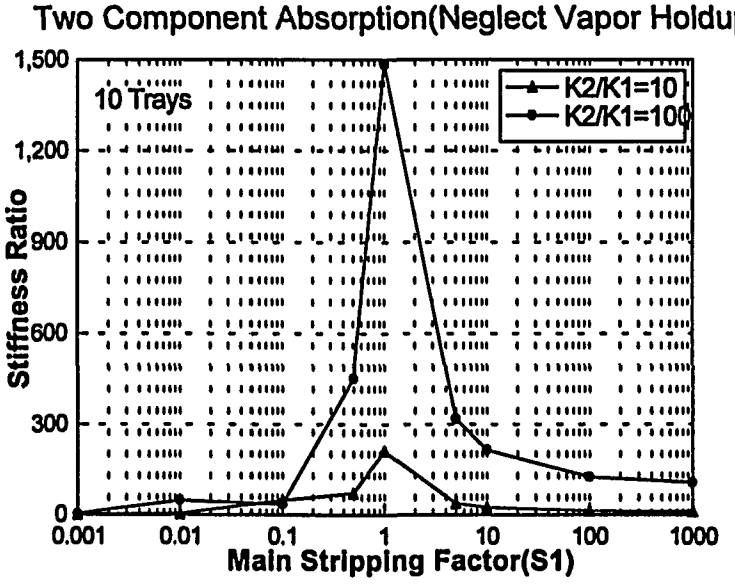

Figure 5-5: Stiffness-Effect of Stripping Factor

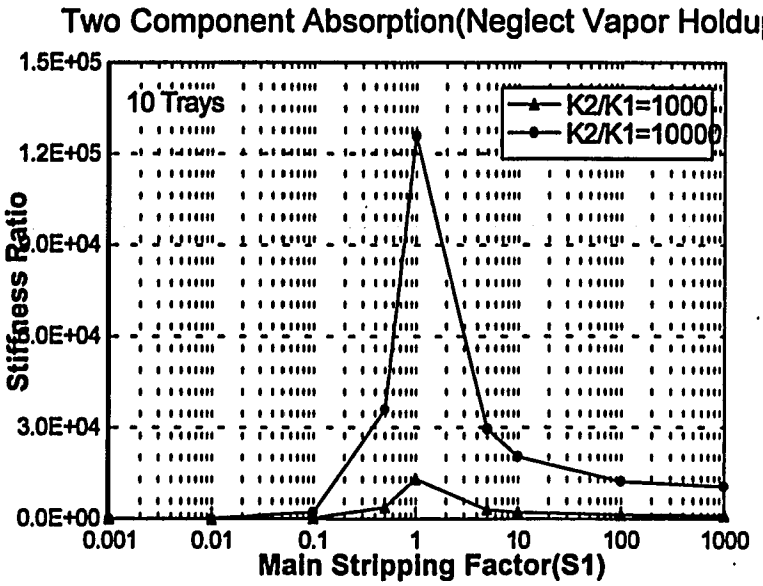

Figure 5-6: Stiffness-Effect of Volatility

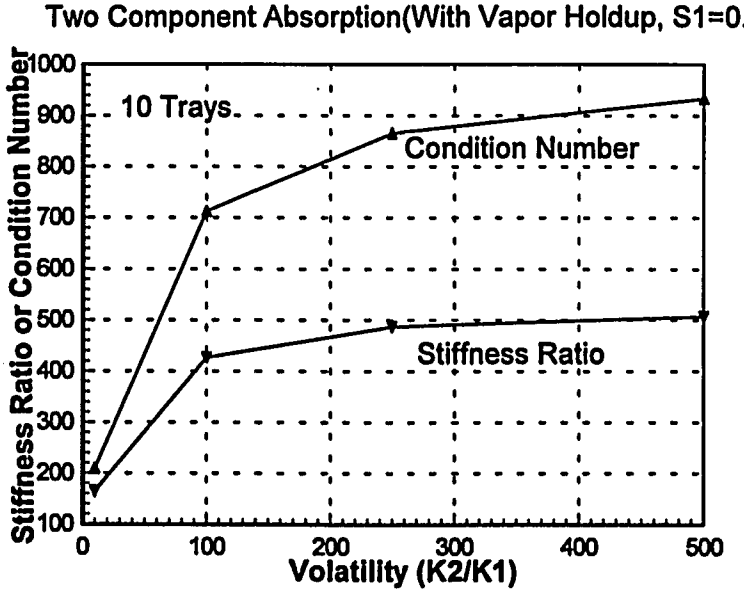

CONCLUSIONS AND RECOMMENDATIONS

A number of conclusions can be drawn from this work that should useful to systems engineers responsible for the dynamic modeling of process systems.

(1) The index A (as developed in Chapter Two) for correlating the effects of the non-ideality of VLE models on model fidelity appears useful forchoosingg the appropriate VLE model. The critical value for this index, at least with regard tochoosingg between the Wilson and Ideal K-value models is 1.0. Under no circumstances should the Ideal VLE model be used if this index exceeds 1.5. Further, if the mixture contains azeotropes, then a non-ideal VLE should definitely be used.

(2) Except for systems containing components of very high volatility (such as slightly soluble supercritical components in gas absorption), the vapor phase holdup can be neglected compared to the liquid for most types of equipment. An exception would be a flash drum operating with a very low liquid level. For almost all distillation systems, the vapor phase holdup can be neglected. An index R was developed in Chapter Three which allows one to decide whether or not to include the vapor phase holdup.

(3) The dynamic effects introduced by variable flow-over-the-weir on distillation and gas absorber trays should be included in any model if liquid flow rate changes are anticipated. Outlet composition responses to inlet composition changes are not affected. This is not a severe requirement since it only increases the number of ODE's per stage by one.

(4) On the other hand, downcomer dynamics can be important with respect to the response of outlet compositions to inlet composition changes. Neglecting the downcomer dynamics appears to be acceptable out to the critical frequency for components whose stripping factor is near unity. More volatile components ($S > 10$) will be significantly affected by neglecting the downcomer dynamics. Including the downcomer dynamics will approximately double the number of ODE's per stage.

(5) Another important decision is whether or not to use a non-equilibrium stage model. Our results show that if the liquid phase holdup is prorated for an ideal-tray model so that the total liquid holdup is the same as that the non-ideal column would have, then responses to changes in total flow rates are essentially the same. However, the response to composition dynamics is significantly different, primarily due to the higher order of the non-ideal tray model (more stages than the ideal tray model). A non-ideal tray model is recommended even though this can significantly increase the number of ODE's required for the column model.

(6) Due to its simplicity, the CMO model is attractive for dynamic distillation modeling. However, it should not be used if the system is significantly non-ideal as indicated by index A.

(7) Most multi-stage dynamic models are both stiff and ill-conditioned, the two appearing to be correlated. This stiffness increases with the number of stages and with the range of the relative volatilities being separated. Including pressure dynamics also increases

stiffness. The use of an implicit Gear-type integrator produces dramatic reduction in the computer time required for the simple absorber model whose Jacobian is constant. For a two-component 10-tray column with a stiffness ratio of 8000, the real time factor (RTF) is reduced by a factor of 20 over explicit integration.

The results are not as clear when applied to the distillation models for which the Jacobian is not constant. The RTF actually increases for a 30 tray column using the CMO model. However, the Jacobian was generated internally via finite differences, an approach which is not very efficient and is not recommended by the developers of LSODE. A user-supplied Jacobian is the recommended approach, but one that time constraints precluded for this work.

(8) There was notable decrease in the RTF when the Wilson model was used rather than the ideal. This decrease varied from a factor of about three using a fixed-step Euler or Runge-Kutta integration to about 1.3 using LSODE in the explicit integration mode. However these results are only indicative. The penalty for using should increase with the number of components. Also, the use of VER0A of DYSIM which has a high overhead probably minimizes the true difference between the two VLE models.

There are several recommendations for additional work to further validate the conclusions developed in this work.

(1) At least one other VLE model should be evaluated.

(2) The effect of composition on the distillation models should be evaluated.

(3) The RTF's for distillation should be determined using an internally generated Jacobian.

(4) The pressure dynamics model needs to be evaluated in more detail. In particular, a lumped model should be compared with the stage-to-stage model used in this work in the hopes of relieving the stiffness problem somewhat.

NOMENCLATURE

A	-	interfacial area, m^2
F	-	feed flow rate, Kmol/s
H	-	stream enthalpy, Kcal/Kmol
h	-	liquid level, m
h_i	-	partial molal enthalpy, Kcal/Kmol
K_i	-	K-value for ith component
L	-	liquid flow rate, Kmol/s
l	-	liquid holdup, m^3
M	-	vector of input variables
P	-	pressure, atm
q_k	-	kth heat flux, Kcal/m^2-s
S	-	cross section area, m^2
T	-	temperature, K
t	-	time, hour
U	-	internal energy, Kcal/Kmol
V	-	vapor flow rate, Kmol/s
x_i	-	mol fraction of ith component in the liquid phase
Y	-	state variable vector
y_i	-	mol fraction of ith component in the vapor phase
Z	-	algebraic variable vector
z_i	-	mol fraction of ith component in a feed stream
α_{ij}	-	relative volatility of component I with respect to component j
γ_i	-	activity coefficient of the ith component in a mixture
ϵ	-	liquid fraction
N	-	total mass transfer flux, Kmol/m^2-s
$\eta_{i,k}$	-	mass transfer flux of component i to the kth phase, Kmol/m^2-s
ρ	-	molar density, Kmol/m^3
ϕ	-	system volume, m^3
Ψ	-	primary vector of conserved quantities
ψ_n	-	holdup of ith component on the nth tray
Υ	-	augmented vector of conserved quantities
υ	-	molar volume
$\varphi_{i,n}$	-	holdup of ith component on the nth tray

Appendix A: Flash Drum Design Data

A flash drum was designed to handle the following feed:

Feed flow rate (kg/hr.)	14000.
Composition (mol fraction):	
water	0.6
methanol	0.3
ethanol	0.1
Temperature (K)	300.0

Operating specifications:	
Operating pressure (atm)	1.0
Heat input (j/hr.)	4.0×10^9
Liquid residence time (min) (One-third full)	10.0
Vapor velocity - % of flooding flooding	80.
Height to diameter ratio	3/1 to 4/1

Based on these specifications, the drum has the following performance:

1) Based on the ideal VLE model:

Operating temperature (K)	360.16
<u>Vapor</u>	
Flow rate (kg/h.)	4060.38
Composition (mol fraction):	
water	0.4447
methanol	0.4290
ethanol	0.1263
<u>Liquid</u>	
Flow rate (kg/hr.)	9939.62
Composition (mol fraction):	
water	0.7206
methanol	0.1885
ethanol	0.0909

2) Based on the Wilson VLE model:

Operating temperature (K)	353.46
Vapor	
Flow rate (kg/hr.)	4465.05
Composition (mol fraction):	
water	0.3888
methanol	0.4408
ethanol	0.1704
Liquid	
Flow rate (kg/hr.)	9534.95
Composition (mol fraction):	
water	0.7455
methanol	0.1802
ethanol	0.0743

The drum size that meets the design specification is:

Diameter (m)	1.2
Height (m)	4.5

Appendix B: Gas Absorber Design Data

A gas absorber was designed to scrub acetone from air using water as the absorption liquid at an operating pressure of 1.0 atm. This design is based on the example given by Douglas (1989) which, in turn, is based on an AIChE Student Contest Problem.

The feed conditions to the absorber are:

Feed flow rates (lbmol/min.):

Liquid	37.7
Air containing acetone	11.7
Mol fraction of acetone in air	0.01
Mol fraction of acetone in lean water	0

The following are the operating and design specifications for the column:

Tray type	Sieve
Number of trays	10
Height between trays (ft)	2
Weir height (in)	2
Active tray area (% of total)	75
Vapor velocity (% of flooding)	65
Operating temperature (C)	25
Operating pressure (atm)	1

Based on these specifications, the column size was determined as follows:

Height (ft)	26
Diameter (ft)	5
Weir length (ft)	3.65

APPENDIX C. ABSORBER TRANSFER FUNCTIONS

The following are the details of the derivations of the transfer functions relating the compositions of the streams leaving an absorber as functions of the feed compositions and the vapor and liquid flow rates. The basic equation for an absorber equilibrium stage is

$$(D\text{-}1) \qquad \varphi_i \frac{dx_{i,n}}{dt} = VK_i x_{i,n-1} - (VK_i + L_n)x_{i,n} + L_{n+1}x_{Dn+1}$$

$$where \quad \varphi_i = S[(h_T - h)\rho_V K_i + h\rho_L]$$

For the reference model, $L_n = L_{n+1} = L_{N+1}$ and $x_{Dn+1} = x_{n+1}$. For a well-mixed downcomer,

$$(D\text{-}2) \qquad \phi_D \frac{dx_{Di,n}}{dt} = L_n(x_{i,n} - x_{Di,n})$$

and $L_n = L_{n+1} = L_{N+1}$. For variable flow over the outlet weir,

$$(D\text{-}3) \qquad S\rho_L \frac{dh_n}{dt} = L_{n+1} - L_n$$

where the flow rate leaving each stage is given by the Francis weir formula,

$$(D\text{-}4) \qquad L_n = C_w l_w (h_n - h_w)^b$$

Linearizing and Laplace transforming Eqns. D-1 through D-4 results in the following equation for the compositions on the nth stage

$$(D\text{-}5) \qquad -S_i \Delta x_{i,n-1} + A(s)\Delta x_{i,n} - B(s)\Delta x_{i,n+1} = \beta_n \frac{\Delta V}{V} - C_n(s)\frac{\Delta L_{N+1}}{L}$$

where S_i is the stripping factor for the ith component, i.e., $S_i = V K_i/L$. The functions A(s),

B(s), and $C_n(s)$ depend upon the specific absorber model as follows:

	Reference Model	*Downcomer Model*	*WeirModel*
$A(s)$	$\tau_L s + S_l + 1$	$\tau_L s + S_l + 1$	$\tau_L s + S_l + 1$
$B(s)$	1	$\frac{1}{\tau_D s + 1}$	1
$C_n(s)$	β_n	β_n	$\frac{(\tau_W s + 1)x_{l,n} - x_{l,n+1}}{(\tau_W s + 1)^{N-n+2}}$

where $C_n(s)$ and β_n are also functions of the steady-state solution

$$(D\text{-}6) \qquad x_{l,n} = \frac{S_l^{N+1} - S_l^n}{S_l^{N+1} - 1} x_{l,0} + \frac{S_l^n - 1}{S_l^{N+1} - 1} x_{l,N+1}$$

$$where \quad x_{l,0} = \frac{y_{l,0}}{K_l}$$

These functions are

$$(D\text{-}7) \qquad \beta_n = S_l(x_{l,n-1} - X_{l,n})$$

$$= \left[\frac{S_l - 1}{S_l^{N+1} - 1} (x_{l,0} - x_{l,N+1})\right] S_l^n$$

$$= \beta_l S_l^n$$

and

$$(D\text{-}8) \qquad C_{l,n}(s) = \frac{(\tau_w s + 1)[\gamma_{l,n} x_{l,0} + (1 - \gamma_{l,n}) x_{l,N+1}] - \gamma_{l,n+1} x_{l,0} + (1 - \gamma_{l,n+1}) x_{l,N+1}}{(\tau_W s + 1)^{N-n+2}}$$

$$where \quad \gamma_{l,n} = \frac{S_l^{N+1} - S_l^n}{S_l^{N+1} - 1}$$

While it is possible to solve Eqn. D-5 for the general case of N stages, the resulting transfer

functions are not particularly instructive as to the underlying dynamic behavior. Instead, we have chosen to look at these transfer functions for absorbers containing a small number of stages. If Eqn. D-5 is solved for N=2, one gets the following general transfer functions for the reference and downcomer models:

$$(D\text{-}9) \qquad \frac{\Delta x_{l,1}}{\Delta x_{l,0}} = \frac{S_l}{A^2 - BS_l}$$

$$\frac{\Delta x_{l,1}}{\Delta x_{l,3}} = \frac{B^2}{A^2 - BS_l}$$

$$\textit{and} \quad \frac{\Delta x_{l,1}}{\Delta F} = \beta S_l \frac{A + BS_l}{A^2 - BS_l}$$

$$\textit{where} \quad \Delta F = \frac{\Delta V}{V} \quad \textit{or} \quad -\frac{\Delta L}{L}$$

The first transfer function gives the response of the liquid composition from the bottom tray to the composition of the vapor feed; the second to the composition of the liquid feed; and the third to changes in either vapor or liquid flow rates. For the weir model, the first two transfer functions remain the same but the third becomes

$$(D\text{-}10) \qquad \frac{\dfrac{\Delta x_{l,1}}{\Delta L}}{L} = \frac{AC_1 + BC_2}{A^2 - BS_l}$$

Substituting for A, B, and C gives, for the reference model

$$(D\text{-}11) \qquad \frac{\Delta x_{l,1}}{\Delta x_{l,0}} = S \frac{\tau_L s + S_l + 1}{\tau_L^2 s^2 + 2(S_l + 1)\tau_L s + S^2 + S + 1}$$

$$\frac{\Delta x_{l,1}}{\Delta x_{l,3}} = \frac{1}{\tau_L^2 s^2 + 2(S_l + 1)\tau_L s + S^2 + S + 1}$$

$$\textit{and} \quad \frac{\Delta x_{l,1}}{\Delta F} = \beta S \frac{\tau_L s + 2S_l + 1}{\tau_L^2 s^2 + 2(S_l + 1)\tau_L s + S^2 + S + 1}$$

for the downcomer model

$$(D\text{-}12)\qquad \frac{\Delta x_{i,1}}{\Delta x_{i,0}} = \frac{(\tau_L s + S_i + 1)(\tau_D s + 1)}{\tau_D \tau_L^2 s^3 + \tau_L(\tau_L + 2(S_i+1)\tau_D s^2 + (S_i+1)(2\tau_L + (S_i 1)\tau_D)s + S_i^2 + S_i + 1}$$

$$\frac{\Delta x_{i,1}}{\Delta x_{i,3}} = \frac{1}{(\tau_D s + 1)[\tau_D \tau_L^2 s^3 + \tau_L(\tau_L + 2(S_i+1)\tau_D s^2 + (S_i+1)(2\tau_L + (S_i 1)\tau_D)s + S_i^2 + S_i + 1]}$$

$$\textit{and}\quad \frac{\Delta x_{i,1}}{\Delta F} = \frac{\tau_L \tau_D s^2 + [\tau_L + (S_i+1)\tau_D]s + 2S_i + 1)}{\tau_D \tau_L^2 s^3 + \tau_L(\tau_L + 2(S_i+1)\tau_D s^2 + (S_i+1)(2\tau_L + (S_i 1)\tau_D)s + S_i^2 + S_i + 1}$$

The response to liquid flow rate transfer functions for the weir flow model is the only one that differs from the reference model. It is

$$(D\text{-}13)\qquad \frac{\frac{\Delta x_{i,n}}{\Delta L}}{L} = \frac{(\tau_L s + S + 1)[(\tau_W s + 1)x_{i,1} - x_{i,2}] + (\tau_W s + 1)[(\tau_W s + 1)x_{i,2} - x_{i,3}]}{(\tau_w s + 1)(\tau_L^2 s^2 + 2(S_i+1)\tau_L s + S_i^2 + S_i + 1)}$$

Similarly, the transfer functions for a three-stage absorber (N=3) are, in general

$$(D\text{-}14)\qquad \frac{\Delta x_{i,1}}{\Delta x_{i,0}} = \frac{A^2 - BS}{A(A^2 - 2BS)}$$

$$\frac{\Delta x_{i,1}}{\Delta x_{i,4}} = S\frac{B^3}{A(A^2 - 2BS)}$$

$$\textit{and}\quad \frac{\Delta x_{i,1}}{\Delta F} = \beta S\frac{A^2 - BS(1-A) + B^2S^2}{A(A^2 - 2BS)}$$

For the reference model these become

$$(D\text{-}15)\qquad \frac{\Delta x_{l,1}}{\Delta x_{l,0}} = S\frac{(\tau_L s+S+1)^2-S}{(\tau_L s+S+1)[(\tau_L s+S+1)^2-2S}$$

$$\frac{\Delta x_{l,1}}{\Delta x_{l,4}} = \frac{1}{(\tau_L s+S+1)[(\tau_L s+S+1)^2-2S}$$

$$\textit{and}\quad \frac{\Delta x_{l,1}}{\Delta F} = \beta S\frac{(\tau_L s+S+1)^2+S(\tau_L s+S)+S^2}{(\tau_L s+S+1)[(\tau_L s+S+1)^2-2S}$$

While for the downcomer model these are

$$(D\text{-}16)\qquad \frac{\Delta x_{l,1}}{\Delta x_{l,0}} = \frac{(\tau_D s+1)(\tau_L s+S+1)^2-S}{(\tau_L s+S+1)[(\tau_D s+1)(\tau_L s+S+1)^2-2S]}$$

$$\frac{\Delta x_{l,1}}{\Delta x_{l,4}} = \frac{1}{(\tau_D s+1)^2(\tau_L s+S+1)[(\tau_D s+1)(\tau_L s+S+1)^2-2S]}$$

$$\frac{\Delta x_{l,1}}{\Delta F} = \frac{(\tau_D s+1)^2(\tau_L s+S+1)^2+S(\tau_L s+S)(\tau_D s+1)+S^2}{(\tau_D s+1)(\tau_L s+S+1)[(\tau_D s+1)(\tau_L s+S+1)^2-2S]}$$

For the weir model, the general transfer function is

$$(D\text{-}17)\qquad \frac{\frac{\Delta x_{l,1}}{\Delta L}}{L} = \frac{C_1(A^2-SB)+C_2AB+C_3B^2}{A(A^2-2SB)}$$

What is of interest is the order of the transfer functions for each of the models. This is summarized in Table C-1. Each entry in table is of the form Nnum:Nden where Nnum is the order of the numerator polynomial and Nden that of the denominator polynomial.

Table C-1. Absorber Transfer Function Analysis

		Model					
Transfer		Reference		Downcomer		Flow-over-Weir	
Function	Ntray =	2	3	2	3	2	3
$\Delta x_1/\Delta x_0$		1:2	2:3	2:3	3:4	n/a	n/a
$\Delta x_1/\Delta x_N$		0:2	0:3	0:4	0:6		
$\Delta x_1/\Delta F$		1:2	2:3	2:3	4:5		
$\Delta x_1/(\Delta L/L_)$						2:3	3:7

Regardless of the model and the number of stages, $\Delta x_1/\Delta x_0$ is asymptotically first order. The asymptotic order for $\Delta x_1/\Delta x_N$ is N for the reference model and 2N for the downcomer model. The asymptotic order of $\Delta x_1/\Delta F$ is always one regardless of the number of stages. However, the asymptotic order of the flow-over-the-weir model increases with the number of stages.

Appendix D. Distillation Column Design Data

A distillation column was designed to separate a mixture of methanol, ethanol, and water.

The column operating conditions are:

	Mol fraction				
	Water	Methanol	Ethanol	Flow rate(kg/hr.)	Temperature(K)
Feed	0.65	0.25	0.10	7000	357.15
Distillate	0.1174	0.6568	0.2259	3630	342.96
Bottom Pro	.0.9708	0.0050	0.024	3370	372.01

Reboiler

Reboiler feed rate	20000 kg/hr.
Reboiler vapor out	5843 kg/hr.
Duty	1.25×10^{10} j/hr

Total Condenser

Duty	-1.245×10^{10} j/hr.
Reflux Ratio	2.14

Operating pressure 1 atm.

Column Design

Tray type	Sieve, single crossflow tray, segmental downcomers and straight weir
Number of trays	9
Feed tray location	5
Tray spacing	0.6 m
Diameter	1.2 m
Column height	8.4 m
Weir length	0.84 m
Weir height	0.06 m

Residence times

Condenser	10 min.
Bottom	10 min.
Reboiler	30 seconds
Tray	20 seconds

REFERENCES

Angel, S., Marmur, A., and Kehat E., "Comparison of Methods of Prediction of Vapor Liquid Equilibria and Enthalpy in a Distillation Simulation Program," *Computers & Chem. Eng.*, Vol. 10, No. 2, pp. 169-180 (1986)

Arbel, A., I. H. Rinard and R. Shinnar, "Dynamics and Control of Fluidized Catalytic Crackers. 2. Multiple Steady State and Instabilities," *Ind. Eng. Chem. Res.*, Vol. 34, No. 9, pp. 3014-3026 (1995)

Asbjørnsen, O.A., "A Systems Engineering Approach to Process Modeling," *Shell Process Control Workshop*, D.M. Prett and M. Morari, Eds., Butterworth, Boston, pp. 139-182, (1987)

Barrett, A., and Walsh, J. J., "Improved Chemical Process Simulation Using Local Thermodynamic Approximations," *Computers & Chem. Eng.*, Vol. 3, pp. 397-402 (1979)

Bennett, D. L., Agrawal, R., and Cook, P. J., "New Pressure Drop Correlation for Sieve Tray Distillation Columns," *AIChE Journal*, Vol. 29, No. 3, pp. 434-442 (1983)

Benson, R., "Process Systems Engineering: Past, Present and a Personal View of the Future," *Computers & Chem. Eng.*, 13 (11/12), 1193-1198 (1989)

Berber, R., and Brosilow, C. B., "A New Algorithm For Dynamic Simulation," *Computers & Chem. Eng., Escape-2*, pp. S367-S372 (1993)

Biardi, G., and Grottoli, M. G., "Development of a New Simulation Model for Real Trays Distillation Model," *Computer & Chem. Eng.*, 13 (4/5), 441-450 (1989)

Boston, J. F., "Inside-Out Algorithms for Multicomponent Separation Process Calculations," *Computer Applications to Chemical Engineering*, ACS Sym. Series 124, Am. Chem. Soc., Washington, D.C. pp. 135-151 (1980)

Boston, J. F., and Britt, H. I., "A Radically Different Formulation And Solution of The Single-Stage Flash Problem," *Computers & Chem. Eng.*, Vol. 2, pp. 109-122 (1978)

Boston, J. F., and Sullivan, S. L. Jr., "A New Class of Solution Methods for Multicomponent Multistage Separation Processes," *Can. J. Chem. Eng.*, Vol. 52, pp. 52 - 63 (1974)

Boston, J. F., and Sullivan, S. L. Jr., "An Improved Algorithm for Solving the Mass Balance Equations in Multistage Separation Processes," *Can. J. Chem. Eng.*, Vol. 50, pp. 663-669 October (1972)

Brandani, S., Brandani, V., Del Re, Giovanni, and Di Giacomo, Gabriele, "Activity Coefficients From a Virial Expansion about Their Infinite Dilution Values," *The Chem. Eng. Journal*, Vol. 46, pp. 35-42 (1991).

Brenan, K.E., S.L. Campbell, and L.R. Petzold, *Numerical Solution of Initial-Value Problems in Differential-Algebraic Equations*, North-Holland/Elsevier, New York, (1989)

Byrne, G. D., and Ponzi, P. R., "Differential-Algebraic Systems, Their Applications and Solutions," *Computers & Chem. Eng.*, Vol. 12, No. 5, pp. 377-382 (1988).

Cameron, I. T., and Gani, R., "Adaptive Runge-Kutta Algorithms for Dynamic Simulation," *Computers & Chem. Eng.*, 12 (7), 705-718 (1988).

Cameron, I. T., Ruiz, C. A., and Gani, R., "A Generalized Dynamic Model for Distillation Columns-II. Numerical and Computational Aspects," *Computers & Chem. Eng.*, Vol. 10, No. 3, pp. 199-211 (1986)

Chimowitz, Eidred H., Anderson, Thomas F., Macchietto, S., and Stutzman, Leroy F., "Local Model for Representing Phase Equilibria in Multicomponent, Nonideal Vapor-Liquid and Liquid-Liquid Systems. 1. Thermodynamic Approximation Functions." *Ind. Eng. Chem. Process Des. Dev.*, Vol. 22, No. 2, pp. 217-225 (1983)

Chimowitz, Eidred H., Anderson, Thomas F., Macchietto, S., and Stutzman, Leroy F., " Local Models for Representing Phase Equilibria in Multicomponent, Nonideal Vapor-Liquid and Liquid-Liquid Systems. 2. Application to Process Design," *Ind. Eng. Chem. Process Des. Dev.*, Vol. 23, No. 3, pp. 609-618 (1984)

Cook, W. J., J. Klatt, and C. B. Brosilow, "Simulation of Large Scale Dynamic System-II. A Modulator Simulator for the Dynamics of Distillation Systems," *Computers & Chem. Eng.*, Vol. 11, No. 3, pp. 255-264 (1987)

Denn, M.M., *Process Modeling*, Longman, White Plains, NY, (1986)

Douglas, J.M., *Conceptual Design of Chemical Processes*, McGraw-Hill, New York, Chapter 3, (1989)

Drozdowicz, B., and Martinez, E., "Reduced Models for Separation Processes in Real-Time Simulators," *Computers & Chem. Eng.*, Vol. 12, No. 6, pp. 547-560 (1988)

Eckert, E., and Kubicek, M., "Modeling of Dynamics for Multiple Liquid-Vapor Equilibrium Stage," *Ind. Eng. Sci.*, Vol. 49, No. 11, pp. 1783-1788 (1994)

Evans, L. B., "Process Modeling: What Lies Ahead," *Chem. Eng. Prog.*, pp. 42-44, October (1990)

Fair, J. R., "Distillation: Whither, Not Whether," *Chem. Eng. Res. Des.*, Vol. 66, pp. 363-370(1988)

Fieg, G., Wozny, G., and Kruse, C., "Experimental and Theoretical-Studies of the Dynamics of Startup and Product Switchover Operations of Distillation-Column," *Computers & Chem. Eng.*, Vol. 32, No. 5, pp. 283-290 (1993)

Franks, R. G. E., *Modeling and Simulation in Chemical Engineering,* Wiley-Interscience, New York (1972)

Fuentes, C., and W.L. Luyben, "Control of High-Purity Distillation Columns," *IEC Proc. Des. Devel.*, Vol. 22, pp. 361-366 (1983).

Gallun, Steven E., and Hollan, Charles D., "Gear's Procedure for the Simultaneous Solution of Differential and Algebraic Equations with Application to Unsteady State Distillation Problems," *Computers & Chem. Eng.*, Vol. 6, No. 3, pp. 231-244 (1982)

Gani, R., and Cameron, I. T., "Modelling for Dynamic Simulation of Chemical Processes: the Index Problem," *Chem. Eng. Sci.*, Vol. 47, No. 5, pp. 1311-1315 (1992)

Gani, R., and Cameron, I. T., "Extension of Dynamic Models of Distillation Columns to Steady-State Simulation," *Computers & Chem. Eng.*, Vol. 13, No. 3, pp. 271-280 (1989)

Gani, R., and Hytoft, G., "*Dynamic Simulation of Distillation Operations: New Features*," AIChE Annual Meeting, St. Louis, Nov. 7-12 (1993)

Gani, R., Ruiz, C. A., and Cameron, I. T., "A Generalized Model for Distillation Columns-I: Model Description and Applications," *Computers & Chem. Eng.*, Vol. 10, No. 3, pp. 181-198 (1986)

Gani, R., and Toneva, G., "Simultaneous Steady State and Dynamic Simulation of Chemical Processes," *Computers & Chem. Eng.*, Vol. 13, No. 4/5, pp. 563-570 (1989)

Gosset, R., Heyen, G., and Kalitventzeff, B., " An Efficient Algorithm to Solve Cubic Equations of State," *Fluid Phase Equilibria*, Vol. 25, pp. 51-64 (1986)

Grassi, V.G. II, "Rigorous Modelling and Conventional Simulation," *Practical Distillation Control*, W.L. Luyben, Ed., Van Nostrand Reinhold, Chap. 3, (1992)

Grottoli, M.G., Biardi, G., and Pellegrini, L.," A New Simulation Model For A Real Trays Absorption Column, " *Computers & Chem. Eng.*, Vol. 15, No. 3, pp. 171-179 (1991)

Gundersen, T., " Numerical Aspects of the Implementation of Cubic Equations of State in

Flash Calculation Routines," *Computers & Chem. Eng.*, Vol. No. 3, pp. 245-255 (1982)

Hanna, O. T., "New Explicit and Implicit 'Improved Euler' Methods for the Integration of Ordinary Differential Equations," *Computers & Chem. Eng.*, 12 (11), 1083-1086 (1988)

Henley, E. J., and Seader, J. D., *Equilibrium-Stage Separation Operations in Chemical Engineering*, John Wiley & Sons, New York, (1981)

Hillestad, M., Sorlie, C., Anderson, T. F., Olsen, I., and hertzberg, T., "On Estimating the Error of Local Thermodynamic Models-A General Approach," *Computers & Chem. Eng.*, Vol. 13, No. 7, pp. 789-796 (1989)

Hoffman, H., "Future Trends in Chemical Engineering Modeling," *Computers & Chem.* Eng., 12 (5), 415-420 (1988)

Holl, P., W. Marquardt, and Gilles, E. D., "DIVA-A Powerful Tool for Dynamic Process Simulation," *Computers & Chem. Eng.*, 12 , pp. 421 (1988)

Holland, C. D., and Liapis, A. I., *Computer Methods for Solving Dynamic Separation Problems*, McGraw-Hill, New York, (1983)

Holmes, M. J., and Van Winkle, M., "Prediction of Ternary Vapor-Liquid Equilibria From Binary Data," *Ind. Eng. Chem.*, Vol. 62, No. 1, pp. 21-31 (1970)

Ishii,Y., and Otto, F. D., "A General Algorithm for Multistage Multicomponent Separation Calculations," *Can. J. Chem. Eng.*, Vol. 51, pp. 601-606 (1973)

Jacobsen, E. W., and Skogestad, S., "Inconsistencies in Dynamic Models for Ill-Conditioned Plants: Application to Low-Order models of Distillation Columns," *Ind. Eng. Chem. Res.*, Vol. 33, No. 3, pp. 631-640 (1994)

Jacobsen, E. W., and Skogestad, S., "Instability of Distillation Columns," *AIChE Journal*, Vol. 40, No. 9, pp.1466-1478 (1994)

Jacobsen, E. W., and Skogestad, S., "Multiple Steady States in Ideal Two-Product Distillation," *AIChE Journal*, Vol. 37, No. 4, pp.499-511 (1991)

Jelinex, J., "The Calculation of Multistage Equilibrium Separation Problems With Various Specifications," *Computers & Chem. Eng.*, Vol. 12, No. 2/3, pp. 195-198 (1988)

Kilakos, A., and Kalitventzeff, B., "A New Implementation For Analytical Derivatives of Thermodynamic Properties and its Beneficial Application on Dynamic Simulation,"

Computers & Chem. Eng., Vol. 17, No. 5/6, pp. 441-450 (1993)

Kim, Changse, and Friedly, John C., " Approximate Dynamic Modeling of Large Staged Systems," *Ind. Eng. Chem. Process Des. Dev.*, Vol. 13, No. 2, pp. 177-181 (1974)

King, C. J., *Separation Processes*, 2nd Edition, McGraw-Hill, New York, (1980).

Kinoshita, M., and Takamatsu, T., "A Powerful Solution Algorithm for Single-Stage Flash Problems," *Computers & Chem. Eng.*, Vol. 10, No. 4, pp. 353-360 (1986)

Kooijman, H. A., and Taylor, R., "A Nonequilibrium Model for Dynamic Simulation of Tray Distillation Columns," *AIChE Journal* Vol. 41, No. 8, pp. 1852-1863 (1995)

Kremser, A., *Nat. Pet. News*, 22(21), pp. 42 (1930)

Krishnamurthy, R., and Taylor, R., "A Nonequilibrium Stage Model of Multicomponent Separation Processes, Part: I, Model Description And Method of Solution," *AIChE Journal,* Vol. 31, No. 3, pp. 449-455 (1985)

Lagar, G., Paloschi, J., and Romagnoli, J.A., "Numerical Studies in Solving Dynamic Distillation Problems," *Computers & Chem. Eng.* , Vol. 11, No. 4, pp. 383-394 (1987)

Lapidus, L., and Amundson N. R., "Stagewise Absorption and Extraction Equipment-Transient and Unsteady State Operation," *Ind. Eng. Chem.*, Vol. 42 No. 6, June (1950)

Leesley, M. E., and Heyen, G., "The Dynamic Approximation Method of Handling Vapor-Liquid Equilibrium Data In Computer Calculations for Chemical Processes," *Computers & Chem. Eng.*, Vol. 1, pp. 109-112 (1977)

Levy, R. E., Foss, A. S., and Grens, E. A., "Response Modes of a Binary Distillation Column," *I & EC Fundamentals*, Vol. 8, No. 4, pp. 765-776 (1969)

Lundstrom, P., Flatby, P., and Skogestad, S., "Effect of Flow Dynamics, Energy Balance and Pressure Dynamics on the Overall Response of Distillation Columns," AIChE Annual Meeting, St. Louis, Nov. 7-12 (1993)

Luyben, W. L., *Process Modeling, Simulation and Control for Chemical Engineers,* 2nd Edition, McGraw-Hill, New York (1990)

Macchietto, Sandro, Chimowitz, Eldred H., Anderson, Thomas F., and Stutzman, L.F., "Local Models For Representing Equilibria in Multicomponent Nonideal Vapor-Liquid and Liquid-l Systems. 3. Parameter estimation and Update," *Ind. Eng. Chem. Process Des. Dev.*, Vol. 25, No. 3, pp. 674-682 (1986)

Marquardt, W., "Dynamic Process Simulation - Recent Progress and Future Challenges," *Chemical Process Control-CPCIV*, Arkun, Y., and Ray, W. H., eds. CACHE/AIChE Publications, New York, pp. 131-180, (1991)

Martin J. J., "Cubic Equations of State-Which?" *Ind. Eng. Chem. Fundam.*, Vol. 18, No. 2, pp. 81-97 (1979)

Mathias, P. M. and Klotz, H. C., "Take a Closer Look at Thermodynamic Property Models," *Chem. Eng. Prog.*, pp. 67-75 June (1994)

Michelsen, M.L., "Phase Equilibrium Calculations. What is Easy And What is Difficult?" *Computers & Chem. Eng.*, Vol. 17, No. 5/6, pp. 431-439 (1993)

Muher, C.A., and W.L. Luyben, "Batch Distillation," *Practical Distillation Control*, W.L. Luyben, Ed., Van Nostrand Reinhold, Chap. 25, (1992)

Nisenfeld, A. E., "Reflux or Distillate: Which to Control?" *Chem. Eng.*, Oct. 6, pp. 169-171 (1969)

Palmer, David A., "A Practical Synthesis of Experimental and Correlation Techniques for Modeling Highly Nonideal Systems with Many Components." *Ind. Eng. Chem. Process Des. Dev.*, Vol. 23, No. 2, pp. 259-266 (1984)

Pantelides, C.C., "SpeedUp-Recent Advances in Process Simulation," *Computers & Chem. Eng.*, 12(7), pp. 745-756 (1988)

Papadourakis, A., and J.E. Rijnsdörp, "Approximate and Simplified Models," *Practical Distillation Control*, W.L. Luyben, Ed., Van Nostrand Reinhold, Chap. 4, (1992)

Perry, R. H., and Chilton C. H., *Chemical Engineers' Handbook*, 5th Edition, McGraw-Hill, New York (1984)

Petzold, Linda, "Differential/Algebraic Equations Are not Ode's," *SIAM J. Sci. Stat. Comput.*, Vol. 3, No. 3, pp. 367-384 (1982)

Pinto, J. C., and Biscaia, E. C. JR., "Order Reduction Strategies for Models of Staged Separation System," Computers & Chem. Eng., Vol. 12 No. 8, pp. 821-831, (1988)

Ponton, J. W., and Gawthrop, P. J., "Systematic Construction of Dynamic Models For Phase Equilibrium Processes," *Computers & Chem. Eng.*, Vol. 15, No. 12, pp. 803-808 (1991)

Preisig, H., Kimmich, M., and Rippin, D. W. T., "A Study of Dynamic System Modeling," *Computers & Chem. Eng.*, 12(5), 455-460 (1988).

Rademaker, C., J.E. Rijnsdorp, and A. Maarveld, *Dynamics and Control of Continuous Distillation Units,* Elsevier, New York, (1975)

Ranzi, E., Rovaglio, M., Faravelli, T., Biardi G., "Role of Energy Balances in Dynamic Simulation of Multicomponent Distillation Columns," *Computers & Chem. Eng.*, Vol. 12, No. 8, pp. 783-786 (1988).

Reid, R. C., Prausnitz. J. M., and Poling, B. E., *The Properties of Gases and Liquids*, 4th Edition, McGraw-Hill, New York, (1987).

Rinard, I. H., "Model Fidelity Considerations in Simulation," AIChE Annual Meeting, Chicago, November (1990).

Rinard, I.H., "Sensitivity to Modeling Errors in Steady-State Progress Simulation," Computer & Chem. Eng., Vol. 11, No. 6, pp. 707-712 (1987).

Rinard, I.H., and B.W. Benjamin, "Control of Recycle Systems. Part 1. Continuous Systems," ACC, WA5 (1982).

Rose, L. M., and Hyka, J., "Analysis of Operating Distillation Column Data," *Ind. Eng. Chem. Process Des. Dev.*, Vol. 23, No. 3, pp. 429-437 (1984).

Rovaglio, M., Ranzi, E., Biardi, G., and Faravelli, T., "Rigorous Dynamics and Control of Continuous Distillation Systems Simulation and Experimental Results," *Computers & Chem. Eng.*, Vol. 14, No. 8, pp. 871-887 (1990).

Ruiz, C. A., Cameron, I. T., and Gani, R., "A Generalized Dynamic Model for Distillation Columns-III. Study of Startup Operations," *Computers & Chem. Eng.*, Vol. 12, No. 1, pp. 1-14 (1988)

Ruiz, C. A., and Gani, R., "Simulation and Design of Distillation Columns, Part 1. Hydraulic Model and Dynamic Behavior," *Lat. Am. J. Chem. Eng. Appl. Chem.*, Vol. 16, pp. 277-305 (1986)

Sanderson, R. V., and Chien, H. Y., "Simultaneous Chemical and Phase Equilibrium Calculation," *Ind. Eng. Chem. Process Des. Dev.*, Vol. 12, No. 1, pp. 81-85 (1973)

Schiesser, W. E., *The Numerical Methods of Lines*, Academic Press, New York (1991)

Shah, V. M., Bienkowski, P. R., and Cochran, H. D., "Generalized Quartic Equation of State for Pure Nonpolar Fluids," *AIChE Journal*, Vol. 40, No. 1, pp. 152-159 (1994)

Silebi, C. A., and W. E. Schiesser, *Dynamic Modeling of Transport Process System*, Academic Press, New York(1992)

Sorlie, C., Hillestad, M., Strand, K., and Flatby, P., "Experiences of Applying Local Thermodynamic Models in Dynamic Process Simulation," AIChE Spring Meeting, 58-d, (1992)

Stryjek, R., and Vera, J. H., "A Cubic Equation of State for Accurate Vapor-Liquid Equilibria Calculation," *Can. J. Chem. Eng.*, Vol. 64, pp. 820-926 October (1986)

Taylor, R., Kooijman, H. A., and Hung, J. S., "A Second Generation Nonequilibrium Model for Computer Simulation of Multicomponent Separation Processes," Computers & *Chem. Eng.*, Vol. 18, No. 3, pp. 205-217 (1994).

Taylor, R., and Krishna, R., *Multicomponent Mass Transfer*, John Wiley & Sons, Inc. New York (1994)

Tyreus, B. D., "Optimization and Multivariable Control of Distillation Column," *Proceedings of the ISA-87, Anaheim, California*(1987)

Vogel, E. F., "An Industrial Perspective on Dynamic Flowsheet Simulation," Chemical Process Control-CPCIV, Arkun, Y., and Ray, W. H., eds. CACHE/AIChE Publications, New York, pp. 181-209 (1991)

Wahl, E. F., and Harriott, P., "Understanding and Prediction of the Dynamic Behavior of Distillation Columns," *Ind. Eng. Chem. Process Des. Dev.*, Vol. 9, No. 3, pp. 396-407(1970)

Walas, Stanley M., *Phase Equilibrium in Chemical Engineering*, Butterworth, MA (1985)

Wankat, P. C., *Equilibrium Staged Separations, Elsevier*, New York, (1988)

Weigand, W. A., Jhawar, A. K., and Williams, T. J., "Calculation Method for the Response Time to Step Inputs for Approximate Dynamic Models of Distillation Columns," *AIChE Journal*, Vol. 18, No. 6, pp. 1243-1252 (1972).

Wong, D. S. H., and Chang, C. F., "Simulation of Dynamics and Phase Pattern Changes for a Azeotropic Distillation Collum," *Computers & Chem. Eng.*, Vol. 15, No. 5, pp. 325-335 (1991)

Wooley, R. J., and Goldfarb, S. M., "The Utility of Using Infinite Dilution Activity Coefficients in Process Design," AIChE Spring National Meeting, April 3 (1989)